UNIVERSITÀ DEGLI STUDI
DI TRENTO

DEPARTMENT OF INFORMATION ENGINEERING AND COMPUTER SCIENCE
ICT International Doctoral School

BROADBAND RADIO INTERFACES DESIGN FOR "4G AND BEYOND" CELLULAR SYSTEMS IN SMART URBAN ENVIRONMENTS

Talha Faizur Rahman

Advisor

Prof. Claudio Sacchi PhD

Università degli Studi di Trento

December 2015

Abstract

Broadband, ubiquitous and energy-efficient wireless networking is one of the pillars in the definition of a really smart urban environment. The latest developments in such a field concern with the forthcoming LTE-A standard, which will also involve small cell deployment for broadband coverage yielding increased quality of experience and reduced power consumption. Some open issues related to small cell LTE-A networking for smart city applications are discussed, together with feasible solutions that are investigated in terms of robust PHY-layer configurations, and fully-wireless backhaul (point-to-point transmission, point-to-multipoint etc.). One such issue is related to power-constrained uplink transmission, where cooperative multipoint (CoMP) in small cell network is considered assuring better quality of service and energy efficiency for user terminal. Moreover, a novel MIMO detection is conceived for LTE-A application based on MCBEP criterion that is suited for size-constrained small base station and guaranteeing near-optimum performance. A door open to upcoming mobile standards by proposing constant envelope techniques in the uplink providing flexible tradeoff between spectral and power efficiency for 5th generation applications. A complete wireless backhaul based on millimeter wave (mmWave), for network of small cells, is considered due to its cost effectiveness and flexible operations. A robust PHY-layer waveform based on space-time MIMO techniques have proven to be the right choice for non-line of sight operations whereas TH-IR UWB techniques are providing significant data rates in line-of-sight case. SDR-Implementation of advanced wireless strategies is important in order to realize network reconfigurability in future cellular networks where network functionalities can be changed "on the fly".

Keywords
[LTE-A, PHY-layer, Cooperative communications, Mm-wave communications, Software-Defined-Radio]

To my family
Abdur Rahman, Saeeda Rahman, Saadi, Rabbya and Umna.

Acknowledgements

Firstly, I would like to express my sincere gratitude to my advisor Prof. Claudio Sacchi for the continuous support of my Ph.D study and related research, for his patience, motivation, and immense knowledge. His guidance helped me in all the time of research and writing of this thesis. I could not have imagined having a better advisor and mentor for my Ph.D study.

Besides my advisor, I would like to thank Dr. Christian Schlegel at Dalhousie University, Canada for interesting and rewarding cooperation.

I am truly grateful to Prof. Lajos Hanzo at University of Southampton, England for allowing me to visit his research lab SOUTHAMPTON WIRELESS where i happened to work on some very interesting research topics that my Ph.D research encompasses. I would like to thank Dr. Mohammed El-Hajjar at University of Southampton for his insightful comments and encouragement during my stay at SOUTHAMPTON WIRELESS.

I am truly thankful to Dr. Mohammed Zafar Ali Khan of Indian Institute of Technology Hyderabad, India for his suggestions and valuable comments during my research. Working with such esteem and respectful personalities is nothing less than a blessing from Allah.

I am grateful to my former and present colleagues at the Information Engineering and Computer Science Department (DISI) of the Univrsity of Trento. During my Ph.D, I happened to supervise some very hardworking Masters Students, Patricia Atungire and Desalegn Melkamu Getu, to mention but a few. My thanks to the members of Multimedia Signal Processing and Understanding Lab (mmLAB) with whom I spent very memorable time. In particular, I express my grattitude to Duc-Tien Dang Nguyen and his beautiful wife, Minh Th Phm, for everything they did for me during my three years of Ph.D research. Forever, I will treasure the time we spent together.

I would like thank my very own Pakistani student community at DISI for their support in difficult times. The people I met were awesome, and I had a great time with them.

Last but not the least, I would like to thank my family. My father, Abdur Rahman, for constantly motivating me through thick and thin of my entire academic career. Even though I am not strong academically and all my life I struggled with education career, he was the one who put faith in me and believed in me for this Ph.D . Of course, alongside my father is my mother, Saeeda Rahman, who brought me up on her own and made me a respectful young man. My brother, Saadi Rahman, and his wife, Anum Saadi, who gave birth to one beautiful soul, *Rania* just a week before my Ph.D defense. My sister Rabbya

Khan who has beautiful little princess, Emaan Khan, are one of few reasons of my happiness. My youngest sister, Umna Usman, got married at the time when I had unavoidable committments with research and couldn't able to be part of ceremony. Lastly, I would like to thank Mrs. Seemeen for her support during my Ph.D career. She supported me through my difficult times and made me believe that I can do this. Indeed, my family will be the happiest family after my this accomplishment. May Allah bless us all with happiness and joys. Ameen!

Talha Faizur Rahman

Contents

List of Tables

List of Figures

Chapter 1

Introduction

Urban population constitutes 80 % of the world population. A possible reason behind this huge population in urban areas is the availability of opportunities and better facilities as compare to rural areas. However, on the other hand, such increase in urban population has made resources, available to citizens, scarce. Today cities are trying to provide better facilities to their citizens e.g., in terms of medics, transportation, telecommunications etc, with available resources. But there is a perception about heterogeneous distribution of such facilities among citizens, i.e. a gap in quality of life indicators. This gap has widened after the economical crisis in 2008 that left the global economy in turbulence. In order to minimize this inability of cities, the concept of *Smart City* is presented in [22] where the aim is to improve quality of life for average population. Following the operational definition of "Smart City", reported at page 6 of [22], a city is said to be "smart" when investments in human and social capital and traditional (transport) and modern (ICT) communication infrastructure fuel sustainable economic growth and a high quality of life, with a wise management of natural resources and through participatory governance. Such ambitious goals can be acheived if research and innovation are done as a function of social requirements of citizens and muncipalities. For this reason, smart cities has open up new research horizons, from socio-economic to ICT areas. ICT will be the core of smart city concept and require transforming solutions.

1.1 ICT for Smart Cities: communication and networking aspects

ICT is believed to have control on some of keys services/applications provided by smart city. In this regard, the significance of ICT on global environment can not be ruled out. Researchers from the Centre for Energy-Efficient Telecommunications (CEET) and Bell

Labs explain that the information communications and technology (ICT) industry, which delivers Internet, video, voice and other cloud services, produces more than 830 million tons of carbon dioxide (CO_2), the main greenhouse gas, annually. Thats about 2 percent of global CO_2 emissions the same proportion as the aviation industry contributes. With the increased usage of smart devices, this figure will be doubled by 2020. Future smart cities will allow to improve environmental sustainability but also offer services/applications aiming to raise quality of life. In such a model the stakeholders in smart cities (Citizens, cities and utilities) can get benefits from developed technology [6].

This model revolves around ICT, especially wireless networking. Keeping this in mind, several service/application providers have deployed their testbeds in smart cities around the world. Many of these devices (running applications) may not be transmitting at huge amount of data but their connectivity in the network could be challenging for the core network. Connection setup and power efficiency are some of the key issues related to such low-cost low-powered devices. Smart cities are usually conceived with large amount of such devices deployed to provide utilities to the citizens. The CO_2 emissions as a result of such deployment is enormous.

Moreover, cellular/mobile network contributes to these emissions, in a sense that large scale network with significant amount of equipment in operation put a considerable dent in the environment system. Therefore, future cellular infrastructure should not only provide spectrally efficient solution but should also be seen as "green" i.e., energy efficient. Small cell technology in smart city context has recently been proposed in [26] where LTE-A small cell technology is considered as right choice for smart city thanks to inherent eco-friendly system design of small cell (short radio footprints). Small cell technology enables battery-limited devices to transmit at low power. The upcoming mobile cellular standards, like LTE-A [1], can act as a communication "*pillar*" for future smart-cities to guarantee broadband access and efficient service mobilization. Small cell LTE-A as forecasted in [82] will represent a technological breakthrough in the wireless networking. As a consequence of smaller radio footprint, user-to-BS proportion is fewer and unit-frequency reuse is possible, shown in Fig 1.1. Hence small cell network inherent the characteristics of "green" and spectral efficient cellular system. Therefore, cellular systems based on small-cell would be fertile for interactive applications requiring loads of information exchange among the entities of smart city.

1.2 The Motivation

Current cellular strategies will be out-dated, in next couple of years and, for smart city scenario where forecasted information flow is many-folds. Next generation cellular network

Figure 1.1: Small cell coverage [26]

LTE-A should overcome the *triple C* bottlenecks of current cellular network, i.e. capacity, cost, and complexity. Smart city applications are to be conceived under the umbrella of LTE-A small cell network, as shown in Fig. 1.2. Such wide range of applications comprise of low data rate sensor and broadband services. Liabilities like power consumption and cost associated with small cell LTE-A should be minimized in the framework of smart city.

Strategies like, cooperative communication, efficient backhaul, radio resource management etc, increase the available capacity by enabling a support of system bandwidth upto 100 MHz, with potential throughput of 1 Gb/s for downlink and 500 Mb/s for uplink [21]. Additionally, if we consider that each small cell site can host also machine to machine (M2M) gateways, richer applications can be conceived targetting both communication and city governance services [26]. It is foreseen that most of the traffic will be originated in the uplink, thanks to interactive relationship between citizens and utilities as described in model proposed in [6]. Hence cellular uplink should be vigorous to stand the originated traffic load. With small cell network, the uplink link quality in LTE-A can be landscaped by visualizing novel and advanced system level strategies.

An improved power efficient LTE-A system can be favorable for smart-phone users, as power/energy efficiency is highly desired for battery-limited devices. Exploiting small

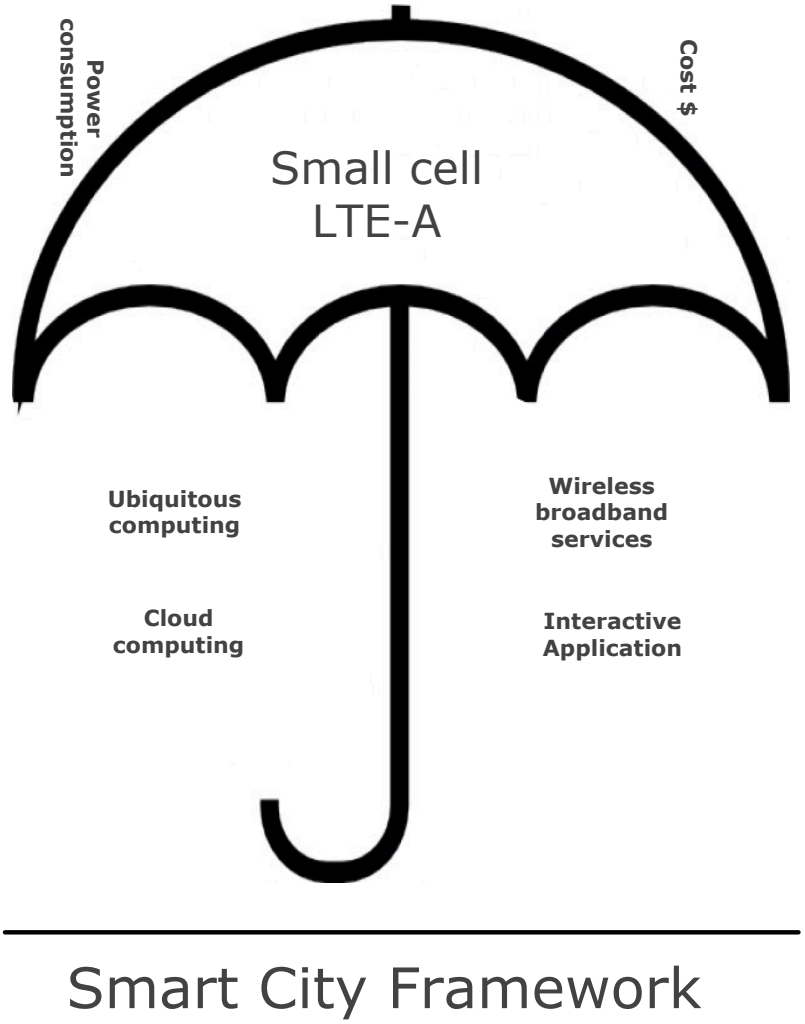

Figure 1.2: Smart city LTE-A umbrella

cell radius, cooperation among BSs, *aka* cooperative multipoint (CoMP), can be anticipated for improved link level performance both in terms of bit-error-rate (BER) and power efficiency. Radiations due to terminal transmission increases with the increase in urban population. It would be a challenge for smart city communication infrastructure to minimize this issue without incurring additional cost at terminal level and gurantees adequate link level performance.

In order to boost uplink capacity, multi-user MIMO (MU-MIMO) configuration is feasible. Indeed high capacity broadband solutions are welcomed in smart city. Uplink cellular scenario is often characterized by large received antenna arrays at base station and single antenna terminals, i.e., $(N_R \geq N_T)$, N_R is receiver antenna elements and N_T is transmit antenna elements. This allows to manipulate signal processing at receiver

with affordable linearly ordered complexity algorithms with performance approaching optimum. The motivation here is to have low complexity receiver design that is able to attain performance close to optimum.

Plug-n-play and self organized small cell BS follow unplanned network infrastructure installed on street poles and connected to core-network via wireless backhaul. In this case, wired solution to backhaul is also not viable and requires high capital expenditures. Wireless backhaul, on the other hand, at millimeter frequency bands provides cost effective and high speed high capacity backhaul solution.

Most of smart city requirements are actually the requirements that are also demanded by 5th generation (5G). In this regard, there is a need to adopt solutions in smart city context that pave the way towards 5G.

1.3 Problems and their Solutions

Smart city should provide an eco-friendly and efficient cellular infrastructure that is able to cope with the needs of citizens. It is believed number of smart city will be fourfold by 2025. LTE-A is an evolution to the current cellular systems as new advancements (in particular, small cell technology) have been standardized for better performance in the future. Some related issues need prompt solution in the context of smart cities keeping in mind that city trends are changing rapidly towards smart city infrastructure.

In this regard, small cell LTE-A uplink is targetted where better performance in terms of throughput and energy efficiency is desired. The proposed appraoch is to enable uplink cooperation among neighboring base stations that are in vicinity. Taking cooperation to base station level will shift the computational complexity burden to high powered base station. Hence terminal gets benefits out of this without increasing hardware complexity and avoids radiating large power to meet the requirements. Indeed ideal signal processing operations at base station will help terminal attaining good quality of service. In the presence of non-idealities (like, non-ideal channel estimation) CoMP in uplink provides interesting insights about link performance and energy efficiency. Such an approach is different from state-of-the-art, because performance analysis is done in terms of user-centric metrics (bit error rate and power consumption).

With the consideration of millimeter wave technology for upcoming 5th generation (5G) standards, different physical layer transmission waveforms proposals have been taken into account to date. Of the important ones are multicarrier techniques like orthorgonal frequency division multiplexing (OFDM) and single-carrier frequency division multiple access (SC-FDMA). Such techniques are efficient in exploiting wide bands available in mmWave frequency range. However, these multicarrier techniques are not power efficient

due to their high peak to average power ratio (PAPR). Hence large backoff is required in order to avoid non-linear distortions. Not only that, these multicarrier techniques are prone to non-ideal oscillator phase noise that might cause destructive effects on the performance. MmWave operations are sensitive to these hardware non-idealities and care must be taken when designing a system.

A possible solution to work around this problem is to have constant envelope (CE) waveform exhibiting 0dB PAPR. Also CE waveforms are robust against phase noise because phase noise is additive to the actual information. CE techniques combined with multicarrier waveforms provide a adequate system capacity with considerable reduced power consumption. In this regard, CE-OFDM and CE-SCFDMA are the possible candidates. Recently, these CE- multicarrier techniques are tested in non-linear LEO satellite channels and have shown remarkable performance improvement over classical OFDM and SC-FDMA systems (detail discussion is in chapter 2).

Multiuser detection in SC-FDMA (uplink of LTE-A) is proposed by linear and non-linear designs in the literature. However, the current SC-FDMA receiver designs are based on maximization of signal power at the output of detector. Practical implementation of one such receiver design, ideal-minimum mean square error (MMSE), is not trivial. In particular, it is often preferred to have adaptive implementation of MMSE criterion in practice. Though linear but such techniques are clearly sub-optimal because MMSE assumes noise is gaussian distributed. In such scenarios where white noise in the system gets colored by multi-user interfering signals, receiver designs based on maximization of output signal-to-interference-noise ratio (SINR) clearly do not yield optimal results. A new strategy is proposed for MU-MIMO uplink LTE-A systems that is based on rather different criterion, called minimum conditioned bit error rate. Minimizing conditioned error probability, in the presence of interference, aims at minimizing the bit error rate at an affordable linear complexity under $N_R \geq N_T$. The proposed strategy is fast in convergence and pose low receiver complexity.

Average throughput inside a small cell is a function of backhaul (BH) links transporting cellular traffic to the core. Fragile BH links will severely degrade the performance inside the cell and users might experience second-rate quality of services. Wireless BH solutions, providing reasonable data rates and link performance, can be conducive as capital expenditures (CAPEX) and maintaince costs are lower than that of wired solutions. Millimeter wave (mmWave) freqeuncy bands can be exploited to meet capacity requirments ranging Gbps with adequate link level performance in terms of bit-error-rate. Efficient PHY-layer waveform design is vital to overcome propagation issues associated with mmWave as a robust waveform should be able to cope with extreme environmental conditions. For LOS BH application, time-hopping impulse radio (TH-IR) is proposed in

the presence of hardware imparments whereas for NLOS case a more robust transmission scheme based on space time shift keying (STSK) is proposed. STSK technique provides diversity and multiplexing gains in conditions where multipath channel fading is severe and hardware impairments are significant.

Future networks are fully reconfigurable. Several infrastructure gains are expected from software defined radio (SDR). For example, to improve network performance, the operator will reconfigure its network by adding additional functionalities to the already deployed network. SDR makes this reconfigurability easy and will become an enabler for terminal and network reconfigurability through software download. Network reconfigurability will be ground breaking developement in smart city context. In case of extreme conditions (e.g., floods, festivals, etc), the operator should be able to reconfigure the network to cope with the needs of the situation. Such reconfiguration should be fast and flexible, and will be playing vital role in smart city where rich applications are being conceived with different requirements. To verify such claims, futuristic strategies should be tested in Lab over hardware to see performance in a realistic environment. An SDR-based cooperative relaying conceiving LTE-A downlink. By simply changing the software (Relay or not to relay), improved link performance through coverage extension is made possible in case of relaying. Another SDR-testbed developement based on uplink CoMP for LTE-A systems is under testing. The aim is to see how network reconfigurability achieves better performance w.r.t conventional systems in LTE-A uplink.

1.4 Research Contribution

The research from this Ph.D work has been publish in international conferences and journals. The work presented in chapter 2 related to small cell technology in the framework of smart city has been presented in one journal paper:

- Cimmino, Antonio, et al. "The role of small cell technology in future smart city applications." *Transactions on Emerging Telecommunications Technologies* 25.1 (2014): 11-20.

Physical layer transmission schemes for efficient LTE-A uplink in section 3.1 has been presented in one conference paper:

- T.F. Rahman,; C. Sacchi,; C. Schlegel, "Link performance analysis of cooperative transmission techniques for LTE-A uplink," in 2015 *IEEE Aerospace Conference*, vol., no., pp.1-8, 7-14 March 2015

The work related to Constant envelope SCFDMA in section 3.2 has been presented in one conference paper:

- R. Mulinde,; T.F. Rahman,; C. Sacchi, "Constant-envelope SC-FDMA for nonlinear satellite channels," in 2013 *IEEE Global Communications Conference (GLOBECOM)*, vol., no., pp.2939-2944, 9-13 Dec. 2013

The low complexity minimum conditioned BEP (MCBEP) receiver discussed in section 3.3 has been accepted for an upcoming conference:

- T.F. Rahman,; C. Sacchi,"A Low-complexity Linear Receiver for Multi-User MIMO SC-FDMA Systems," *Accepted* in 2016 IEEE Aerospace Conference.

Line of sight wireless backhaul based on TH-IR techniques of section 4.1 has been presented in one conference paper:

- T.F. Rahman,; C. Sacchi; C. Stallo, "MM-wave LTE-A small-cell wireless backhauling based on TH-IR techniques," in 2015 *IEEE Aerospace Conference*, vol., no., pp.1-9, 7-14 March 2015

Non line of sight wireless backhaul based on STSK in section 4.2 has been under review in one journal:

- T.F. Rahman,; C. Sacchi; M. El-Hajjar,; L.Hanzo, "Space-Time MIMO Techniques for Millimeter Wave NLOS Backhaul in Dense Urban Environment," *Under Review* IEEE Transactions in Communications.

SDR based cooperative relaying in LTE-A downlink of chapter 5 has been presented in one journal paper:

- P. Atungire,; T.F. Rahman; F. Granelli,; C. Sacchi, "Open-field emulation of cooperative relaying in LTE-A downlink using the GNU radio platform," in *IEEE Network*, vol.28, no.5, pp.20-26, September-October 2014

1.5 Structure of the Thesis

This thesis consists of six chapters. The outline of each chapter is as follows.

Chapter 1, gives an overview of the motivations, problem statement and proposed solutions. Moreover, it also includes research contribution and outline of this dissertation.

Chapter 2 discusses the state-of-the-art related to small-cells and LTE-A in the framework of smart city. Moreover, PHY-layer aspects are dealt for LTE-A in the form of transmission, detection, and backhauling. Then state-of-the-art related to SDR-based reconfigurability is discussed in LTE-A framework.

Chapter 3 discusses the uplink cooperative communication in small cell LTE-A networks. Also minimum conditioned BEP (MCBEP) is discussed. Lastly, CE-SCFDMA is highlighted for 5G cellular communications in the chapter.

Chapter 4 is related to wireless backhauling in small cell LTE-A where TH-IR techniques are studied for LOS case and space time MIMO techniques are considered for NLOS case.

Chapter 5 deals with SDR implementation of cooperative relaying in LTE-A downlink.

Chapter 6 draws the conclusions and shed some light on future works.

Chapter 2

Smart cities, small cells, current 4G standards

Smart city as defined in wikipedia [97], "*A smart city uses digital technologies or information and communication technologies (ICT) to enhance quality and performance of urban services, to reduce costs and resource consumption, and to engage more effectively and actively with its citizens*". The Smart City paradigm is a vision for future cities centered around the concept of connectivity. Indeed, connectivity is the core requirement for Smart Cities to exist, enabling tight integration among citizens, devices and service providers. However, it is also a mean for interoperable access and interconnection among different services.

2.1 Smart city: communications and networking aspects

An interesting example of cooperative model, targeted at supporting the creation of innovative services and applications with real value of economy and citizens, is proposed by the consortium of EU OUTSMART project [6]. The OUTSMART model is based on a stakeholders' triangle whose vertices are represented by citizens, utilities and cities, shown in Fig 2.1:

- *Citizens* are the main beneficiaries of smart cities. Smart cities are to provide citizens with smart services in order to enhance their quality of life. Moreover, citizens shall be empowered with more control for resource management by collaborating in economical and environmental issues.
- *Utilities* are what citizens can be benefitted from. Generally speaking, utilities can be classified in two entities: service providers and network providers. Service providers are responsible for providing services to the citizens or to a smart city at large.

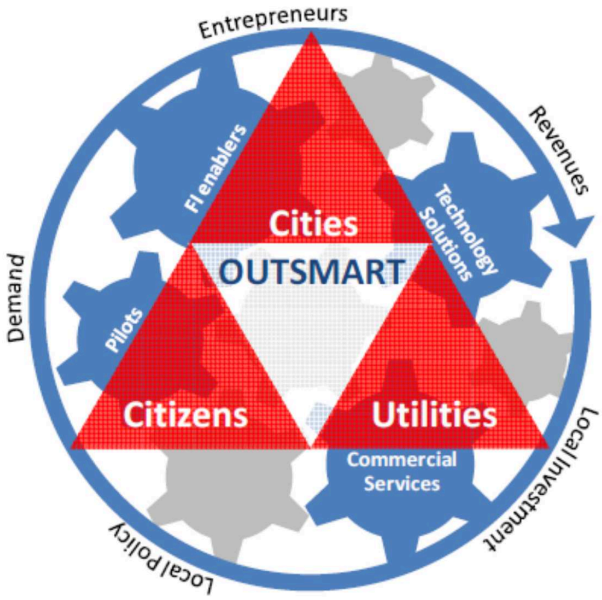

Figure 2.1: Smart City Ecosystems [6]

Network providers take care of network infrastructure that enables services. Their aim is to allow utility companies to improve the management of their resources: optimization of resource distribution, prevention of resource outages, easy and rapid maintenance actions, etc. Besides this, utility providers will benefit from the new environment, becoming able to develop and deploy added-value network-facilitated services for users. This will simplify and accelerate service delivery, reducing the operational costs and enhancing a faster return of investment. The collaborative ecosystem and interactions will make services tailored for customers specific needs and preferences.

- *Cities* are constituted by its inhabitants. With the increase in urban population, citizens are facing numerous problems in every aspect of their life e.g. security, pollution, traffic congestion, infrastructure maintenance, asset management, etc. Hence, this has put a question mark on facilitating general population with adequate quality of life. There exists a interacting relationship between citizens and the city environment

such that citizen adapt according to the environment they living in. So much effort has been made to closely monitor the environment in real-time through the use of networked sensors and actuators deployed in the city and take actions according to varying environment. These actions can be taken without or with minimum human intervention. With this, city municipale are able to provide the better lives to its citizens.

In the model described above, ICT and, in particular, wireless networking play a key role to transform city into "smart city". Indeed, ICT is fully capable of providing added-value services to users.
Some recent work has been done in this regard in which ICT is incooperated into the framework of smart cities. In [38] a smart city testbed, named SmartSantander (related to the Santander city in Spain), is presented. The aim is to deploy a network of sensors in order to keep a track on environmental changes and tailor human lives accordingly. The application considered is related to distributed environmental monitoring using wide-area WSNs based on IEEE 802.15.4. In [45] a testbed is presented targeting at ubiquitous computing and operational in Oulu, Finland. A middleware layer has been added on top of Oulu metropolitan WiFi access network in order to allow ubiquitous computing with sensing and communication resources embedded in urban elements. A cloud architecture for smart cities based on near field communication (NFC) technology is proposed in [110]. All these solutions, in [38], [45], and [110], are based on local area networking infrastructures, providing hot-spot rather than ubiquitous broadband connectivity. Broadband connectivity available anytime and anywhere will be one of the key requirements of future intelligent cities, where people will not only be connected to others but also keep themselves up-to-date through interactive services. According to survey conducted by ABI research [2], in which it is shown that a population of 1.4 billion and counting own a smart phone or gadget. Consequently, the user data rate requirement will be immense resulting the need for ubiquitous broadband connectivity in smart cities.

Long term evolution advanced (LTE-A) is an emerging set of standards and technologies that will be able to provide wireless-data payload at the speed of Gbps. ICT in smart city can leverage LTE-A for the provisioning of broadband connectivity. Small cells are already considered as an enabler due to their lower energy consumption and broadband coverage capacity (see [52]). Some recent works (e.g., [25]) have already considered the integration of macro, micro and small cells with the aim of building service platforms for Smart Cities.

2.1.1 Communication requirements in future smart cities

Looking at the retrospect of internet one would realize that how slow the evolution was as first Advanced research projects agency network (ARPANET) took around twenty two years to evolve into world-wide web (WWW) development. One of the major reason of such slow evolution was unmaturity of electronic industry when transistors were vaccum-tube. Anyhow evolution of technology has taken a rapid pace over the years thanks to high speed computing helping in solving science and engineering problems rapidly. Surely, future services and intentions will take less time to be finalized, since prerequisites are already available. Likewise the anticipated services for smart cities will quickly be come into existence thanks to the existed infrastructure that is operational in cities. For instance, optical fibre or copper cables used by service providers to deliver internet access to the citizens as well as 3G/4G cellular infrastructure for mobile users. After mentioning the pros of already deployed infrastructure in the context of future smart cities, the constraints like, integration of some communication facilities hindered by local regulations or ownership, or by architectural issues, could also pose a challenge to speedy roll out of smart city features.

Moreover, it is believed that internet of things (IoT) could possibly be the "killer application" that will drive the explosion and growth of smart city concept. Based on IoT several testbeds are functional providing services for community in general (like, public transport, street lights, etc.) or citizen (e.g., parking services, smart metering etc.). More recently, the concept of 'Big data' has been integrated in to smart cities where huge amount of data is put to use to analyse to reveal patterns, trends, or associations related to human behaviour and interaction. Some recent examples of 'Smart' cities (Singapore, Rio de Janeiro, etc.) are focusing on big data services considering integration and processing of huge amount of data generated by heterogeneous sources (e.g. weather, traffic conditions, crimes, best routes across the city, etc.) but the offered services are rather traditional. As a result, the pattern of traffic at network level is extremely uncertain. Hence designing and dimensioning of a proper communication infrastructure should be a challenge. Such communication infrastructure would be capable of adapting to the needs of fluctuating and ever-changing scenario. The possible requirements of future communication and networking are:

1. *Interoperability*, future communication infrastructure should allow to connect all possible data sources through global content provider (e.g, Cloud computing) to support new services.

2. *Scalability*, the communication and networking infrastructure in a smart city should provide flexible use of bandwidth and scalable performance that can easily be up-

graded with time as the number of population and services grow.

3. *Fast deployment* of an infrastructure is desirable favouring less bulky and easy-to-install machinary. Such an infrastructure can be deployable in case of big events like, earth quake affected areas, flood relief activities, etc.

4. *Robustness* of an infrastructure should be guaranteed to order to be assured availability of smart city services even in extreme conditions.

5. *Limited power consumption* is a challenge in future smart cities as communication infrastructure should have minimal impact on environment and low power consumption to minimize operating and management costs.

6. *Multi-modal access* allows inhabitant of smart city to access services using single wireless terminal. Access to Smart City services should follow the AAA principle: Any-time, any-where, any-device.

LTE-A (4th generation, 4G) solution to these aforementioned issues could be technological breakthrough. Evolution of telecommunication standards doesn't stop at 4G rather continues to evolve into further releases (5th generation, 5G). 5G has promised to address a broader range of applications with requirements such as, energy efficiency, cost effectiveness, easy deployement etc., that are still to be addressed. Therefore, latest release of LTE-A 3GPP Rel-13 has introduced small cell technology together with innovative solutions and strategies to target future requirements.

2.2 Small cell LTE-A technology

Small cell technology has been seen in the framework of LTE-A (4G) in recent release of 3GPP because of the fact that beyond 4G technologies are relying on small cells due to numerous advantages (e.g., proper coverage, spectral efficiency, power efficiency etc.). In the LTE-A perspective, a small cell is a low-power, low-cost, and less bulky radio base-station, whose primary design target is to provide superior cellular coverage in residential, enterprise and hot-spot outdoor environments. Four main typologies of small cells have been identified in [21]:

- *Pico-cells*, smaller, lighter base-stations that plug directly into an operator core network;
- *Femto-cells*, smallest, and user-deployed base-stations mainly for indoor converage;
- *Trusted WLAN cells*, integrated into the LTE-A system;

- *Relay nodes*, that have been primarily defined in LTE Release 10/11 in order to extend the macrocell coverage or fill a coverage hole.

The desire for innovative services going beyond the simple internet connectivity requires broadband links that can be provided with the help of small cells. High capacity links are inherent to smaller coverage areas. For this reason, small cells will play a key role in a new standardization perspective.
Femtocells, which initially came to market in 2007 and were standardized in 3GPP Rel-8 in early 2009 (HSPA framework) [66], represent a feasible solution to improve indoor and short-range coverage. Femtocells do not only improve spectrum efficiency and throughput, but also enable quick traffic off-loading from macro cellular networks. [19] discuss femto cells deployment and their contribution in enhancing system rate. It has been shown that regardless of the typology of femto cell deployment, closed-access or open access, system throughput can be increased. As a consequence of instinctive femtocell deployment, interference from macro to femto can not be ruled out. The high cost of the femtocellular systems made them not competitive with Wi-Fi access technologies. Hence, femtocells can not be seen as fitting solution to meet futuristic demands of smart cities. Therefore small cells should be seen as a general plug-play, as studied by Liu, Wu, and Koh in [72].

Outdoor small cells are usually operator-deployed BSs in order to complement macrocell BSs e.g., in terms of coverage enhancement and system throughput. However, small cells can also be deployed without macro coverage without prior planning. Due to outdoor setup, a flexible cooperative system level structure can be realized aiding to achieve ambitious goals of broadband connectivity, see Fig 2.2. For this reason, LTE-A release-13 has focused on the enhancement of outdoor small cells. In [49] the authors highlight factors that are responsible for CO_2 emission in cellular networks and then propose techniques to minimize such emission and cost related to cellular networks. Indeed, base stations produce high amount of CO_2 emission in cellular network due to heavy equipment installed and air-conditioning system. Power amplifers consumes around 50 % of energy, of which 80-90 % of energy is wasted as heat. Air-conditioners are required to avoid over heating of PAs. The authors propose sleep mode protocols to reduce energy waste in PAs under no traffic load. Literatures have shown that renewable energy source is more eco-friendly, and less costly as compared to diesel or other carbonized fuels. Hence it is proposed that small cells located in rural areas can be functional using renewable energy (e.g., solar energy). In [114], an adaptive network architecture is proposed in which overlaid small base stations can be switched off if traffic load is light. Because of their short-range coverage, small BSs do not require high-rise towers and can be mounted on street light poles, building side walls, etc. This signifies environmentally friendly behaviour of small cells. [48] gives an overview about trade-off among capacity, energy and cost. It shows that small

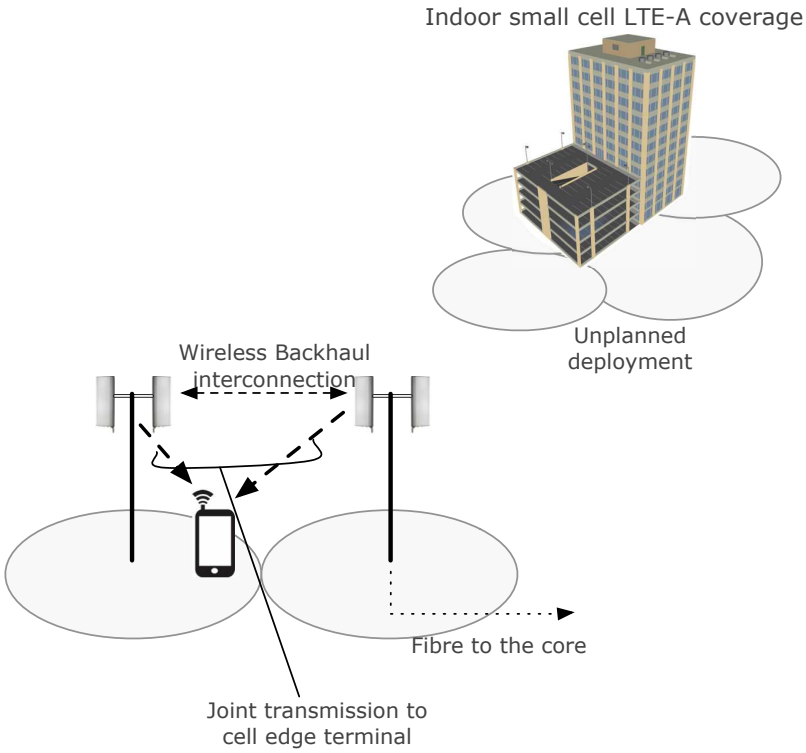

Figure 2.2: LTE-A small cell technology at a glance

cells deployment can consume 30% less energy than macro cells but small cells incur cost, which is 14% more than that of macro cells. According to authors, this is due to backhaul cost for small cells. But providing wireless multi-hop connections among small cells BSs, the cost can be reduced. In [53], concept of green outdoor small cells is conferred. After some realistic assumptions, simulation results have shown that small cells are capable of meeting future demands in economical and ecological way. Small cells in the form of Wifi access points, 3G/4G small cells and micro cells can ease the burden on macrocells (big cells) by offloading mobile traffic [36]. It has been shown that small cells in these forms can provide better quality of service, support to new revenue-generating services and better coverage provided that issues like deployment of small cells, interference management, geo-location of hotspots, backhaul and deployment cost are to be resolved. A similar work in [25] has considered the heterogenous network (HetNet) with the aim of building service platforms for smart cities. A detailed description on ICT involved in smart city applications has been given where it is highlighted that LTE-A with HetNet communication infrastructure can meet goals by providing broadband services in smart cities. More recently in [26], where the role of small cell technologies in smart city applications has been discussed. The authors relied on LTE-A small cell technology to meet demands of

smart city as in the Fig. 2.3. Some technological challenges associated with LTE-A in

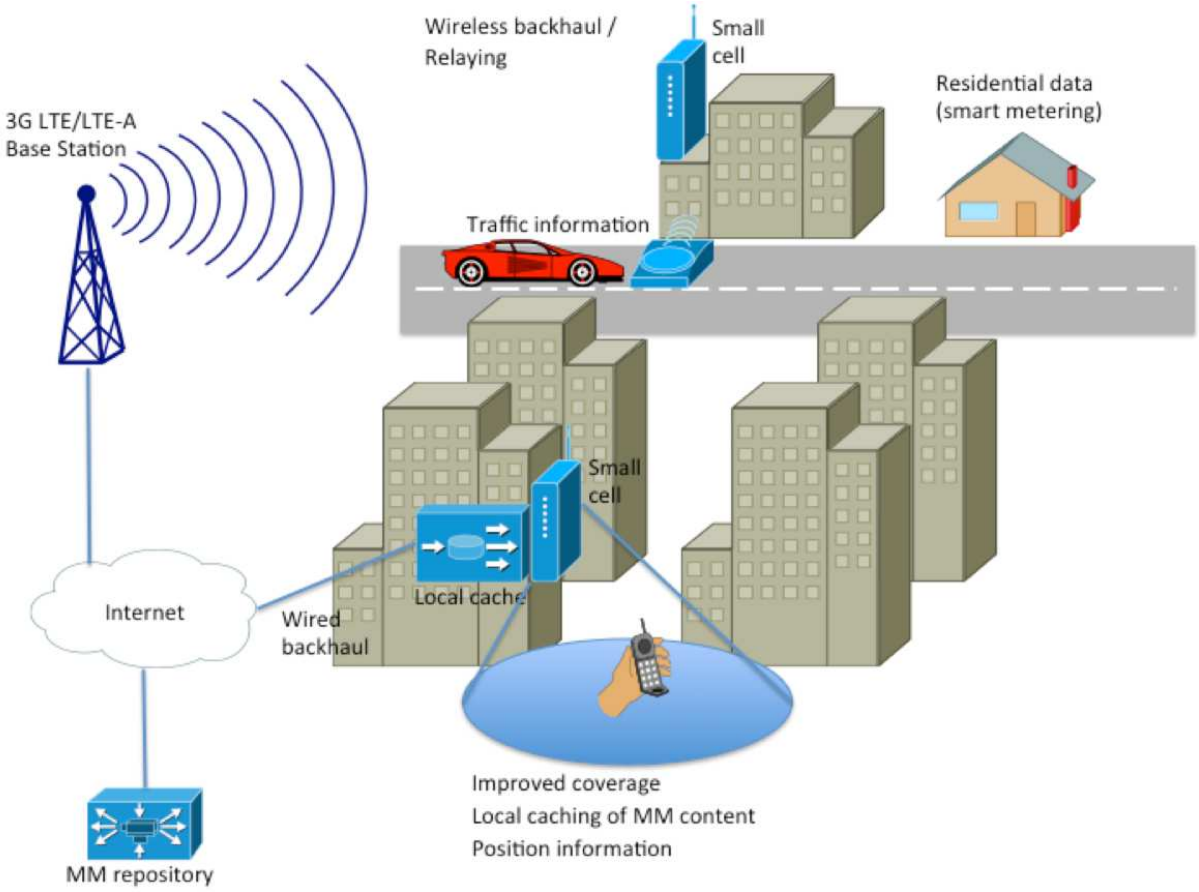

Figure 2.3: Small cell Architecture with possible applications in Smart City [26]

smart city context are mentioned in [26] that should be resolved. These challenges are:

- *Machine-to-machine communication* covers a wide range of applications from massive deployment of low-cost limited-power sensors to remote-controlled utility meters and cameras. Such low powered devices may not be transmitting large amount of data at once but connectivity to the network could be a huge challenge for the core network.

- *Security* of citizens' data is of paramount importance in smart city. The system framework should be able to detect any malicious devices and guarantee the "*safety*" of citizen's privacy.

- *Efficient spectrum utilisation* is desired in smart city applications where wireless resources are to be shared among many consumers. Cognitive radio technology enables the adaptivity in network that allows the exploitation of radio resources in an efficient manner.

- *Backhauling* in small cells is vital in the sense that wired backhaul solution will not be feasible from cost viewpoint. Wireless backhaul solution would be better choice if the provision of gigabit/sec datarate is guaranteed.

Small cells due to their smaller radio footprints are considered as environment friendly and can occasionally be turned OFF and ON depending upon the traffic. Hence, energy saving, economical and quick deployment make them favourite for smart cities applications.

2.3 Physical layer (PHY) solutions for LTE/LTE-A

The two widely deployed 2G cellular systems i.e. GSM and CDMA separately evolved to two different 3G technologies though ITU-Rs 3G intention was to come up with a single wireless cellular system to be deployed worldwide. Now a days, GSM and GSM family systems are widely deployed covering more than 89% of the global mobile market as of February 2010 [104]. Backward compatible technologies were required to extend current services with seamless integration to the new one. In order to meet current traffic growth demand, extensive efforts are currently in progress in 3GPP group to develop new standard for the evolution of GSM/HSPA technology towards a packet-optimized system. The main goal of the group is to define standards to provide higher data rates, low latency and greater spectral efficiency. The first packet switched mobile technology introduced by the group is known as Long-Term Evolution (LTE). Aggressive spectral efficiency targets for LTE system have achieved three to four times higher efficiency than the previous systems [51]. High spectral efficiency is achieved using new advanced radio interface techniques. In LTE low-PAPR SC-FDMA for uplink and OFDMA for downlink access are used. LTE also introduces MIMO antenna technologies, advanced inter-cell interference mitigation techniques, low latency channel structure by reducing the number of nodes in the access network and single-frequency network (SFN) broadcast technique. In the later releases of the group i.e. release-10 and beyond, 3GPP introduced LTE Advanced (LTE-A) system that exceeds IMT-A system requirements. LTE-A significantly enhances LTE Release-8 and supports much higher peak rates, higher throughput as well as coverage area and lower latencies which in turn result in a better user experience. LTE provides high data rate, low latency and packet optimized radio access technology supporting flexible bandwidth deployments [7]. A new network architecture is designed for LTE system to support packet-switched traffic with seamless mobility, quality of service and minimal latency [8]. LTE physical parameters and air interface attributes are summarized in Table 2.1. The system supports flexible bandwidths benefited from OFDMA and SC-FDMA

Parameters	Link	Specifications
Bandwidth		1.4, 3, 5, 10, 15, 20 MHz
Duplexing		FDD, TDD, Half duplex FDD
Mobility		350 km/hr
Multiple access	Uplink Downlink	SCFDMA OFDMA
MIMO	Downlink Uplink	2x2, 4x2, 4x4 1x2, 1x4
Peak data rate in 20MHz	Downlink Uplink	172.8 and 326.4 Mb/s for 2 x 2 and 4 x4 MIMO, respectively 86.4 Mb/s with 1 x 2 antenna configuration
Modulation		QPSK, 16-QAM and 64-QAM
Channel coding		Turbo coding
Other techniques		Channel sensitive scheduling, link adaptation, power control, ICIC and hybrid ARQ

Table 2.1: LTE system radio interface attribute

multiple access schemes. In addition to FDD and TDD, half duplex FDD is allowed to support low cost User Equipments (UEs). Though the system is primarily optimized for low mobile users of speed up to 15Km/hr, the system also supports user mobility up to 350Km/hr with acceptable performance degradation. The system supports downlink peak data rates of 326 Mb/s with 4x4 MIMO antenna configuration within 20MHz bandwidth. Since uplink MIMO is not employed in the first release of the LTE standard, the uplink peak data rates are limited to 86 Mb/s for 20MHz bandwidth. LTE system provides higher spectral efficiency relative to previous systems. Similar improvements are observed in cell-edge users throughput as well as packet transmission latency from UE to the network.

Radio Interface Techniques: OFDMA & SC-FDMA

In the wireless standards of GSM family before LTE, Wide-band Code Division Multiple Access (WCDMA) within 5MHz is used as a radio interface for both uplink and downlink. Due to the presence of multi-path propagation effect which is inherent in wireless communication, the walsh codes used are no longer orthogonal and interference with each other result in Inter-Symbol Interference (ISI). In WCDMA systems, the impact of multi-path can be overcome using advanced receivers which come at the expense of receiver complexity. Multi-path interference problem of WCDMA based systems escalates for larger bandwidths such as 10MHz and 20MHz required by LTE for the support of higher data rates. The chip rate increases for large bandwidth and receiver complexity grows as well

due to increase of multi-path intensity. In addition, it is difficult to implement a system with flexible resource allocation using WCDMA system yet LTE requires the support of smaller bandwidth less than 5MHz. As a result new multiple access schemes are introduced in LTE: OFDMA in downlink and SC-FDMA in uplink. The generic block diagram of OFDMA and SC-FDMA is shown in Fig 2.4.

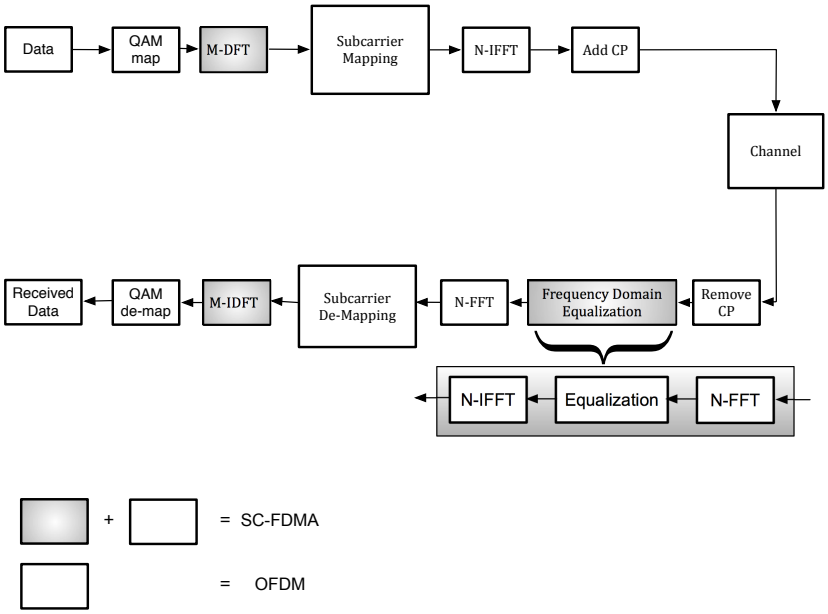

Figure 2.4: Small cell Architecture with possible applications in Smart City

Orthogoanl frequency divison multiple access (OFDMA)

It is simply the multi-user version of the popular OFDM digital modulation technique. Multiple access is achieved in OFDMA by assigning a group of sub-carriers to each individual users. The basic principle of OFDM is to divide the available bandwidth into narrow band parallel channels known as sub-carriers, and information/symbol is transmitted using these channels at a reduced rate. The advantage is to let each channel experience almost flat-fading and simplify the channel equalization process at the receiver. In addition, the frequency response of the channel is overlapping and orthogonal which enhance spectral efficiency. In practice, the orthogonality between carriers can be lost when the signal passes through time-varying channel due to inter-OFDM symbol interference. Cyclic prefix (CP) is introduced used to overcome this challenge. A scalable OFDM transmission/multi-access technique is used in LTE-A downlink that allows high spectrum efficiency by utilizing multiuser diversity in a frequency selective channel. Some of the advantages of OFDM with cyclic prefix are:

- OFDM is efficient in combating the frequency selective fading channel with a simple frequency domain equalizer which makes it a suitable technique for wireless broadband systems such as LTE/LTE-A.
- It is possible to exploit frequency selective scheduling with OFDM-based multiple access (OFDMA) that has a big difference especially in slow time-varying channels.
- The transceiver structure of OFDM with FFT/IFFT enables scalable bandwidth allocation with a low complexity.
- As each sub-carrier becomes a flat fading channel, compared to single-carrier transmission, OFDM makes it much easier to support multi-antenna transmission. This is a key technique to enhance the spectrum efficiency and reach high data rate.
- OFDM enables multicast/broadcast services on a synchronized single frequency network (MBSFN), as it treats signals from different base stations as propagating through a multipath channel and can efficiently combine them.

In LTE specifications, the size of an elements in the time domain is expressed as a sampling time $T_s = 1/(\Delta f \times N_{FFT})$ where Δf is sub-carrier spacing, and N_{FFT} is the size of FFT in the system. As the normal sub-carrier spacing is defined to be $\Delta f = 15KHz$, T_s can be regarded as the sampling time of an FFT-based OFDM transmitter/receiver implementation with FFT size of NFFT (from 128 upto 2048 depending on transmission bandwidth). For 20MHz bandwidth, as an example, T_s becomes $Ts = 1/(15000)$ sec. The sampling frequency, which equals ($\Delta f \times N_{FFT}$, is a multiple or sub-multiple of the UTRA/HSPA chip rate of 3.84MHz. In this way, multi-mode UTRA/HSPA/LTE terminals can be implemented with a single clock circuitry. In addition to the 15kHz sub-carrier spacing, a reduced sub-carrier spacing of 7.5kHz is defined for MBSFN cells that provides a larger OFDM symbol duration in order to combat the large delay spread associated with the MBSFN transmission. In time domain, the downlink and uplink multiple Transmission Time Interval (TTI) is organized into radio frames of duration $T_f = 10ms$. LTE supports both TDD and FDD duplexing [44] methods to support terminal complexity and increase design reuse between both systems. Thus LTE uses two different frame structures for these duplexing techniques.

1. The first frame structure type is used for both half-duplex and full-duplex FDD with three different kinds of units. The smallest one is called slot, and its duration is $T_{slot} = 15360 \times Ts = 0.5ms$. Two consecutive slots are defined as a sub-frame of length 2 slots and radio-frame of 20 slots which are 1ms and 10ms in duration respectively. Channel-dependent scheduling, and link adaptation operate on a sub-frame level. Therefore, the sub-frame duration corresponds to the minimum downlink

TTI of 1ms duration. A shorter TTI is for fast link adaptation and is able to reduce delay. It also helps to better exploit the time-varying channel through channel-dependent scheduling. Each slot consists of a number of OFDM symbols with CP (6 symbols for extended CP and 7 symbols for normal CP). For sub-carrier spacing of $\Delta f = 15KHz$, OFDM symbol duration is $1/(\Delta f)$. In FDD uplink and downlink transmissions are separated in the frequency domain each with 10 sub-frames.

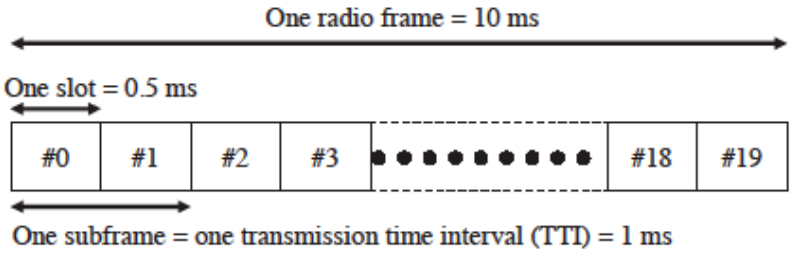

Figure 2.5: LTE FDD frame structure (Type-1 frame) [44]

2. The second frame structure type is for TDD duplexing method. It is designed for coexistence with legacy systems such as the 3GPP TD-SCDMA-based standard. Similar to FDD frame structure, the radio frame for TDD is also 10ms in length which consists of two half-frames of length 5ms each. Each half-frame is divided into five sub-frames with 1ms duration. There are special sub-frames, which consist of three fields: Downlink Pilot Time Slot (DwPTS), Guard Period (GP), and Uplink Pilot Time Slot (UpPTS) yet the total length of these three special fields has a duration of 1ms. These fields are already defined in TD-SCDMA and are maintained in the LTE TDD mode to provide sufficiently large guard periods for the equipment to switch between transmission and reception.

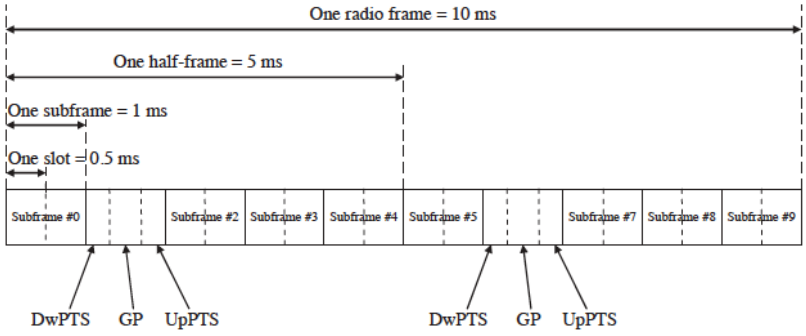

Figure 2.6: LTE TDD frame structure (Type-2 frame) [44]

Single carrier frequency domain multiplex access (SC-FDMA)

It is basically FDMA scheme that deals with the assignment of multiple users to use shared communication resource. SC-FDMA can be considered as linearly precoded OFDMA as it uses addition DFT processing preceding the OFDMA processing. The feature that distinguishes SC-FDMA from OFDMA is the "single-carrier" form of transmit signal. Subcarrier mapping can be achieved using either localized mapping or distributed mapping. Localized mapping is considered for LTE standard because of ease of implementation of such mapping technique with standard frame structure. SC-FDMA is implemented in the uplink communication of LTE due to lower peak-to-average power ratio (PAPR) that greatly enhances mobile terminal transmit power efficiency and reduce the cost of transmitter power amplifier. Indeed SC-FDMA with a CP is adopted in practice for uplink transmission to combat the multi-path propagation environment.

Since the input data stream is blended in frequency domain that results in higher complexity of SC-FDMA receiver which, however is not considered to be an issue in the uplink transmission since computational capability at the base station is eminent [44]. Radio resources in the uplink have resemblance with that of the downlink though only localized resource allocation on consecutive sub-carriers is allowed in the uplink yet limited number of MIMO modes are supported for mobile terminals transmit to base stations. The uplink frame structure is similar to that for the downlink. The minor difference is that now we talk about SC-FDMA symbols and SC-FDMA sub-carriers instead of OFDM symbols and OFDM sub-carriers. In frame structure type-1, a uplink radio frame consists of 20 slots of 0.5ms duration, and one sub-frame consists of two slots of (1ms duration similar to downlink transmission. Frame structure type 2 consists of ten sub-frames with one or two special sub-frames including DwPTS, GP, and UpPTS fields. A CP is inserted prior to each SC-FDMA symbol. Each slot carries seven SC-FDMA symbols in the case of normal CP and six SC-FDMA symbols in the case of extended CP.

2.4 MIMO technology for LTE/LTE-A

MIMO technology uses multiple antennas at transmitters and receivers to improve performance of a communication system as it offers significant increase in data throughput and link quality without additional bandwidth and increased transmit power. MIMO transmission and detections are broad topics that require seperate details for proper understanding.

2.4.1 MIMO transmission

MIMO operation literally includes spatial multiplexing, pre-coding and transmit diversity [51]. The very fundamental principle behind spatial multiplexing is the sending signals from two or more different antennas with different data streams and separating the data streams by advanced signal processing techniques at the receiver, hence increasing the peak data rates by a positive multiple factor (theoretically 2 for 2x2 and 4 for 4x4 antenna configuration). Open loop spatial multiplexing is a form of MIMO in LTE systems that involves sending information which can be transmitted over two or more antennas. However there is no feedback from the terminal but transmitter rank indicator (TRI) is transmitted from terminal that can be used by the base station to determine the number of spatial layers [17]. In contrast, close loop spatial multiplexing incorporates a feedback where terminal communicates pre-coding matrix indicator (PMI) with the base station through feedback link. This enables the transmitter to pre-code the data to optimize the transmission and enable the receiver to more easily seperate the different data streams [17].

LTE MIMO utilizes the transmission of the same information stream from multiple antenna to obtain transmit diversity. LTE supports 2-antenna or 4-antenna arrays for this technique. Using space-time or space-frequency block codes, information is coded at the transmitter to combat multipath channel effects. With such encoding schemes, signal quality improves at the receiver but the rate stays at unity. Hence transmit diversity strategies are not spectrally efficient but robust against channel impairments.

Closed loop pre-coding is another form of LTE MIMO where single codeword is transmitted over a single spatial layer. This can be seen as a fall back mode for closed loop spatial multiplexing and it may also be associated with beamforming as well.

The first release of the LTE system does not support single-user MIMO spatial multiplexing in the uplink. However, multi-user MIMO (MU-MIMO) operation where two UEs are scheduled on the same resource blocks in the same subframe is permitted in the latest release of LTE. Multiple receive antennas give eNBs degrees of freedom to separate signals from the two UEs by using techniques such as Minimum mean square error (MMSE) algorithm. The multi-user MIMO operation in the uplink can improve over all cell capacity and significantly enhance cell edge users throughput [115].

2.4.2 MIMO detection techniques

The promise of high data rates in the LTE-A systems can be fulfilled by use of MIMO configuration in both UL and DL. In order to support general MIMO systems, several receiver designs are proposed for SC-FDMA and OFDMA systems with linear and non-

linear complexity. In this section only SC-FDMA receiver design will be discussed. The optimal solution for single carrier (SC) systems has often high computational complexity that is nearly impracticable. [40] derives the optimal maximum liklihood (ML) bounds for single carrier FDMA systems that are applicable for general SC systems for correlated and uncorrelated rayleigh channels. In order to have reduced complexity and near optimal performance in SC-FDMA systems, a suboptimal approach is considered in [84] where minimum mean square error (MMSE) based ML detection is proposed. MMSE estimation is done prior to ML and improves the detection process. The proposed algorithm of [84] has shown significant improvement over conventional MMSE detetor but complexity of such algorithm is still high due to ML operation. A modified frequency domain linear equalization is proposed for MIMO SCFDMA systems in [70] with analytical SINR expressions. It is shown that performance of proposed technique is improved w.r.t MMSE for improper modulation techniques.

In another work [54], decision feedback equalizer (DFE) is proposed in the context of SCFDMA that outperforms linear equalizers. However, computational complexity of such equalizers is significant as compared to linear equalizers. Iterative multiuser detection is another interesting way to detect MIMO signals at the receiver. SC-FDMA with iterative multiuser detection is studied in [119] where multiuser interference (MUI) is randomized using user-specific interleavers and is cancelled out using frequency domain equalization afterwards.

All previous mentioned techniques aim at maximization of output SINR that might not reach optimality. Rather maximization of SINR, direct minimization of bit-error-rate (BER) results in performance improvement. Linear equalization based on minimum bit error rate (MBER) for OFDMA systems is proposed in [14] where it is shown that MBER based on steepest descent outperforms MMSE (based on maximization of SINR). MBER techniques are iterative strategies (gradient descent, genetic algorithms, etc) for finding the filter weights that minimizes the MBER solutions. [13] shows similar work as [14] where genetic algorithm is employed to find MBER solution. The complexity of MBER based detectors is exponential with the number of transmitting antennas. The complexity can be reduced by minimizing the conditional probability of error that is linear to the number of transmitting antennas [30] at the expense of performance. The authors in [30] present MCPOE detector for MC-CDMA systems where the performance is comparable to MMSE detector with reduced computational complexity. Sacchi et al. in [33] considered MCPOE approach STBC MC-CDMA systems where performance of MCPOE outperforms adaptive LMS-based MMSE and MMSE strategies.

2.5 Cooperative MIMO in LTE-A

In early stages, LTE included full support of single user MIMO for downlink using a maximum of four antenna ports and four transmission layers. It also has basic support for MU-MIMO in the downlink. Later in Release 9, dual layer beamforming is introduced to enable eNBs transmit to two receive antennas that can be located on one or two mobiles. As part of release 10, dual layer beamforming technique is extended to provide full support for downlink MU-MIMO by increasing the maximum number of base station antenna ports to eight; that is, 8x8 MIMO antenna configuration technique is introduced. The technique for single user MIMO (SU-MIMO) support is achieved by utilizing the eight antennas with the help of eight layer transmission method. This enables the network to choose between single-user MIMO when the channel is uncorrelated (maximize single UE data rate) and multi-user MIMO in correlated channel condition (maximize overall cell throughput). Also in LTE-A, the uplink is enhanced to support single-user MIMO using up to four transmit antennas and four transmission layers reaching a data rate of 600Mb/s in the uplink in release 10.

Peak data rate and cell-edge user throughput can be enhanced greatly by the help of Relaying and Coordinated multi-point (CoMP) that are newly introduced to LTE-A standard. Below we shed some light on these techniques in the context of LTE-A.

2.5.1 Relaying in LTE-A

Relaying is a vital method introduced in LTE-A to extend mainly the coverage area of a cell. Relaying increases the data rate at the edge of a cell, by improving the signal to interference plus noise ratio (SINR). In general, relays provide coverage in new areas, facilitate temporary network deployment, enhance cell-edge throughput, achieve coverage of high data rate, and improve group mobility to the system [1]. Relaying can be accomplished with the help of low cost and light weight radio control units as complex signal processing is not done at relays. Mobile UE can also be seen as relay nodes however a proper relay with high antenna gains, larger transmitter and better receiver serves the purpose appropriately [65]. It has been shown that relaying helps in low SNR conditions that is case for cell-edge users. Hence relaying provides capacity gains and range extension under specific conditions. Relay selection is not trivial in a scenario where number of relays are large. An isolated relay selection and power allocation scheme for cooperative networks is considered in [61]. A heuristic algorithm is presented to find near optimal relay assignment and power allocation when users are supported by only single relay. Optimal solution is not possible with this approach due to isolated design approach. [11] discusses this relay selection together with radio allocation for multi-user OFDMA networks. Op-

timal schemes are presented with polynomial computation complexity. However, through sub-optimal techniques of relay selection with radio allocation, quality of service (QoS) can also be guaranteed in the system [11].

The improvements due to relaying technique can be grouped into two: coverage extension and throughput enhancement advantages. The overall cost of a relay is usually less than that of an eNB due to reduced hardware complexity. Relaying can minimize the power consumption of overall network due to location of relay that is closer to UE. Energy efficient relay selection rule in cooperative network is discussed in [75] where it is shown tha optimal cooperative-relay schemes can outperform non cooperative ones in terms of energy efficiency. In another work, an energy efficient channel dependent scheduling is proposed for multi-user SCFDMA uplink systems in [120]. With different relaying strategies discussed in [120], significant gains can be attained in case of high shadowing environment over non-cooperative scenario.

Both inband and outband relaying can be conceived, where in former same frequency band is used by RN and eNB, and different frequency band is used by the two in latter case. In [69] Li et al. investigated the radio resource allocation for heterogeneous networks with cooperative relaying, where the relay nodes (RNs) with in-band backhaul act as micro base stations (BSs), able to serve the user equipment (UE) independently or cooperatively with the BSs.

2.5.2 Coordinated Multi-point (CoMP)

CoMP techniques can be seen as CoMP transmission for downlink (DL) coordination and CoMP reception for uplink (UL) coordination. For DL transmission, coordinated scheduling/beamforming (CS/CB) and Joint transmission (JT), as in Fig 2.7 are the most briefly studied cooperative techniques.

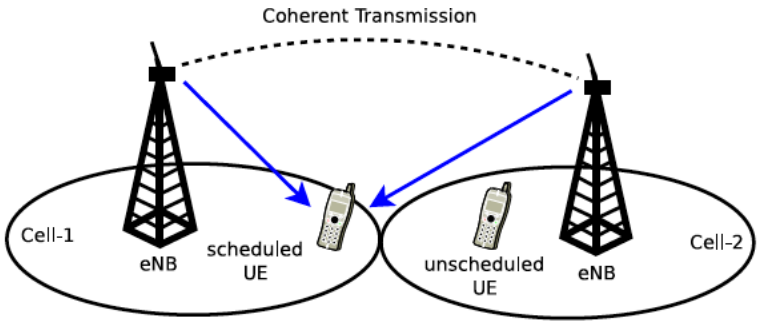

Figure 2.7: CoMP joint transmission in the downlink [67]

In the uplink, joint detection (JD) of the physical uplink shared channel (PUSCH)

is taking place, and various receiver diversity techniques is used at the central/serving eNB to maximize the received signal to noise ratio (SNR) [67, 10], as shown in Fig 2.8. Most of the CoMP techniques require sharing of some scheduling information regarding the users at different base stations. A very-low-latency links are required to exchange information between coordinated nodes on the order of milliseconds. As a result, two kinds of architectures are distinguished with respect to the way this information is made available at the different transmission points: centralized and distributed CoMP [24].

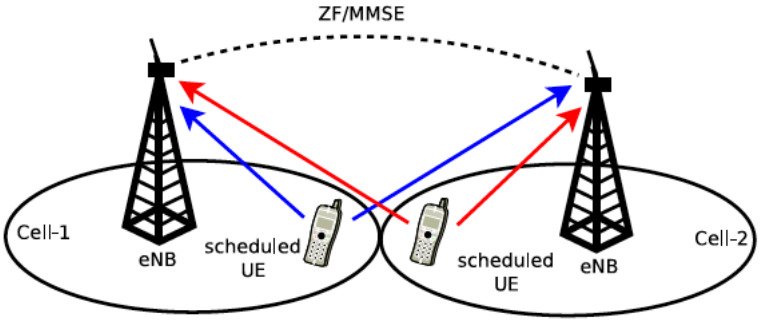

Figure 2.8: CoMP joint detection in uplink [67]

In a centralized approach, the central entity is needed in order to gather the channel information from all the UEs being served by coordinating eNBs, and the entity performs user scheduling as well as signal processing operations such as precoding. Whereas distributed approach is based on the assumption that schedulers in all eNBs are identical and channel information regarding the whole coordinating set can be available to all cooperating nodes. This method removes inter-eNodeB communication links and minimizes the infrastructure and signaling protocol cost associated with these links. A mixed architecture is also promising as they consider the advantages of both architectures and avoid the extreme solutions.

Coordination amongst eNBs (in uplink and downlink) can reduce inter-cell interference in cellular network and achieve considerable performance gain for both the average and the cell-edge user throughputs [109, 108, 57]. High capacity backhaul with low latency plays a key role in CoMP as information sharing has to be done between two eNBs. However, in practice backhaul represents a contrainst due to finite latency and link traffic. In [121], the authors discussed the performance of downlink BS cooperative transmission with limited capacity backhaul. The proposed transmission mode switching enables performance close to the optimal by sharing limited data through backhaul. Marsch and Fettweis in [76] considered a cooperative transmission modality very similar to the one assessed in [121], but used for an OFDMA uplink and subjected to two constraints: limited-capacity

backhaul (like in [121]) and non-ideal knowledge of channel state information (CSI). Results shown in [121] and [76] demonstrate the effectiveness of CoMP for next-generation mobile communications both in terms of inter-cell interference cancellation capability and capacity enhancement even under realistic operating conditions. Virtual MIMO (*aka* network MIMO) is another interesting application of cooperative communications, which is strictly related to CoMP. As stated in [41], multi-cell MIMO cooperation can literally exploit inter-cell interference by allowing users to be jointly processed by several interfering base stations. In [41], numerous applications of multi-cell cooperation are considered, namely:

- Interference coordination, based on the CSI sharing among different cells obtained via feedback channels. Such kind of coordination is targeted at interference cancellation;
- MIMO cooperation, where different cells share not only CSI, but also the full data signal of their respective users in order to exploit diversity;
- Rate-limited MIMO cooperation, based on limited sharing of CSI and allowing partial interference cancellation;
- Relay-assisted cooperation, based on the relay nodes assistance instead of direct cell backhauling.

It is clearly highlighted in [41] that MIMO cooperation is theoretically more powerful than the other kinds of cooperative models mentioned above. Indeed, MIMO cooperation would make the multi-cell network into a multi-user MIMO channel for which all propagation channels are exploited to improve system diversity and link capacity. However, in order to make feasible MIMO cooperation, eNBs should be linked by high-capacity and delay-free links.

2.6 MmWave communications in LTE/LTE-A

As the mobile networks data demand grows, the sub-3GHz spectrum is becoming increasingly crowded. On the other hand, a large amount of spectrum in the 3-300 GHz range remains underutilized. Although by traditionally the 3-30 GHz is referred to as the super high frequency (SHF) and 30-300 GHz spectrum is referred to us the extremely high frequency (EHF) or mmWave band, in this thesis we can refer these two bands as mmW bands (with wavelengths ranging from 1 to 100mm). This is because radio waves both in SHF and EHF bands share similar propagation characteristics. Millimeter wave technology (mmWave) is under study by researchers across the globe as it is believed that future cellular communication wil be based on mmWave [93]. For this reason, there is a

need to have a smooth transition from 4G to 5G by gradually introducing the mmWave technology in envolving standards like 4G (5G is yet to be evolved). MM-Wave communication systems that can achieve mulit-gigabit (multi-Gbps) data rates at a distance of up to a few kilometers range already exists [35]. However, the component electronics used in these systems, including power amplifiers, low noise amplifiers, mixers and antennas are too big in size and consume too much power to be applicable in mobile communication with acceptable cost. In search of unlicensed and multi-Gbps short range wireless communications, recently much more efforts has been made in developing more power efficient 60 GHz RFICs [21]. Hence many of these technologies can be brought to other mmW bands. Moreover, the very small wavelengths of mmWave signals put in line with the current advances in low power CMOS RF circuit technologies can help to have large number of miniaturized antennas in small dimensions. This in turn enhances to form high gain, highly directional antennas for much higher bit rates needed for the higher aggregate capacity for many simultaneous users.

Transmission loss of mmWave is principally accounted for free space loss. The general misconception in the wireless radio waves perception is that free-space propagation loss depends on frequency, so higher frequencies propagates less than higher frequencies. Even though there are impairments in the mmWave propagations due to the physical properties of high frequency radio transmissions in the presence of atmospheric conditions, receiver power can be improved with frequency if reflector antenna is used whose gain increases with frequency [27]. To look more deeper into this, we consider the generic friis equation,

$$P_r = P_t \left(\frac{\lambda}{4\pi r} \right)^2 \tag{2.1}$$

where P_r is the received power, P_t is the transmitted power, λ and r is the distance between two antennas. But this assumption is made to calculate the path loss at specific frequency between two isotropic antennas whose effective aperture area increases with the wavelength (decreases with frequency). An antenna with a larger aperture has normally a larger gain than a smaller one since it can capture more energy of the radio waves. Nevertheless, with shorter wavelengths more antennas can be packed on same area. Hence, for the same antenna apertures, higher frequencies shouldnt have any inherent disadvantage compared to lower frequencies in terms of free-space path loss [86, 21]. On top of that, larger number of antennas enables transmitter and receiver beamforming with high gains. For instance, in [86, 21] it stated that, a beam at 80 GHz will have about 30dB more gain (pencil beam) than a beam at 2.4GHz if the antenna areas are kept constant. The other important consideration in dealing with mmWave propagation is penetration and other losses such as foliage losses, rain attenuation and gaseous losses. While signals at lower frequencies can penetrate more easily through buildings, mmWave signals do not pene-

trate most solid materials very well. Foliage losses are also significant for mmWave and can be a limiting factor for propagations in some cases. In [86] for instance, penetration losses for foliage of 5, 10, 20, and 40m depths are discussed and it is stated that at 80GHz and 10m foliage penetration, the loss can be about 23.5dB, which is about 15dB higher than the loss incurred by 3GHz frequency.

Furthermore, mmWave transmission can face with significant attenuations in the presence of heavy rain. Rain drops are roughly the same size as the mmW radio wavelengths and hence can cause the scattering of the radio signals. The attenuation in terms of dB/km can be calculated from the rain rates (mm/hr). Figure 2.9 for instance indicates the curves plotted for mmWave frequencies allowing link fading to be understood with respect to the rain falls. Light rain at a rate of 2.55mm/hr yields just over 1dB/km attenuation while heavy rain at the rate of 25mm/hr results over 10dB/km attenuation at E-band frequencies. Nevertheless, with proven models of worldwide rain distribution characteristics (as the most intense rain tends to fall in much selected countries of the world) link distances of many miles in most part of the globe can be realized.

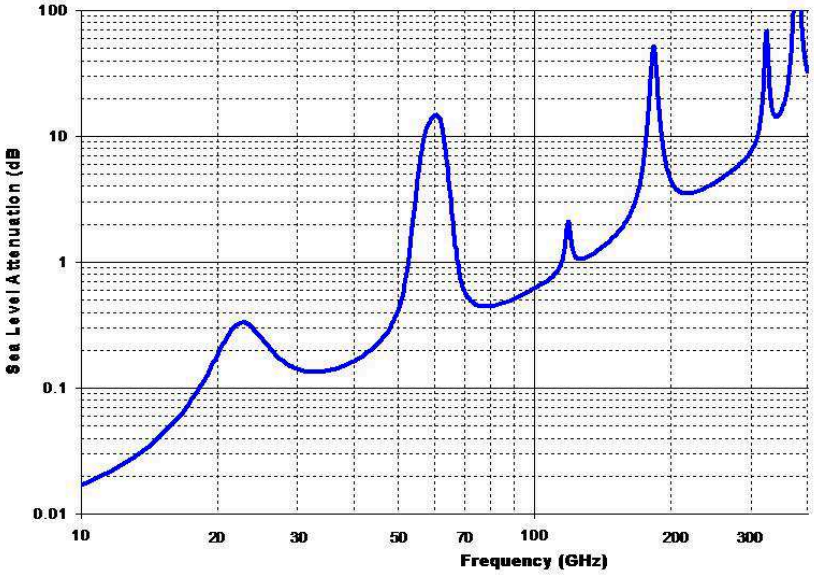

Figure 2.9: Atmospheric and molecular absorption at mmWave frequencies [4]

Taking all the above mentioned factors in to account, there is a viability of using mmWave frequencies that allows for higher data transfer rates. Millimeter-wave frequencies also allow for larger bandwidth allocations, which transfer directly to higher data transfer rates. By increasing the RF channel bandwidth for mobile radio channels, the latency of digital traffic is greatly decreased thus supporting more internet based appli-

cations of LTE-A. Considering the availability of contagious spectrum in addition to the propagation characteristics, mmWave can support the backhauling of lower-mobility, high data rate LTE-A small cell users. The mmWave radio signal experiences elevated propagation losses, compared to the lower frequencies, can also be advantageous for small cells which can have a shorter radio footprint with better reuse factor as a consequence.

From Figure 2.9, it can be seen that there is a drop in the atmospheric and molecular absorption in the E-band region (around 70GHz and 80GHz) as well as around 30GHz frequencies. Hence, these mmW frequencies can offer a window of opportunity for LTEA small cell backhauling. Furthermore, they have wider channel bandwidths which can be helpful to offer high data rate transmissions in the ranges of gigabits per second. What is more important to harness these frequency regimes is a feasible transmission technique.

Transmission rate inside a cell is the function of backhaul througput as it carries the data to core network. A reliable backhaul infrastructure can directly impact the quality of service that a user experiences. Taking these concerns into mind, mmWave is employed thanks to availability of excess bandwidth that is still underutilized. The rate demand on backhaul links is not so high in small cells because of shorter radio footprint that covers a limited population of users.

[55] has discussed different type of solutions for backhaul, namely optical fibre, microwave and mmWave. The author examines different characteristics associated with these backhaul solutions and remarked where these solutions are most appropriated to be deployed. The author indicated that cells covering larger area with huge population should have optical fibre as backhaul whereas wireless backhaul is advisable where population is paltry. In terms of cost, capital expenditures (CAPEX) of mmWave is lowest amongst the mentioned solutions. CAPEX of optical fibre is enormous and is two-times the cost of mmWave. For this reason, mmWave solution to backhaul provides a better tradeoff between CAPEX and requirements. Future cellular networks are based on small cells where subscribers/cell ratio is high hence mmWave solution can be taken into consideration. In addition, there are certain requirements for backhaul in heterogeneous LTE-A network to improve data rates. Such requirements are discussed in [59] where authors highlight that backhaul should guarantee high data rates, low latency and precised synchronization to meet future cellular demands. Similarly, backhaul requirements for CoMP in LTE-A systems are analyzed in [58]. CoMP requires sharing of information among cooperating eNBs in order to harvest gain out of cooperation. This calls for increase in backhaul capacity and it has been shown through qualitative results that the capacity requirement ranges to 5Gbps for upstream and 20Gbps for downstream. Due to high CAPEX, fibre optic solution is infeasible. However short range fibre to the home (FTTH) can greatly reduce the cost. Another workaround to the increased capacity issue

is to exploit 70GHz band with higher spectral efficiency (higher order QAM) for CoMP applications [58]. [37] discusses the advantages of using 80GHz band in the backhaul. Attaining high data rates without incurring increase in operator's cost, 80GHz band is suitable candidate for emerging 4G mobile deployments. Enabling high antenna gains at higher frequencies, high microwave frequencies at 28GHz are considered in [27] for NLOS small cell backhauling. Single carrier with adaptive equalization with frequency division duplex (FDD) is considered in 2×56Mhz channels using 512-QAM. For comparison, a sub-6 Ghz band is chosen where a typical link configuration is employed using time division duplex (TDD) and 64-QAM MIMO-OFDM waveform. The authors have proven through simulation results that benefits of higher frequency bands can be extended to NLOS scenario thanks to higher antenna gains for similar antenna size. Also single carrier transmission technique has shown robustness against multipath channels at higher frequencies.

A similar use case is 5G networks where mmWave is key technology to obtain high data rates. Backhauling in 5th generation (5G) networks is discussed in [39]. 60GHz band is taken into account from millimeter wave bands and compared with high microwave frequencies 5.8 GHz and 28GHz bands. Two different backhauling scenarios are discussed, centralized and distributed. In centralized scenario where there is central entity (macro BS), 5.8GHz outperforms 28GHz and 60GHz bands in terms of energy efficiency whereas in distributed scenario the performance of these three systems are quite close to each other. In general distributed scenario is more energy efficient as compare to centralized scenario. With the increase of small cells in the network, backhaul throughput increases linearly in centralized scenario whereas the increase is exponential in distributed scenario.

In another work [32] , In-band approach is discussed for 5G systems where 60GHz and 70/80GHz frequency bands are discussed. Details about modulation schemes and antennas to be used at these frequencies are presented with a comparison between CMOS and bipolar technologies. Reliable CMOS technology is required to counter hardware impairments (power amplifier and phase noise issues) in the backhaul. Feasibility of inband wireless backhaul for 5G network is presented in [102]. A cost effective and low latency backhaul solution is a strong requirement for backhaul. BS-to-BS scheduling scheme is presented that can be multiplexed with usual BS-to-MS scheduling for an in-band solution. In [28] wireless channel operating at E-band is characterized by considering the propagation limits and rain impairments on transmission link availability. Given the constraints of rain attenuation and figure of merit, an optimized modulation scheme is derived. It has been shown that E-band is able to provide high capacity upto 3Gbps to all access points. Multicell processing for uplink SCFDMA with limitations on backhaul is discussed in [18]. Network topology is defined where all BSs are connected to RNC

through wireless backhaul and quantized information is shared among the BSs. Greedy algorithm is proposed for rate allocation with quantizer design aiming to increase network throughput. Such a work is based on increasing the network throughput with emphasis on quantizer design and rate allocation algorithm.

2.7 LTE/LTE-A: software-defined radios solution

The Software Defined Radio(SDR) has gained increasing popularity in the electronics and communications field mainly because radios so developed can be easily reconfigured and thus can work on various heterogeneous networks. In addition, these radios guarantee software portability which results into considerable capital investment savings. An SDR can be used to implement the physical and some of the MAC layer of a communication protocol. However, it is limited by the capabilities of what the software can do and also the processing power of the processor on which the software is deployed. Due to the enormous possibilities that arise when the implementation of certain radio components is done in software, more research is being carried out to ensure that the SDR can be used to a maxim without considerably degrading the system performance. The concept of a Software Radio is based on the fact that some of the signal processing functionality of the radio, for example, the filtering and modulations, are implemented in software instead of using actual physical elements to carry out these functions. Due to the fact that some components are easier to emulate in software than others, the Software Radio has been classified by the Wireless Innovation Forum in the following ways [7]:

- *Tier 0:* This type of Software Radio is one that cannot be reconfigured by software at all despite having some of its components defined in software. It is also referred to as a hardware radio.
- *Tier 1:* In this type of software radio, only a few of the functions can be altered or controlled in software. However, neither mode nor frequency can be altered in this type without changing the hardware first. It is also referred to as the software choose radio.
- *Tier 2:* In this type,which is also referred to as the software defined radio(SDR), more functions are controlled by software and so is the modulation and the frequency. The software can be used to select a modulation/demodulation scheme and what type of signal to use(whether narrowband or broadband), among others. However, the front end is still non-configurable.
- *Tier 3:* In this type of software radio, the front end is configurable as well in addition to having many more functions controlled by software than Tier 1 or 2. Everything,

except the antenna can be controlled in software. It is also referred to as the ideal software radio.

- *Tier 4:* This software radio is referred to as the ultimate software radio .Everything it consists of- the functions and also the front end- can be reprogrammed. The controlling software though, should be standardised.

These tiers were coined by the forum so as to have a way in which to classify the different software radios that are currently in existence. The software radio has been used to modify transceiver designs, and thus functions in the physical layer. By incorporating a software radio, the transceiver is made more flexible, since it can then produce/receive multiple waveforms and also becomes easily upgadeable thus yielding a radio that can be used for a longer lifespan.

A typical SDR design consists of a radio platform that supports a waveform. The radio platform consists of the hardware and the software systems necessary to produce or receive the waveform. The waveform is the software program that defines the ultimate RF signal, including the frequency, modulation type and message format [106]. An example is the GNURadio Platform: the software portion exist before the digital to analog converter (DAC) and RF front end for the transmitter and after the RF front end and analog to digital converter (ADC) in the receiver. The software part is implemented on a commodity PC and a special board called the Universal Software Peripheral Board (USRP) is used to implement the RF front end.

Despite the seeming simplicity of adopting the software radio technologies, there are a few challenges that have hindered the rapid proliferation of this technology. A first challenge is the need for open standards that make it possible for the software radio to run on heterogeneous networks. These standards will make it easier to develop waveforms that can run on multiple platforms with minimal change. One such open network is the Software Communications Architecture(SCA) that will enable rapid prototyping of waveforms that can run on multiple platforms[106]. Thakare, Musale and Shete in [103] also demonstrate the use of SDR to highlight the importance of an open communication platform with reconfiguring ability in changing environmnental conditions during communication. Their research used an open distributed wireless communication system called ODWCS which is a new architecture for a wireless access system with distributed antennas, distributed processors and distributed controlling through SDR. The authors demonstrate how it is possible to increase data rates considerably using this architecture and the SDR technology.

Whilst most research in SDR is still limited to the military, there are a number of application platforms that have been responsible for the growing interest on the SDR

platform in academia: Matlab and Simulink, the GNURadio Platform and Microsoft Research Software Radio (SORA). These platforms enable programming of most of the signal processing functionality of the developed radio on commodity PC architectures. SORA is still being developed by microsoft researchers in Beijing and is yet to be rolled out to academia. Matlab and Simulink is used to define systems not just for the SDR but also for cognitive radios because they have a family of toolboxes that allow building of these radios to explore various spectrum sensing, prediction and management techniques [100]. When MATLAB is used, it can be used as a simulator. However,in order to facilitate experimental research, it can be ported to an RF front end to emulate a real world scenario. The GNURadio platform is an open source framework that allows the use of python and C++ for the development of signal processing algorithms. Because of open source, it is possible for developers to design their own blocks in C++ which increases the possibilities of what the GNU radio framework can be used for.

LTE-A/4G is offering a variety of advance techniques for improving data rates for end-users, e.g., carrier aggregation, Relaying, CoMP, MU-MIMO etc. With the provisioning of flexibility and reconfigurability, SDR can make it possible to realize such advanced strategies without the use additional hardware. Because LTE-A/4G will be collection of wireless standards, SDR will ensure that a single terminal can seamlessly and automatically connect to available high speed wireless access systems. For instance, if the terminal is moved to indoor environment, it will scan for Wireless local area network (WLAN) for better service without any involvement from user. Considering the same approach at network level, where network adapts to different functionalities depending on the change in parameters (like, traffic load, channel conditions, demanded services at a particular instant, congested band , etc) affecting the overall network performance. Band congestion is the issue that requires the introduction of new concept called cognitive radio (CR). Cognitive radio (CR) enables the use of "*white space*" of bandwidth without causing harm to other users of the same bandwidth. SDR and CR go side by side as adaptive change of spectrum would require adaptive change in transmission scheme in order to cope with the requirements of the technologies currently sharing the spectrum.

There are a number of scenarios in literature that demonstrate the advantages of incorporating a SDR into a communication system. Yoshida et.al in [117] describe a scenario in which a multimode receiver is implemeted by means of SDR. They demonstrate that using the SDR results into an increase in the design flexibility and a reduction in the receiver chains, since only one chain is used for all the modes. Tachwali et.al [101] demonstrate a scenario in which a wireless digital modem is implemented on a hybrid software radio platform using hybrid GPP/DSP/FPGA architecture. They implement and deploy this framework and also provide a description for the basic signal processing logic

design in the FPGA section. This basically illustrates how adopting SDR technology is facilitating experimental research [101]. Additionally, OPNET has been used to demonstrate the use of game theory in software defined radio networks [96]. Silverman et al in [96] shows that in order to model the spectrum usage, radio frequency interference avoidance, and distributed radio resource management, the behavior of Software Defined Radios should be predicted using game theory in an analytic mathematical framework. This application scenario illustrates the fact that SDR is going to be a key technology in future networks and studies like these demonstrate the feasibilty of SDR incorporation into these future networks. What is common to all is that in adopting the technology, the ensuing system is more flexible and results, oft-times, into a more cost effective solution. However, very few cases of research with SDR have focussed on systems developed using GNURadio coupled with USRP boards. The software defined radio has seen growing use in experimental research for the PHY layer of wireless communication protocols partly because the Software Defined Radio(SDR) is an enabling technology for cognitive radio. [123] demonstrates how to implement an adaptive interference avoidance TDCS (Transform-domain Communication System) based cognitive radio via a software defined radio implementation. The designed system uses the GNURadio platform and USRP boards. The developed cognitive radio is able to detect primary users in real time and adaptively adjusts its transmission parameters to avoid interference to primary users.

The SDR has been used extensibly in research in OFDM-based systems. For example, Rahman et al uses the SDR to study OFDM Inter Carrier Interference(ICI) cancellation schemes in the 2.4GHz frequency band [88]. They use the GNU Radio platform along with the USRP boards to demonstrate that the proposed ICI schemes result into a high performance transmission of IEEE-802.11b specification compliant data. [116] provides yet another example of an SDR implementation for OFDM transceivers. They define a SDR system with a reconfigurable architecture based on an adaptable OFDM scheme using BPSK and QPSK modulation. Kelley in [64] proposes a new SDR system using OFDM transceiver styles that jointly minimizes power, maximize algorithm flexibility, and enables rapid software re-programming. In doing this it solves the issue faced by most SDR developers: trying to maintain flexibility while at the same time supporting computationally efficient broadband communications.

2.8 Door open to 5th Generation

Technology is evolving at a rapid pace thanks to availability of increased processing power units. The same is true for cellular technology that starts from analog 1G (First generation) and entering into new era of 5G (5th generation). So much have been discussed

about previous generations; however, in this section the upcoming 5G will be discussed together with some proposals for uplink PHY-layer transmission scheme.

5G is believed to be a perfect wireless technology without limits that is able to meet following requirements:

- Power efficient network;
- Provisioning of high data rates;
- ∼Gbps data rate in mobility;
- Applications with artificial intelligence (AI);
- Low deployment cost;
- Reconfigurable network able to adapt itself depending on the situation;

5G will be a new technology that will enable new applications for it users by using only one device. In this regard visualizing energy efficiency in power-constrained devices, like user terminal, is vital because continuous acitivity will shorten device battery life [23].

For this reason, a power efficient uplink transmission should be conceived in order to prolong battery lifetime. Current LTE-A systems are based on SCFDMA that are characterized by lower PAPR as compare to OFDMA. Still high input backoff (IBO) is still required for high order of modulations schemes (e.g., 16QAM, 64QAM). A non-orthogonal multicarrier technique, filter bank multicarrier (FBMC), is proposed for 5G applications in satellite communications. FBMC has shown PAPR characteristics similar to OFDM and is less sensitive to carrier frequency offset (CFO). Also FBMC demands high IBO for a linear operation. Because 5G is based on mmWave technology, increasing PAPR will be a serious issue. Single carrier with cyclic prefix (or zero padding) techniques are robust against PAPR and carrier frequency offset and is proposed for 5G in [43]. However, increased optimal detection complexity and less spectral efficient are the major drawbacks of single carrier techniques.

Hence a tradeoff between spectral and power efficiency is desired in transmission schemes for 5G uplink service. Thompson *et.al* in [105] proposes constant envelope OFDM (CE-OFDM) that exhibits zero PAPR characteristics by sacrificing slightly the spectral efficiency. The basic principle is to modulate the carrier phase with information signal using real-valued fourier transformation. The power dissipation in power amplifier is reduced significantly hence power loss due to IBO is avoided. Recently, CE-SCFDMA is tested in non-linear satellite channels [81] where CE-SCFDMA has shown significant performance improvement over CE-OFDM. The receiver design is complex in the sense an equalizer is required to remove the channel phase shifts from the signal. Hence such

techniques can meet goals in uplink 5G where receiver is the base station and complexity can be afforded.

Chapter 3

Novel PHY-layer techniques in LTE-A Uplink

In this chapter, study and development of innovative physical layer techniques for LTE-A uplink, based on SC-FDMA. At first, link performance analysis together with energy efficiency improvement is done with the help cooperation among neighboring base stations (BSs) by conceiving virtual MIMO. A power efficient technique, constant envelope SCFDMA, is proposed for uplink LTE-A that is robust against non-linear effects of the channel. Later, a computationally efficient multi-user detection in uplink LTE-A MIMO is considered that is based on minimum bit error probability criterion.

3.1 Efficient transmission scheme based on virtual MIMO

In this section, cooperative communication techniques for LTE-A systems will be described. Cell-edge users often suffer from low-SNR due to mainly two reasons, longer distance from serving BS and inter-cell interference (ICI). User equipments (UE) are characterized by battery limited devices and when transmitting in low SNR conditions, the battery drains out quickly. In such a scenario cooperative communication, especially CoMP, can be auspicious where neighboring BSs cooperate in order to provide better link level performance without increase in transmission power. BS cooperation allows to improve system performance without incorporating advanced system level signal processing functionalities in user terminals. This motivates to analyse deeply the link level performance and energy efficiency as result of BS cooperation.

This analysis presented here is different from state-of-the-art and is a step ahead in the field of cooperative communication, because state-of-the-art aims at improving capacity of cell-edge users using CoMP as discussed in section 2. Moreover, not much efforts are made in uplink cooperative communication but much emphases are done in downlink.

In this work link level performance of uplink cooperative MIMO, in terms of BER, using turbo coded modulation standardized for uplink LTE-A systems. Besides multipath channel, another key issue is considered related to imperfect channel estimation in cooperative MIMO. Energy efficiency is important in uplink and has to be considered in cooperative MIMO context. Energy efficiency model is presented in this work deriving energy consumption in fixed power MIMO systems. In the following section, cooperative MIMO system model is dicussed in detail together with analyses and issues that are briefly discussed.

3.1.1 System Model

The uplink multi-user tranmission configuration is considered where K cell-edge UEs are transmitting over orthorgonal radio resources using single antenna. The signals from UEs are received by the cooperating BSs, each one having N_r antenna elements. Thanks to orthorgonal radio resource usage by transmitting UEs, receiver architecture becomes simpler as multi-user detection (MUD) is not required to seperate transmissions from different UEs. However, in the case of Multi-User MIMO (MU-MIMO) configurations, paired UEs are allowed to transmit over same resource blocks simultaneously with multi-user detector employed at BSs. It is evident that BS cooperation in MU-MIMO, joined with affordable MUD algorithms, can strongly reduce user interference, increase spectral efficiency and definitely boost capacity. The MUD receiver design is discussed in section (3.3) In this work, we are interested in how uplink CoMP can enhance performance in terms of BER and energy efficiency. The current analysis will represent the lower bound to the scenario where multi-user inteference (MUI) is enabled. The k-th UE transmits data streams with appropriate channel coding (rate-compatible punctured convolutional turbo coding [16] is adopted, following the guidelines of LTE standard) and occupies the assigned resource blocks (RB) M_k,

$$M_k = \frac{M}{K} \tag{3.1}$$

The assigned RBs are kept contiguous in order to minimize energy consumption at UE (i.e., localized subcarrier mapping). SCFDMA supports two different subcarrier mapping techniques, namely localized and interleaved. In former the data is mapped to adjacent localized subcarriers, whereas the latter allows to fill subcarriers that are equi-distant from each other. Localized-SCFDMA (LFDMA) provides ease of practical implementation, and multi-user diversity if combined with channel dependent scheduling [89]. For these reasons, LFDMA has been adopted in long term evolution (LTE) [51]. On the other hand, interleaved-SCFDMA (IFDMA) is robust against frequency selective channels but

it's practical implementation is un-convenient. In order to have a compliancy with existing and future LTE standards, we will only deal with LFDMA[1] in the thesis.

The cyclic prefix (CP) is added to the signals at each UE after N-IFFT block. CP-length is kept longer than channel impulse response in order to avoid inter-symbol interference (ISI). The unit-power k-th user signal X_k is sent over noisy multipath channel to the B BSs. The SC-FDMA signal formation is described in next chapter of radio resource management. The signal transmitted from k-th UE is then received by the BS b:

$$Y_{kb} = H_{kb}X_k + Z_b, \quad b = 1, .., B \tag{3.2}$$

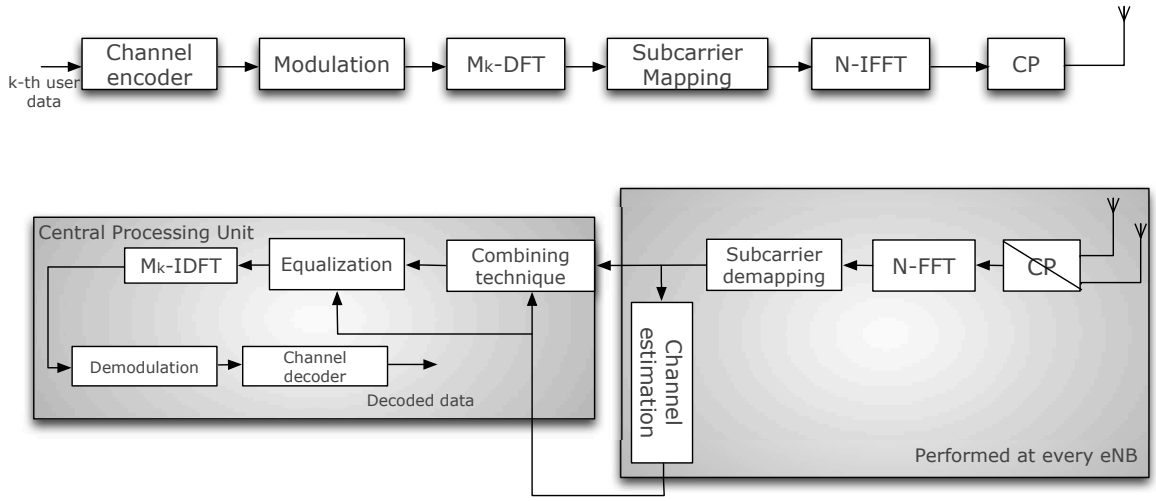

Figure 3.1: Block Diagram of the virtual MIMO LTE-A uplink

where H_{kb} is $N_r \times 1$ complex multipath channel between k-th UE and b-th BS equipped with N_r antenna elements and Z_b is the additive white gaussian noise (AWGN) with zero mean and unit variance. The above procedure is depicted in Fig 3.1. It can be seen that channel estimation is performed by all cooperating BSs whereas the combining and equalization of the signals is performed only at serving BS. In the next section, the cooperative multi-point transmission system based on virtual MIMO diversity will be described in detail for what concerns the signal processing tasks performed by BSs.

3.1.2 CoMP signal processing for Virtual MIMO diversity exploitation

At each BS b, the received signals are converted into frequency domain using an N-FFT block. Channel estimation is done for every transmission time interval (TTI) at BSs. The raw received signal samples $\tilde{Y}_{kb}$ at cooperating BSs together with channel state

[1]We will use "SCFDMA" for LFDMA.

information (CSI) are then sent to central processing unit (CPU *aka* serving BS) through ideal backhaul (i.e., unlimited bandwidth, error-free and zero-latencies). In Fig 3.2, the joint diversity combination of virtual MIMO is pictorially sketched, together with the inter-cell backhaul link.

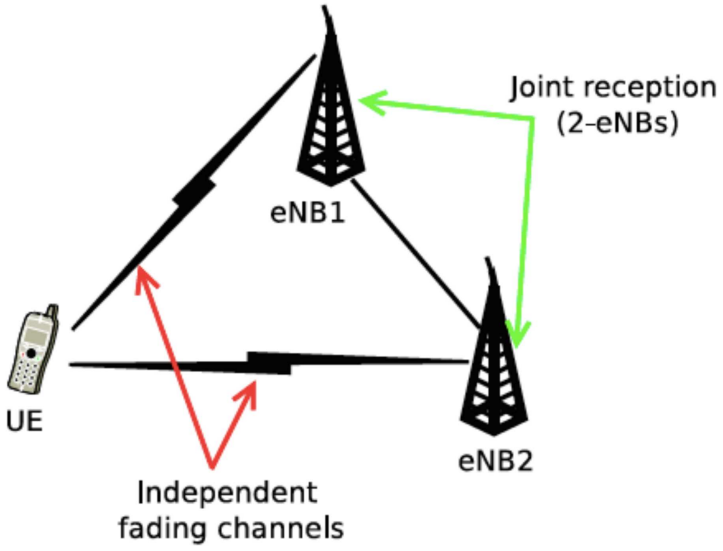

Figure 3.2: Virtual MIMO: two cooperating BSs

The hypothesis of ideal backhaul among small cells is realistic if mmWave wireless solution is adopted. Some very recent works have investigated the capacity bounds of small cell point-to-point and point-to-multipoint backhaul links at 28 GHz (LOS and NLOS) [27] and 80 GHz (mainly LOS) [4]. Considering the shorter backhaul distances involved by small cell networking, appropriate PHY-layer solutions joined with efficient traffic aggregation strategies would allow error-free backhaul rates of the order of 10 Gb/s with latencies less than ~ 3 microseconds.

The received signal Y_{kb} is coherently combined and equalized at CPU or at serving BS using the CSI $\tilde{H}_{kb}$ estimated by all cooperating BSs. In this work, we assumed the processing is done at serving BS. Using Maximal-Ratio Combining (MRC) [46], we obtain for k-th user:

$$\hat{Y_k} = \sum_{i=1}^{B} \sum_{j=1}^{N_R} w_{ki}^{j} Y_{ki}^{j} \tag{3.3}$$

where $w_k = H_k^*$ is the complex conjugate of channel filter coefficients for user k. After MRC combining, the effective k-th user CSI for equalization can be written as,

$$\bar{H}_k = \sum_{i=1}^{B} \sum_{j=1}^{N_R} H_{ki}^{j*} H_{ki}^{j} \tag{3.4}$$

Channel estimation is done using Least Square (LS) method [51]. Pilot symbols are transmitted on fourth slot of a TTI to obtain channel impulse response at BS receiver. The motivation for the choice of LS lies in the good tradeoff between robustness and computational complexity. The achievement of perfect channel estimation providing ideal CSI knowledge has been considered in our simulations in order to appreciate the impact of real channel estimation on the link performance.

The equalization block, based on zero forcing (ZF) technique, is explicitly required by SC-FDMA in order to remove ISI. ZF is preferred in LTE standard to MMSE because it does not require the knowledge of noise covariance matrix, whose estimation would be difficult. The k-th user ZF filter coefficient using $\bar{H}_k$ in (3.4) is given as:

$$W_k^{ZF} = (\bar{H}_k^* \cdot \bar{H}_k)^{-1} \bar{H}_k^* \tag{3.5}$$

where $(\cdot)^*$ is the complex conjugate of the signal in parenthesis. The CSI of N_R antennas from each of B BSs is communicated to serving BS over lossless and zero delay backhaul. The joint diversity combining and equalization is performed at serving BS. The signal $\hat{Y}_k$ in (3.3) after equalization is given as $\bar{Y}_k$,

$$\bar{Y}_k = W_k^{ZF} \hat{Y}_k \tag{3.6}$$

The estimated symbols $\hat{x_k}$ are finally obtained from $\bar{Y}_k$ after demodulation and channel decoding, as shown in Fig. 3.1.

3.1.3 Energy Efficiency in Virtual MIMO

Energy efficiency is considered to play an equally important role with spectral efficiency in future cellular networks. It is believed that future cellular networks will facilitate the subscribers with high data rate that comes with the minimal use of battery energy. Energy dissipation and consumption both in the uplink and downlink need a careful look in order to have a realistic energy model in the system. In uplink where battery limited UEs are transmitting, minimal use of energy is demanded by the user. For this reason, a considerable amount of research work has been carried out in order to obtain energy consumption models capturing the power usage of the UE. Most of these models are based on network parameters like system throughput. However keeping network parameters fixed, we can exploit a link level parameter like the bit-error-rate (BER) to model energy consumption as in [73]-[29]. An energy efficiency model based on BER is being proposed in this paper for uplink virtual MIMO systems where signal processing tasks for MIMO diversity are performed at BS level. With transmit power is fixed at UE, BER can be improved by uplink BS cooperation as most of the transmit power is consumed over data

bits that are correctly received at BSs (i.e., converting large portion of transmitted energy into useful).

Let's denote with N_{total} the data volume in terms of number of information bits to be transmitted from UE to BS and, E_b/N_o the signal-to-noise ratio per bit required to obtain bit-error-rate of P_e at serving BS. E_{total} is the power required by UE to transmit N_{total} and is given by:

$$E_{total} = N_{total} \times E_b \tag{3.7}$$

where E_b is the bit energy and it is given as:

$$E_b = \frac{E_b}{N_o} \times \frac{\sigma^2_{noise}}{R_b} \tag{3.8}$$

σ^2_{noise} is the noise variance at the receiver and R_b is the data rate in the system. Putting (3.8) into (3.7), we have:

$$E_{total} = N_{total} \times \frac{E_b}{N_o} \times \frac{\sigma^2_{noise}}{R_b} \tag{3.9}$$

The energy wasted in bits errors, E_{wasted}, can be computed as follows:

$$E_{wasted} = N_{error} \times \frac{E_b}{N_o} \times \frac{\sigma^2_{noise}}{R_b} \tag{3.10}$$

N_{error} is the number of bits incorrectly received, i.e.

$$N_{error} = N_{total} \times P_e \tag{3.11}$$

The energy spent for transmitting bits that are received correctly, E_{useful}, is obtained from (3.7) and (3.10)

$$E_{useful} = E_{total} - E_{wasted} \tag{3.12}$$

(3.12) is the metric used to analyze energy efficiency. The efficiency expressed in terms of percentage of useful energy against total energy spent by the UE is given by:

$$\eta\ (\%) = \frac{E_{useful}}{E_{total}} \times 100 \tag{3.13}$$

The units of all energy expressions are joules.

3.1.4 Simulation Results

Cooperative multi-point uplink system based on virtual MIMO is simulated in MATLAB/Simulink environment with parameters set according to LTE-A 3GPP standard, as highlighted in Tab 3.1.

A two-user scenario is considered where both the users are associated to same serving cell and transmission is received by multiple neighboring BSs. Also, users are occupying

Table 3.1: Simulation Parameters

Bandwidth	5 MHz
Number of Subcarriers	512
CP length	36
Resource Blocks (RBs)	6
Subcarriers in RB	12
Subcarrier Spacing	15 KHz
Sampling frequency	7.68 MHz
Channel Estimation	Ideal
Channel Impulse response	Extended Vehicular A (EVA)
Modulation	QPSK & 16-QAM
N_R	2
Channel coding	Turbo coding
Code Rate	1/2, 3/4
Baud-rate (Mbaud/sec)	3.6
Receiver	MRC & Zero forcing

orthogonal radio resources and do not interfere to each other. Bandwidth and baud-rate have been fixed according to LTE specifications. Considering the modulation format and the punctured turbo coding rates shown in Table 3.1, the net data rate ranges from 3.6 Mb/s for the 1/2-coded QPSK configuration to 10.8 Mb/s for the 3/4-coded 16-QAM. Cooperative and non-cooperative transmissions are compared for what concerns the BER and energy efficiency performance.

Link Level Analysis

Virtual MIMO is able at providing supreme performance in case of lower order modulation techniques, i.e., QPSK (see Figs 3.4-3.5). We observe a dramatic performance gains achieved by cooperative transmission against non-cooperative one in particular when robust channel coding and ideal channel estimation are considered. In such a case, 2-BS and 3-BS virtual MIMO can provide 5dB and 8dB gains respectively. Performance gain is still significant even in case of real channel estimation (about 5dB). Increasing the code rate to 3/4 requires puncturing of systematic bits from coded data hence making turbo decoding less performing. Having 3-BS cooperation virtual MIMO, we have a maximum of 6dB gain over non-cooperative strategy thanks to receiver diversity gain. Non-cooperative

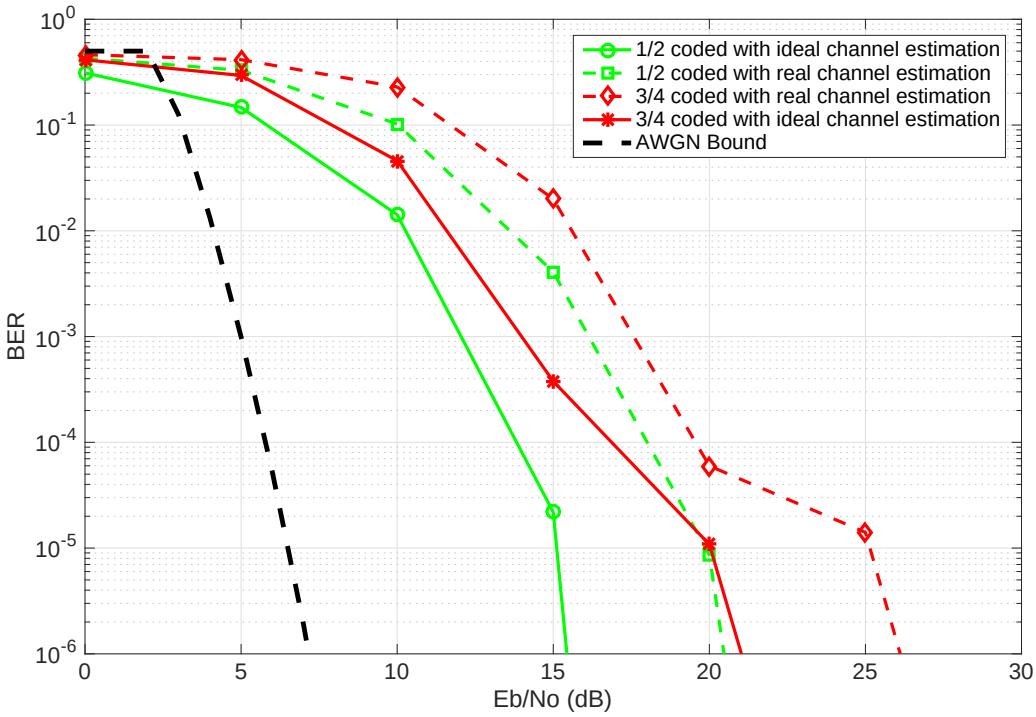

Figure 3.3: BER performance achieved in non-cooperative LTE-A scenario: QPSK modulation.

transmission always perform poorer when real channel estimation is considered, as evident in Fig. 3.3. It should be noted that the impact of real channel estimation on link performance is not negligible both in the cooperative and in the non-cooperative case. Despite the use of a robust and efficient LS channel estimation, the performance degradation with respect to the ideal (perfect) channel estimation is about 5dB for the non-cooperative transmission and is almost independent on channel coding rate. For two cooperating BSs, the measured performance loss remains almost the same as compare to that in non-cooperative case, while it is considerably decreased when three cooperating BSs are considered in conjunction with robust 1/2-rate turbo coding.

Some additional simulation trials for higher modulation level, i.e., 16-QAM, are performed to see how system behaves when spectral efficiency is increased. In such a case, 3-BSs cooperative transmission outperforms non-cooperative approach by $\sim$ 10dB in case of ideal channel estimation and 1/2 code rate. In 3-BSs cooperative transmission scenario, the transmitting energy is received by antennas at all BSs and thanks to joint combining and equalization at serving BS the output SNR increases significantly. Clearly, this is not the case in non-cooperative case In non-cooperative case, cell-edge users are required to spend more energy per transmitted bit in order to achieve larger data rates. For coding

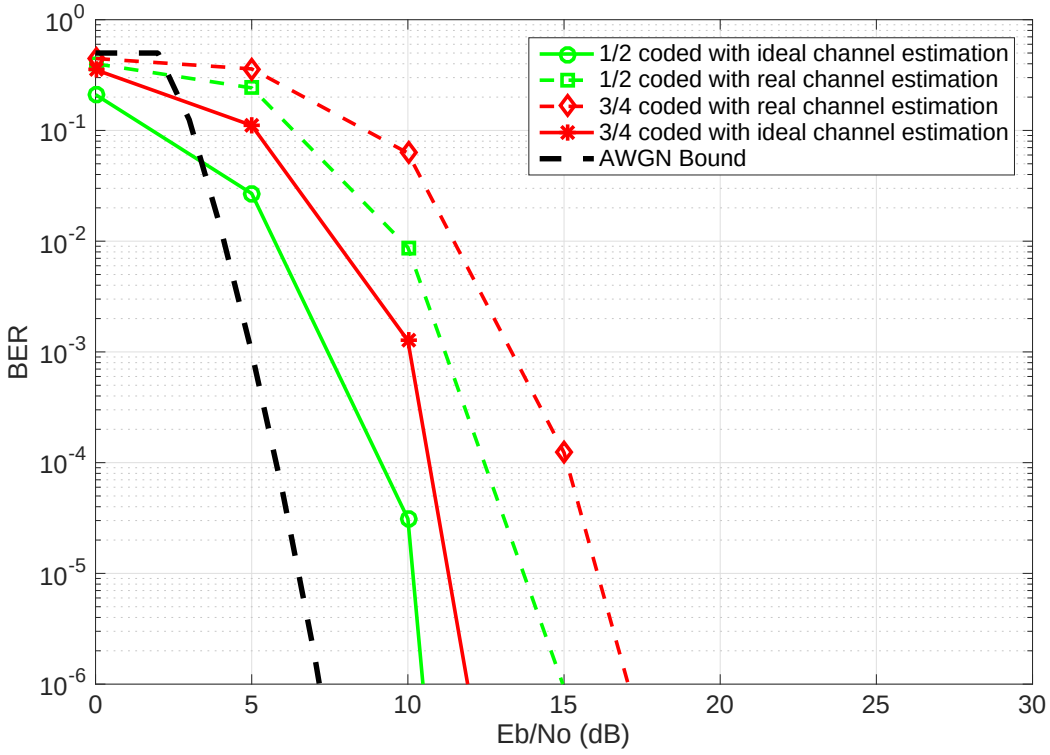

Figure 3.4: BER performance achieved in two-BSs cooperating scenario: QPSK modulation.

rate equal to 3/4, the 3-BS cooperation gain against non-cooperative strategy decreases down to 5dB, as shown in Figs. 3.6, 3.7, 3.8. Increasing the order of modulation, the impact of non-ideal CSI knowledge gets significant and is surprisingly larger when three BSs are cooperating. Increasing the number of antennas at receiver escalate the channel estimation burden and hence due to non-ideal channel estimation the noise in CSI increases. Due to joint diversity and equalization that requires the CSI availability, the non ideal CSI degrades the performance significantly. This is evident in the Fig. 3.8 whereas such loss due to non-ideal channel estimation is not significant in non-cooperation case.

Energy Efficiency Analysis

Energy efficiency is another key performance indicator for in cellular networks especially in uplink. The gain in energy efficiency due to CoMP is quite enormous from battery-limited device's point of view. Cooperative transmission clearly outperforms non-cooperative one also in terms of energy efficiency, because diversity gain reduces the bit-energy spent by the UEs to reach the target BER. Virtual MIMO allows UE to better exploit the available energy resources with respect to non-cooperative transmission. This is evident

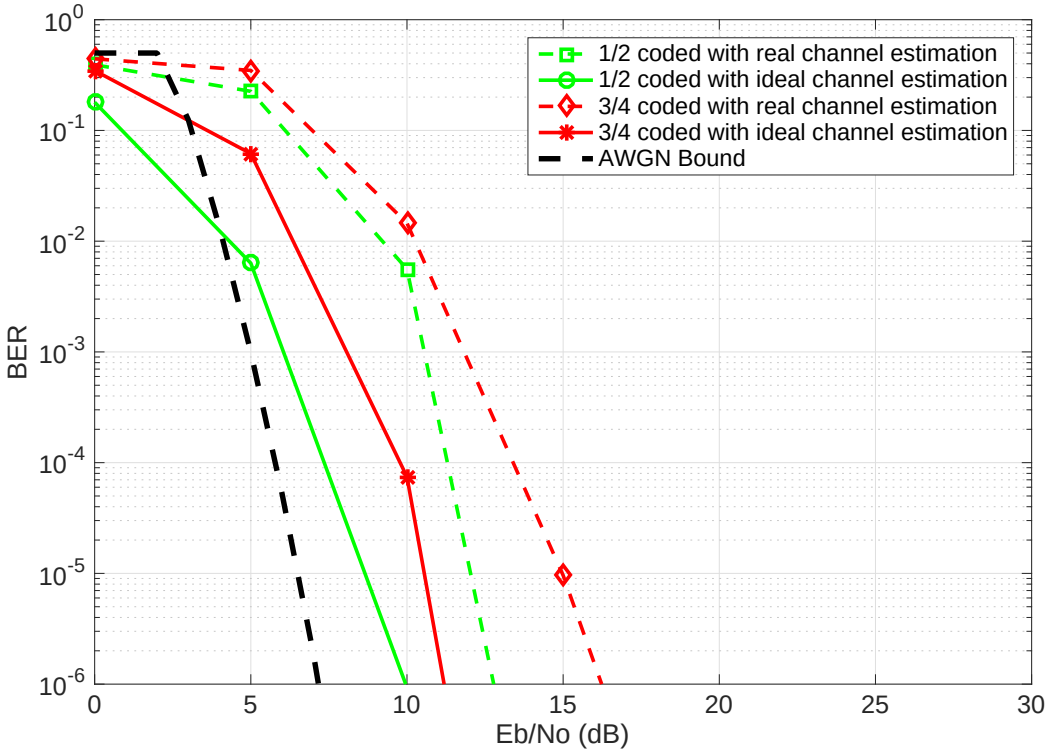

Figure 3.5: BER performance achieved in three-BSs cooperating scenario: QPSK modulation.

in Figs. 3.9, 3.10. Cooperation with 3-BSs brings improvement in energy efficiency as significant percentage of energy, $\sim$ 20 % in 1/2-rate turbo coding and $\sim$ 25 % in 3/4-rate turbo coding. Because of the definition of energy efficiency, channel impairments and non-ideal channel estimation losses have significant impact on energy saving. It is worth noticing here although the performance is improved but the increasing number of cooperating BSs (from 2 to 3) does not significantly improve energy efficiency.

In case of 16-QAM modulation, CoMP transmission is still able to outperform the non cooperative case both with ideal and real channel estimation, but the energy efficiency gain is a bit less than it is for the QPSK. We can see in Figs. 3.11, 3.12 that virtual MIMO attains the maximum energy efficiency at lower SNR-per-bit values. The gained energy efficiency is more significant when 1/2-rate turbo coding is adopted (maximum: 14 percent with 3-BSs), as shown in Fig. 3.11.

As far as the impact of real channel estimation on system energy efficiency is concerned, it is evident from Figs. 3.9-3.12 that non-ideal CSI knowledge involves a significant reduction of the system energy efficiency. Such a reduction may reach 20 percent at low SNR regime and for higher order modulation schemes. This suggests, CoMP requires

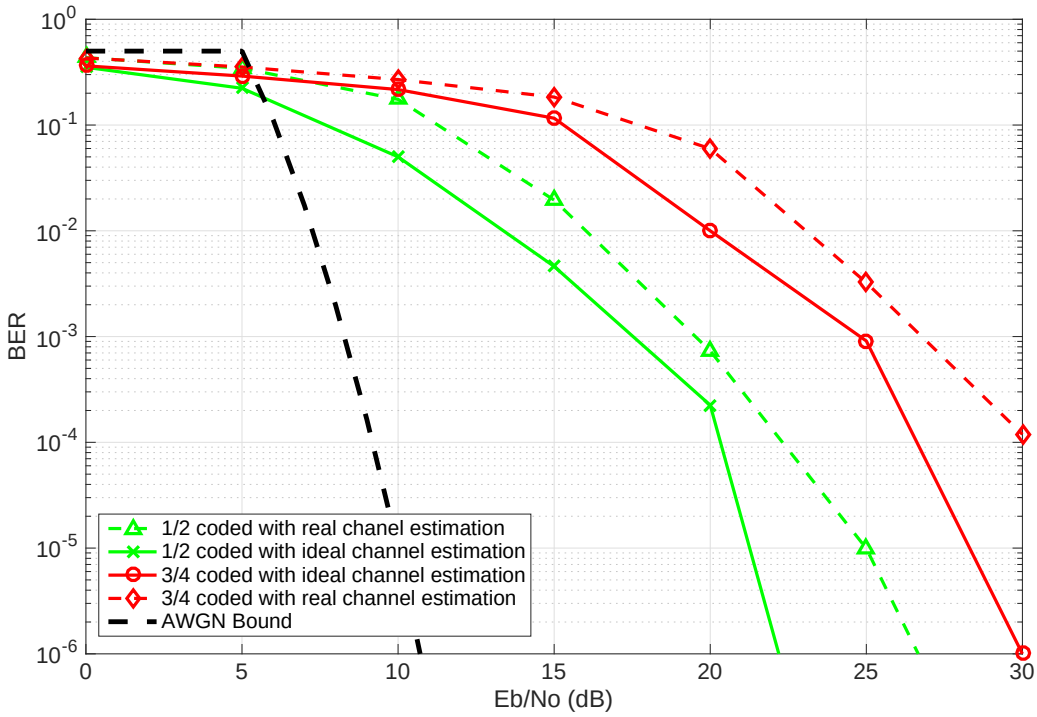

Figure 3.6: BER performance achieved in non-cooperative LTE-A scenario: 16-QAM modulation.

very robust channel estimation techniques to reach the expected targets in terms of link performance and energy efficiency.

3.2 Novel Radio Interface for Uplink 5G Systems

The nonlinear characteristics, due to the presence of high-power amplifiers (HPAs) in the PHY-layer chain, is a hindrance for multicarrier modulations in the uplink. Future mobile networks are based on exploitation of high frequency bands of millimeter wavelengths (38GHz, E-band). Such high frequencies show sensitivity to large free-space pathloss, significant atmospheric and rain attenuations, antenna and demodulation loss [9]. Therefore, expensive power amplifier operating very close to saturation point is desired. However, OFDM and OFDMA (for downlink 4G applications) waveforms are severely affected by the non-linear amplifier characteristics due to high envelope fluctuations and require a large input back-off (IBO) to achieve acceptable performance. SC-FDMA (for uplink 4G applications) has lower envelope fluctuations and perform relatively better than OFDMA. Still they require some dBs of input backoff (IBO) for higher order modulations for which PAPR is not negligible.

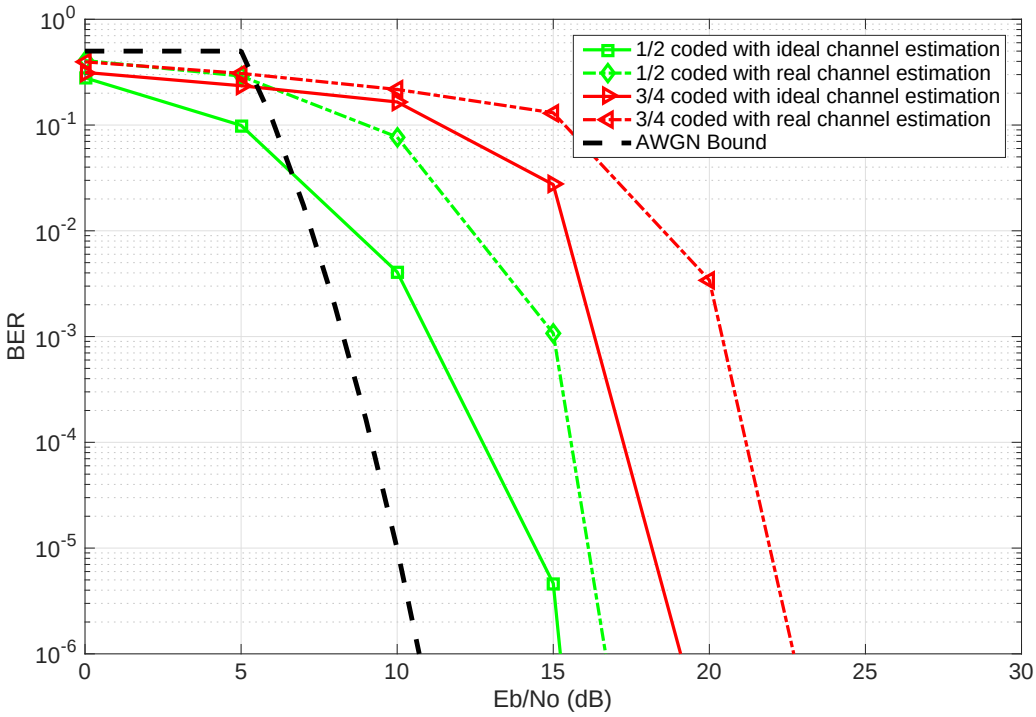

Figure 3.7: BER performance achieved in two-BSs cooperating scenario: 16-QAM modulation.

User convenience is one the key goals in future smart city cellular netowrks. In particular, user terminals should have long battery lifetime to enjoy perks and benefits provided by smart city applications. The situation is critical in uplink where transmission is done at the expense of limited terminal power budget. A power efficient waveform is the solution that does not require backoff for its adequate operations. Thompson *et.al.* in [105] proposes a constant envelope OFDM (CE-OFDM) that is able to exhibit 0dB PAPR and hence IBO is waived off. CE-OFDM has been successfully tested over nonlinear wireless channels affected both by multipath fading and nonlinear distortion. CE-OFDM is realized by applying a nonlinear phase modulation to a real-valued OFDM symbol sequence. Such a transformation ensures that the transmitted signal has 0dB PAPR level. In [81], constant envelope SCFDMA (CE-SCFDMA) is proposed for non-linear satellite channels and it has been shown that CE-SCFDMA technique outperforms CE-OFDM in ricean satellite channels. In another similar work [31], CE-techniques are tested against non-ideal oscillator phase noise and have shown significant resilience against moderate phase noise levels.

Against this background, it is strongely motivated that CE-SCFDMA is capable of addressing power issues related to user terminals in future mobile networks. CE-SCFDMA

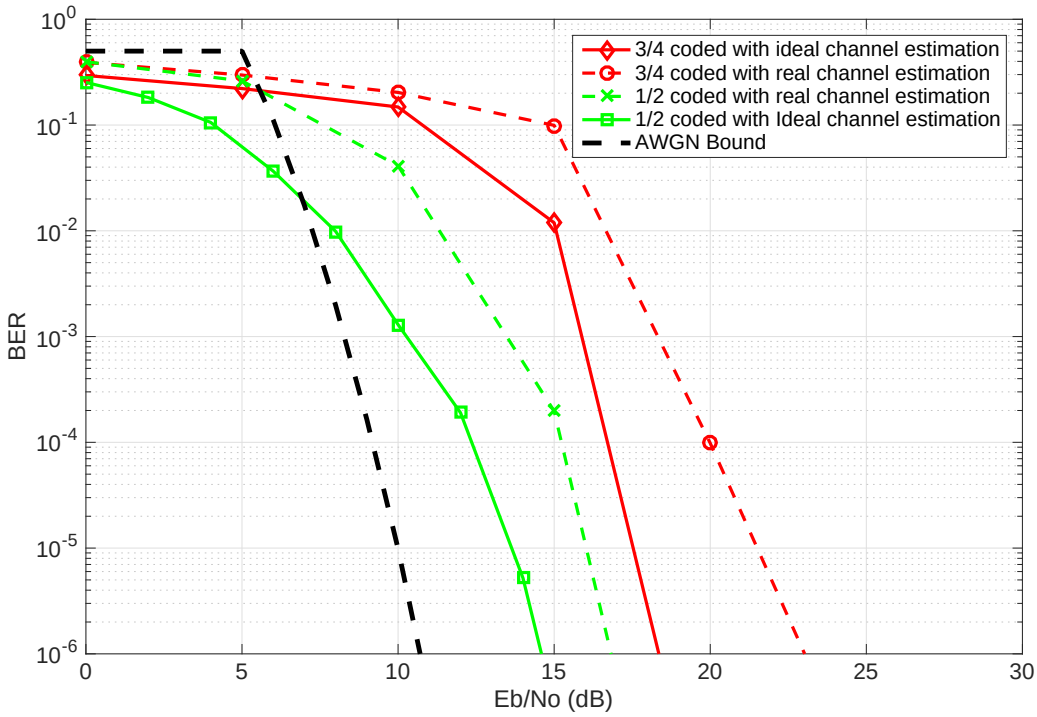

Figure 3.8: BER performance achieved in three-BSs cooperating scenario: 16-QAM modulation.

is proposed for uplink future cellular networks in this work and to prove its significance in LTE-A mobile terrestrial channels, simulations are performed w.r.t current uplink transmission scheme (SC-FDMA).

3.2.1 System Model: Constant Envelope SC-FDMA

Fig. 3.13 shows the block diagram of the CE-SCFDMA baseband transmission system. The N_c-point DFT pre-coding spreads the energy of the mapped QAM data symbols across the bandwidth as is done in the conventional SC-FDMA. Let the pre-coded data sequence generated be denoted by $\{X_k\}_{k=0}^{N_c-1}$, such that

$$X_k = \sum_{k=0}^{N_c-1} x_n exp(-j2\pi nk/N_c) \tag{3.14}$$

The pre-coded symbols are then mapped onto a subset of the available subcarrier set (whose cardinality is $N > N_c$) by the subcarrier mapping operation. The data symbol sequence $\{x_n\}_{n=0}^{N_c-1}$ is composed of L-QAM with $L = 2^a$ where a is the even integer. Two different subcarrier mapping strategies can be adopted in SC-FDMA (and, therefore, in CE-SC-FDMA), namely: Localized-FDMA (L-FDMA), in which contiguous subcarriers

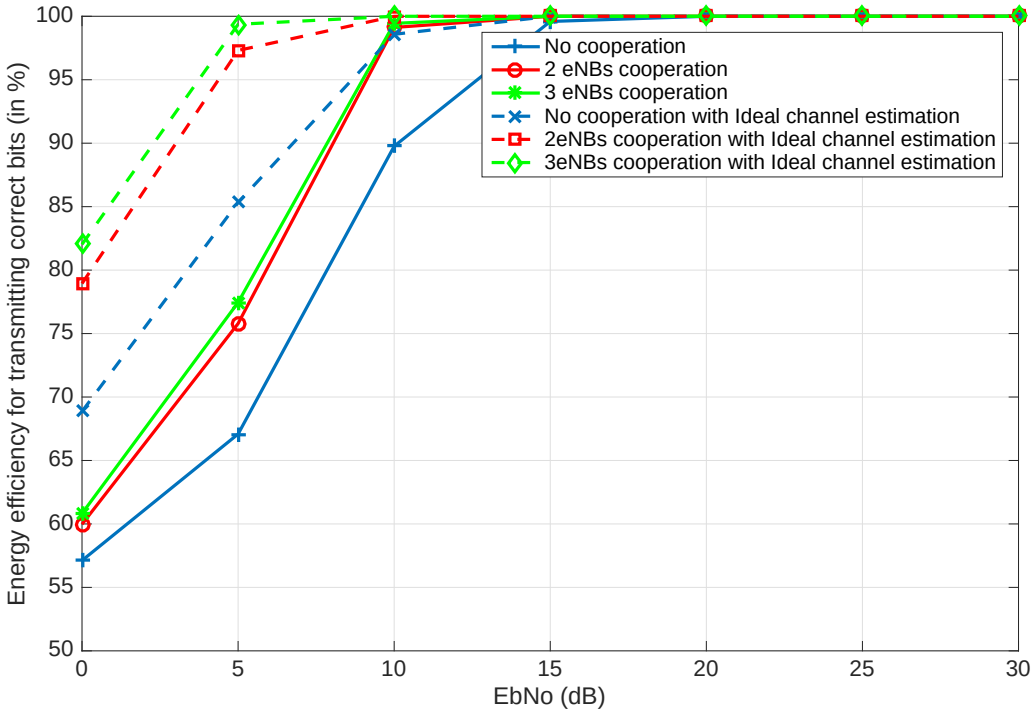

Figure 3.9: Energy efficiency achieved by cooperative and non-cooperative LTE-A uplink: QPSK modulation with code rate = 1/2.

are allocated to the pre-coded user symbols, and Interleaved-FDMA (I-FDMA), in which the input precoded user symbols take on equi-distant subcarriers. It is shown in literature that I-FDMA improves the frequency diversity against frequency-selective channels, at the cost of an increased computational complexity of the receiver. The mapped symbols are then fed to a real-valued IFFT, which generates the CE-SCFDMA signal by using the same methodology shown in [105]. The real-valued transmitted SCFDMA sequence is obtained by applying a conventional I-FFT to an oversampled conjugate symmetric zero-padded sequence [87], i.e.

$$X_{SCFDMA} = \left[0, X_1, X_2, \cdots, X_{N_c}, Z_p, 0, X^*_{N_c}, X^*_{N_c-1}, \cdots, X^*_1\right] \tag{3.15}$$

where X is the pre-coded data sequency as in (3.14), $\underline{Z_p}$ is the zero padding vector of length D_{zp}. Because localized-SCFDMA is standardized for LTE-A application, CE-SCFDMA is also studied in the context of localized subcarrier allocation in this work. The total number of samples of the sequence X_{SCFDMA} is $M = 2N + 2 + D_{zp} \doteq C_{ov}N$ where C_{ov} is the oversampling factor equal to 4 or 8 [105]. Under the hypothesis mentioned above, the output of real-valued IFFT is given by,

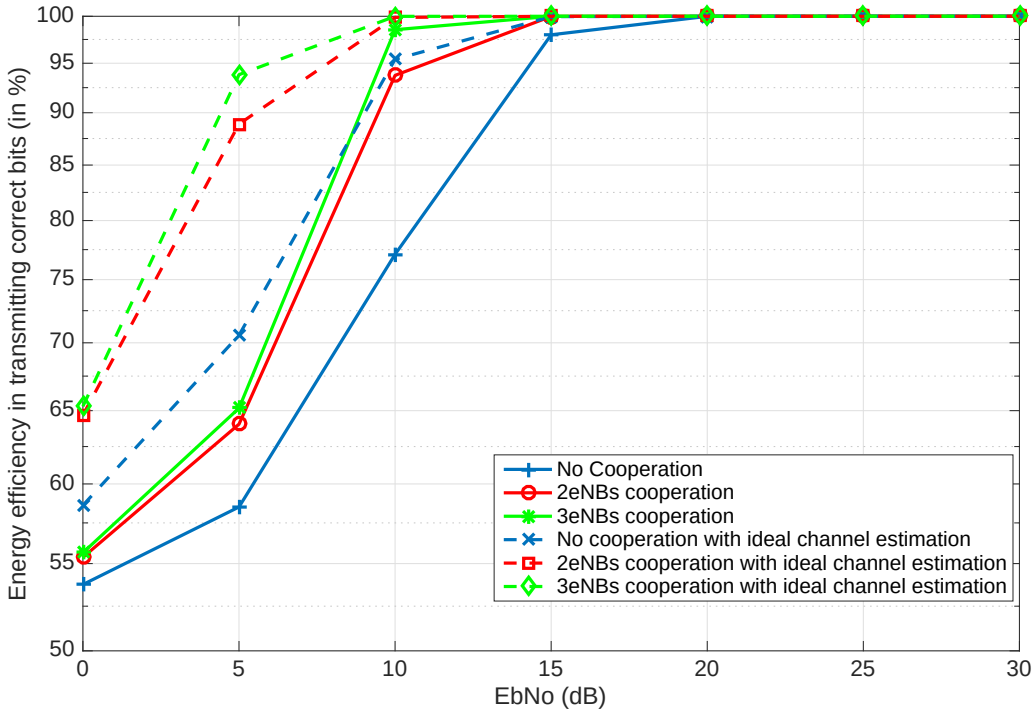

Figure 3.10: Energy efficiency achieved by cooperative and non-cooperative LTE-A uplink: QPSK modulation with code rate = 3/4.

$$\chi_n = \sum_{m=0}^{M-1} X_{SCFDMA}\,[m]\, exp(j2\pi mn/M) \tag{3.16}$$

(3.16) can be written in full as,

$$\chi_n = \frac{2}{Q_c} \sum_{k=1}^{N} \Re\{X_k\}\, cos(2\pi knQ_c/N) - \Im\{X_k\}\, sin(2\pi knQ_c/N) \tag{3.17}$$

In (3.17) $Q_c = N/N_c$ is the energy spreading factor of the DFT precoding. The output signal from the M-point IFFT is fed to phase modulator applying the following non-linear transformation:

$$s_n = exp(j2\pi hC_{norm}\chi_n) \tag{3.18}$$

C_{norm} is the normalization constant and $2\pi h$ is the angular modulation index expressed in radian. For CE-SCFDMA, C_{norm} is equal to $\sqrt{2/N\sigma_l^2}$ with $\sigma_l^2 = N(L^2-1)/3$. The cyclic prefix T_{cp} extension is added to CE-SCFDMA signal after the phase modulation

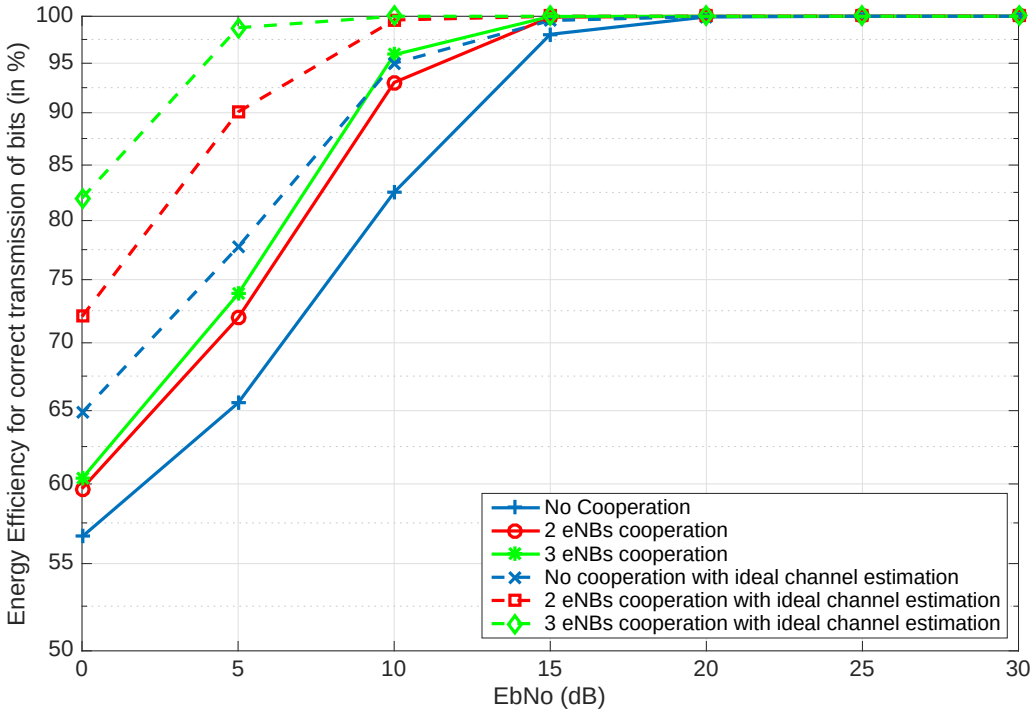

Figure 3.11: Energy efficiency achieved by cooperative and non-cooperative LTE-A uplink: 16-QAM modulation with code rate = 1/2.

of real-value IFFT signal. Therefore, the D/A converted CE-SCFDMA signal can be expressed as follows:

$$s(t) = Aexp(j[2\pi h\lambda(t) + \theta]), -T_{cp} \leq t \leq T \tag{3.19}$$

where A is the signal amplitude, θ is the arbitrary phase offset, and $\lambda(t)$ is the normalized real-valued SC-FDMA signal defined as,

$$\lambda(t) = C_{norm}\chi_t \tag{3.20}$$

where χ_t is the D/A converted real valued SCFDMA signal. Finally, the amplified signal is transmitted onto the multipath channel. At the receiver side, the signal received is digitized using A/D converter. Frequency domain equalization (FDE) is performed on the digital signal after the removal of CP. A state-of-the-art Minimum Mean Squared Error (MMSE) equalizer has been considered in this work. The equalized signal is then fed to the phase demodulator, which consists of a phase unwrapper and an arctangent calculator. The phase unwrapper is needed to avoid phase jumps that might occur when the received phase crosses the π-radian boundary [105]. After the phase demodulation,

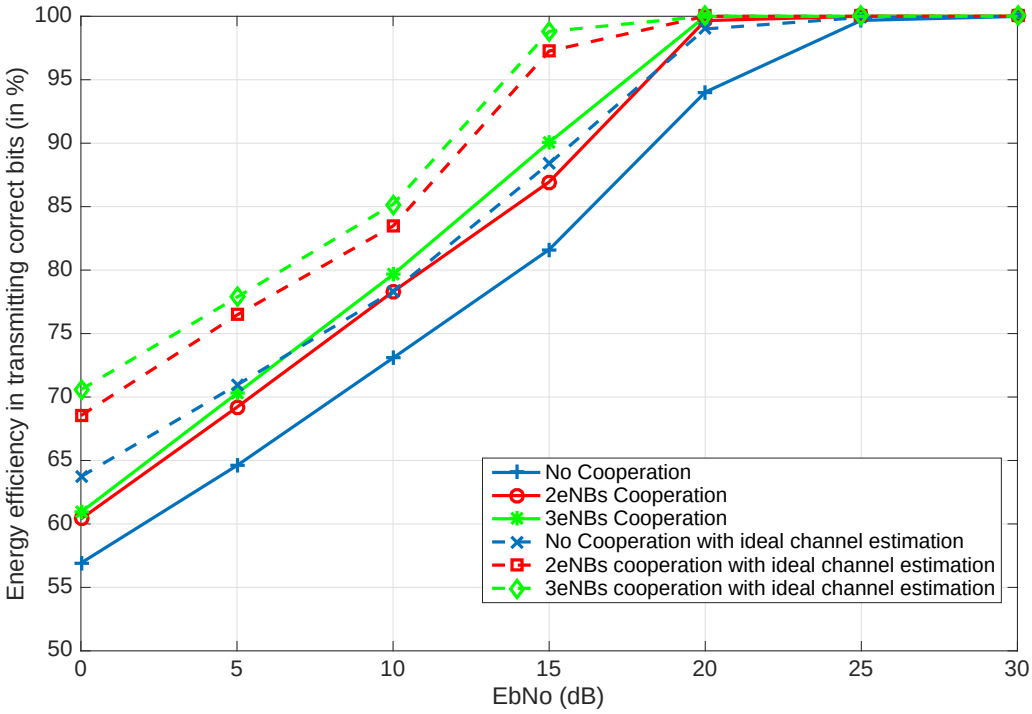

Figure 3.12: Energy efficiency achieved by cooperative and non-cooperative LTE-A uplink: 16-QAM modulation with code rate = 3/4.

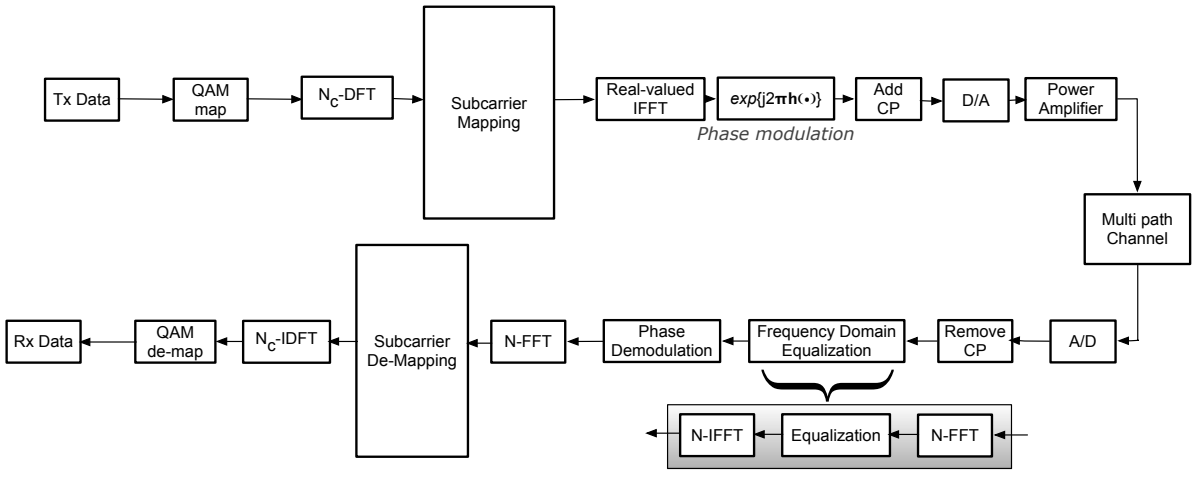

Figure 3.13: Proposed Constant Envelope Single Carrier Frequency Divison Multiple Access (CE-SCFDMA) in Multipath Channel

the usual processing tasks of SC-FDMA detection are performed, i.e.: coherent FFT-based de-mapping, subcarrier de-mapping, N_c-point IDFT and L-QAM de-mapping as

Table 3.2: Simulation Parameters

Parameters	**Numerical value**
N (number of subcarrier)	512
C_{ov}, oversampling factor	4
L (modulation scheme) QAM	4, 16, 64
N_c, block size	126
Bandwidth (B_w)	5 MHz
Channel Model	EPA, EVA

highlighted in Fig. 3.13. The spectral efficiency of the CE-SC-FDMA, which is the same as that indicated in [105] for the CE-OFDM, is a crucial aspect to be considered:

$$S = \frac{R_b}{B_w} = \frac{\log_2 \sqrt{L}}{max(2\pi h, 1)}, bps/Hz \tag{3.21}$$

The spectral efficiency S decreases if $2\pi h$ is larger than 1. In such a case, the phase modulation increases the signal bandwidth. Results shown in [105] indicate that increasing the modulation index does not necessarily provide performance improvement. The proposed CE-SCFDMA scheme inherits the capability of managing the tradeoff between spectral efficiency and BER performance, in a flexible manner from CE-OFDM. This is achieved by tuning two parameters, namely: modulation levels and angular modulation index ($2\pi h$). Such capability is of particular interest in LTE-A systems, where adaptive modulation and coding techniques are often employed. In a comparative framework, a recent paper [113], is worth mentioning, where continuous-phase modulation (CPM) (namely: Minimum Shift Keying, MSK) has been used in conjunction with SC-FDMA in order to produce a constant-envelope SC-FDMA signal. CE-SCFDMA scheme provides increased flexibility in spectrum management with respect to the scheme of [113]. The spectral efficiency of [113] is fixed to 1 bps/Hz].

3.2.2 Simulation Results

The results obtained from the proposed CE-SCFDMA is compared with those of SC-FDMA by means of simulations performed in MATLAB environment. The transmission system parameters used in our simulation trials are reported in Tab. 3.2 .

The channel models considered in simulations are LTE-A standard models, extended pedestrian A (EPA), and extended vehicular A (EVA) [1]. It is an interesting aspect to see how CE-SCFDMA performs in a correlated channel (EPA) w.r.t SCFDMA. With reduced spectral efficiency where L = 4 or 4-QAM, through offline results angular modulation index ($2\pi h$) is measured. It was observed $2\pi h = 0.7$ is the optimal choice for 4-QAM modulation order in CE-SCFDMA technique. Due to 0dB PAPR in CE-SCFDMA, backoff

is not applicable, whereas 6dB of IBO is applied in case of SCFDMA. It can be seen in Fig. 3.14, gain of ∼2dB is in the favour of CE-SCFDMA against SCFDMA at high SNR . The performance of CE-SCFDMA is quite close to lower bound in pedestrian channel.

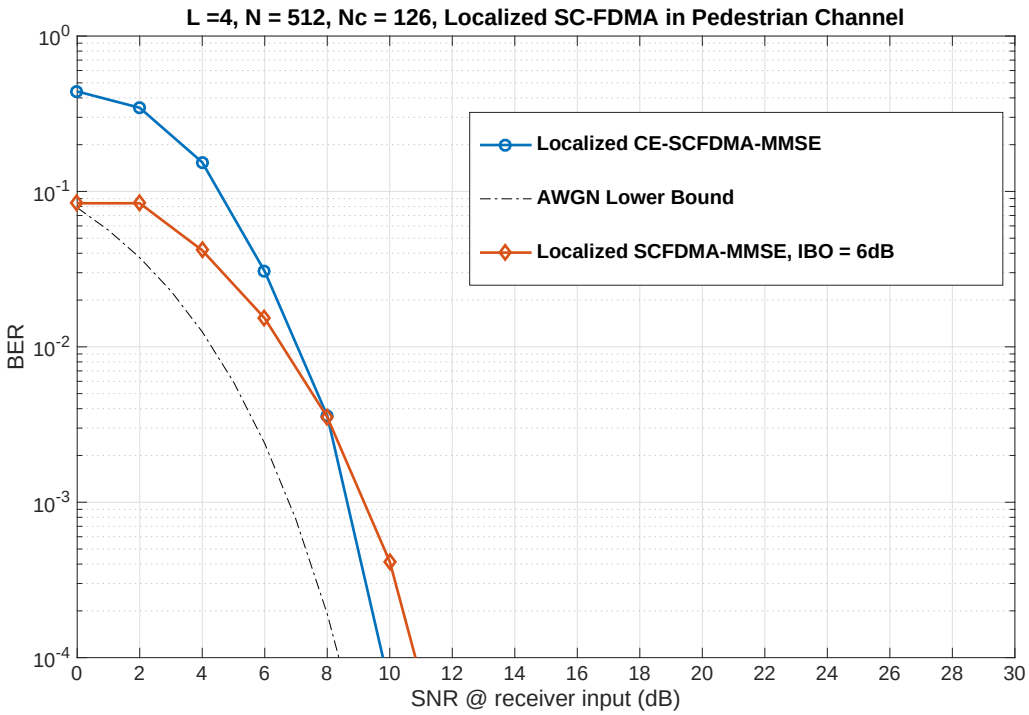

Figure 3.14: Constant Envelope SCFDMA vs. SCFDMA in non-linear pedestrian channel, L = 4, N = 512, $N_c = 126$, $2\pi h = 0.7$.

In case of EVA channel, the performance improvement for CE-SCFDMA is around 2dB over SCFDMA in 4-QAM. Such a performance loss in SCFDMA is due to applied backoff that is mandatory for linear operation of power amplifier.

Increasing spectral efficiency from 4-QAM to 16-QAM requires angular modulation index to be inreased accordingly. Hence $2\pi h$ is set to 1 for 16-QAM as suggested by offline simulations in AWGN channel. The performance improvement is noticeably huge in case of 16-QAM in both the channels. CE-SCFDMA observes a gain as high as 6dB over SCFDMA in pedestrian channel, whereas it is increased to 8dB in EVA.

With 64-QAM modulation, classical SCFDMA technique requires 14dB of backoff. The angular modulation index is set to 1.5 in case of CE-SCFDMA. The CE-SCFDMA outperforms the SCFDMA by clear margin if the backoff is applied to SCFDMA. Indeed, high modulation index is required for higher order of modulations that results in decreasing the overall spectral efficiency as in (3.21). However thanks to 0dB PAPR, CE-SCFDMA strikes a better trade-off between power and spectral efficiency.

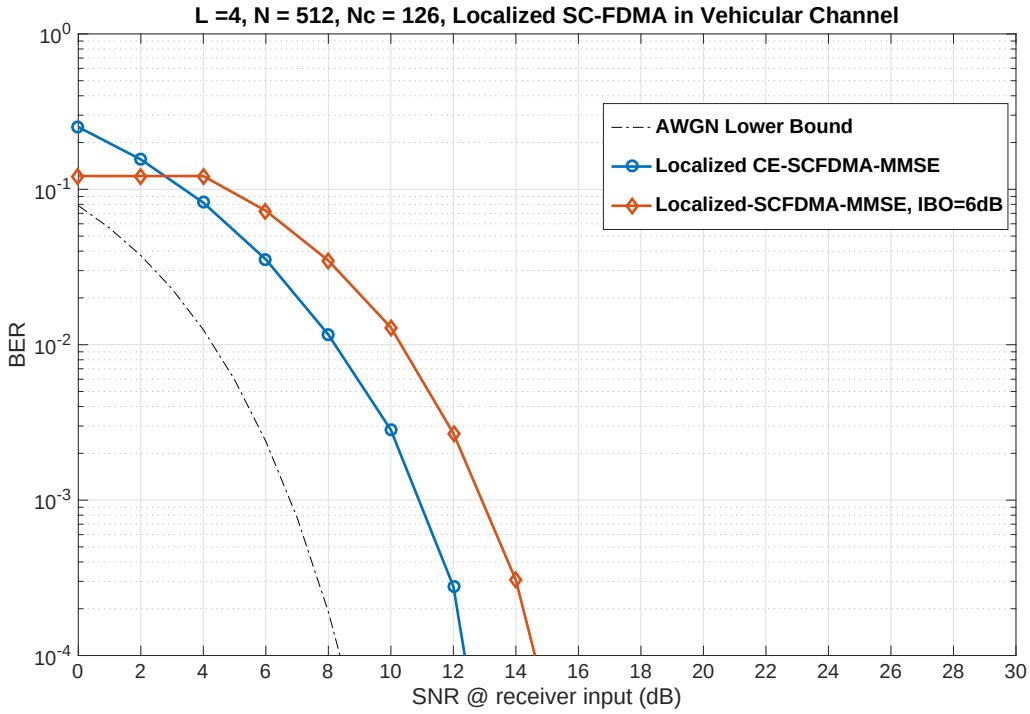

Figure 3.15: Constant Envelope SCFDMA vs. SCFDMA in non-linear vehicular channel, L = 4, N = 512, $N_c = 126$, $2\pi h = 0.7$.

3.3 Near optimum multi-user detection for MIMO LTE-A uplink

In this section, a multiuser receiver design for MIMO LTE-A uplink is described. Because of multi-user MIMO (MU-MIMO) operation, multiple access interference (MAI) caused by multiple users make state-of-the-art detection schemes (minimum mean square error MMSE (Ideal), least mean square LMS-MMSE) to operate far from optimum. Practical implementation of ideal-MSME is not trivial and often implemeted as LMS-MMSE. Such schemes are based on maximization of output signal to interference noise ratio (SINR) that is clearly sub-optimum in inteference environments. An iterative strategy is considered in this work that is based on minimum conditional bit error probability (MCBEP) criterion and directly minimizes the bit error rate (BER). Such a scheme has shown impressive results in state-of-the-art (sec 2) when considered in different context. Fast convergence and near-optimum performance are the standout features of this proposed MU-MIMO scheme. It would be interesting to analyse the performance of this proposed detection scheme in massive MIMO framework where receiving antennas are greater in number as compare to tranmsitting antennas.

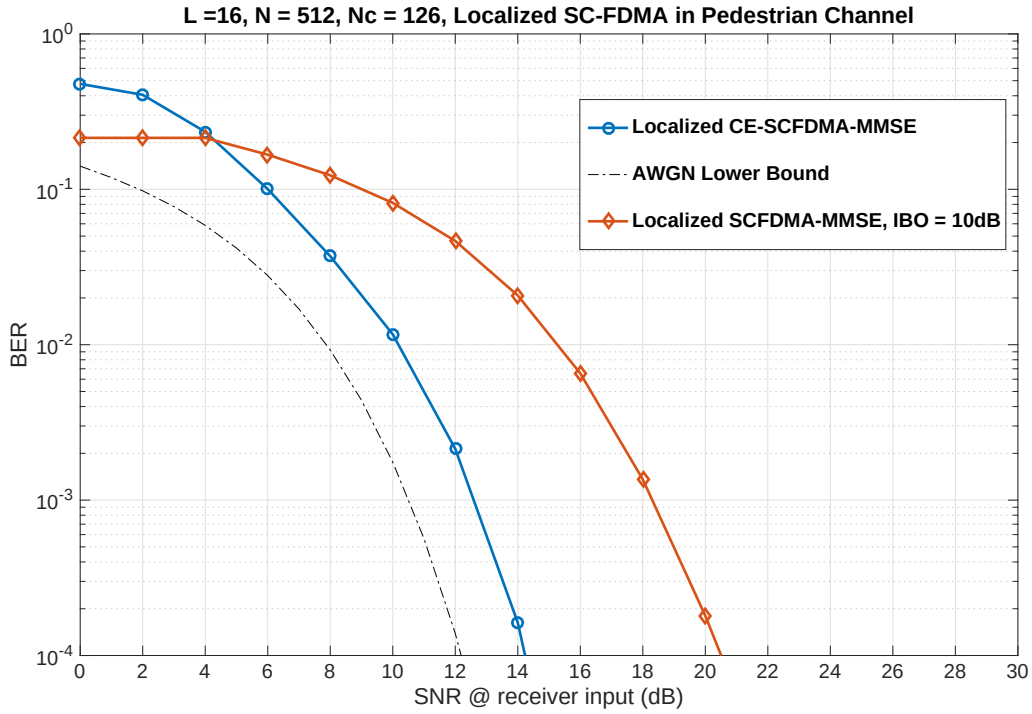

Figure 3.16: Constant Envelope SCFDMA vs. SCFDMA in non-linear pedestrian channel, L = 16, N = 512, $N_c = 126$, $2\pi h = 1$.

3.3.1 System Model

Due to SCFDMA, the system model in this section is not very different from that of in subsection (3.1.1). The only difference is, multiple UEs are transmitting to single base station. The notations used for representation of signal flows and operations in this section will be different from those used in previous sections and are not related.

The conceived scenario is an uplink scenario where user in close proximity form multi-user MIMO depicted in Fig. 3.20. The paired users (say, K) transmit to BS equipped with N_R antenna elements thus forming a $K \times N_R$ MIMO system, employing MUD to remove multi-user interference (MUI) thereby enhancing system throughput and provide required quality of service to the terminals. The information stream of k-th user i.e., $x_k = \left[x_k^1, x_k^2 \cdots x_k^M\right]^T$, is spread over M frequency bins using DFT and mapped to $N > M$ subcarriers using defined subcarrier mapping technique.

The frequency domain reprsentation of k-th user signal is X^k,

$$X_k = F_M x_k = \left[X_k^1, X_k^2, \cdots, X_k^M)\right]^T \tag{3.22}$$

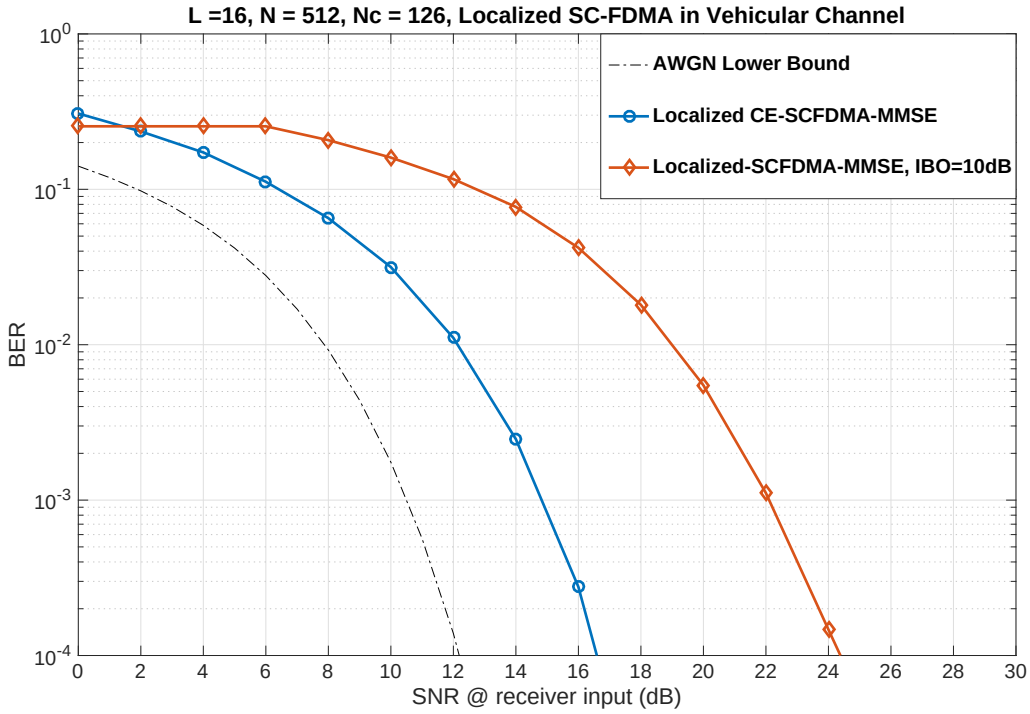

Figure 3.17: Constant Envelope SCFDMA vs. SCFDMA in non-linear vehicular channel, L = 16, N = 512, $N_c = 126$, $2\pi h = 1$.

where F_M is the normalized M-point DFT operator

$$F_M = \frac{1}{M} \sum_{n=0}^{M-1} x_n e^{-i2\pi k \frac{n}{M}}. \tag{3.23}$$

The k-th user SCFDMA signal as in (3.22) is passed through N-IFFT block and is given as,

$$\bar{y}^k = F'_N F_M x^k \tag{3.24}$$

where F'_N is the N-point IDFT matrix. The signal at transmitter is then added with cyclic prefix (CP) of length greater than channel impulse response (CIR). The signal $\bar{y}$ is transmitted over noisy-multipath channel using single antenna at transmitter. Corrupted with MUI and multipath chanel, the K user signals are received by N_R antennas of the receiver. Such MIMO configuration is desirable in uplink wireless systems where, unlike receivers, transmitters are power constraint devices.

The received multi-user signal at r-th receiver antenna $\bar{y}_r$ is given as,

$$\bar{y}_r = \sum_{k=1}^{K} h_r^k \bar{y}^k + z_r \tag{3.25}$$

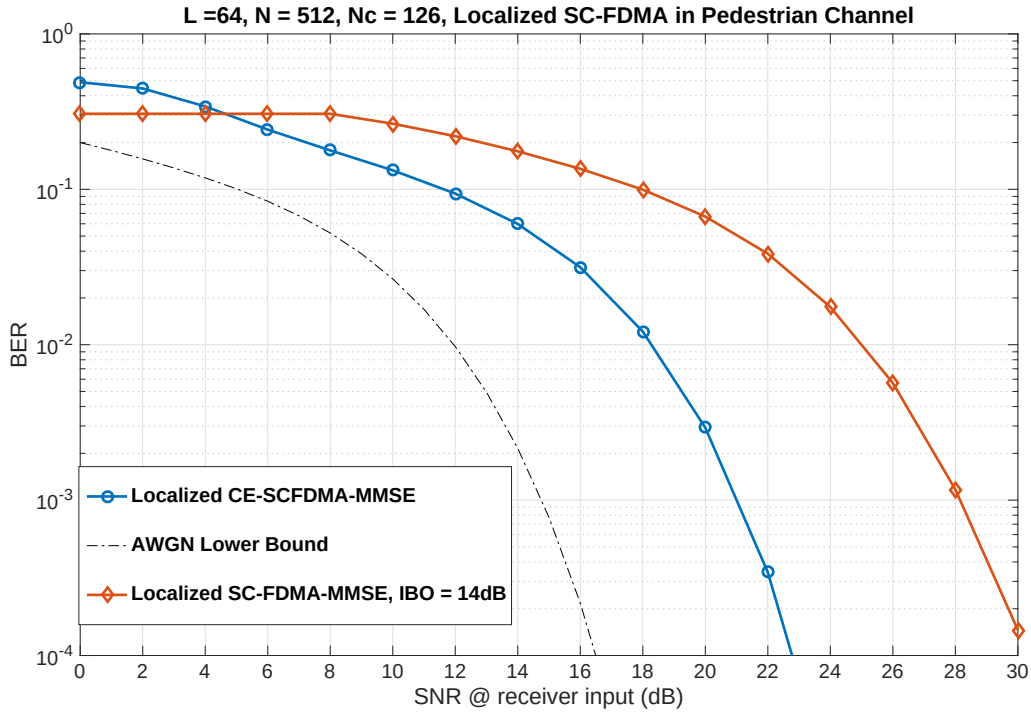

Figure 3.18: Constant Envelope SCFDMA vs. SCFDMA in non-linear pedestrian channel, L = 64, N = 512, $N_c = 126$, $2\pi h = 1.5$.

where h_r^k is the time domain channel impulse response between k-th transmit antenna and r-th receiver antenna and z_r is the independent identically distributed (i.i.d) AWGN samples with zero-mean and covariance σ^2. For the sake of simplicity, we are dropping the user index k and receive antenna index r from the equations as received signals at the receiver are jointly detected at MUD block. The frequency domain matrix representation of 3.25 is,

$$\bar{Y} = H \cdot Y + Z \tag{3.26}$$

In (3.26) $\bar{Y}$ is $R \times 1$ matrix corresponding to signals received at R antennas of receiver and H is the RxK channel matrix between transmit antennas and receive antennas. The received signal is passed to multi-user detector block. The latter removes MUI and other channel impairments with the help of channel state information (CSI) provided by former. In this work we assume ideal channel estimation however in general the channel estimaton operation is performed at receiver for each received antenna. In the following section, we will discuss the the proposed MCBEP receiver for MU-MIMO SC-FDMA system.

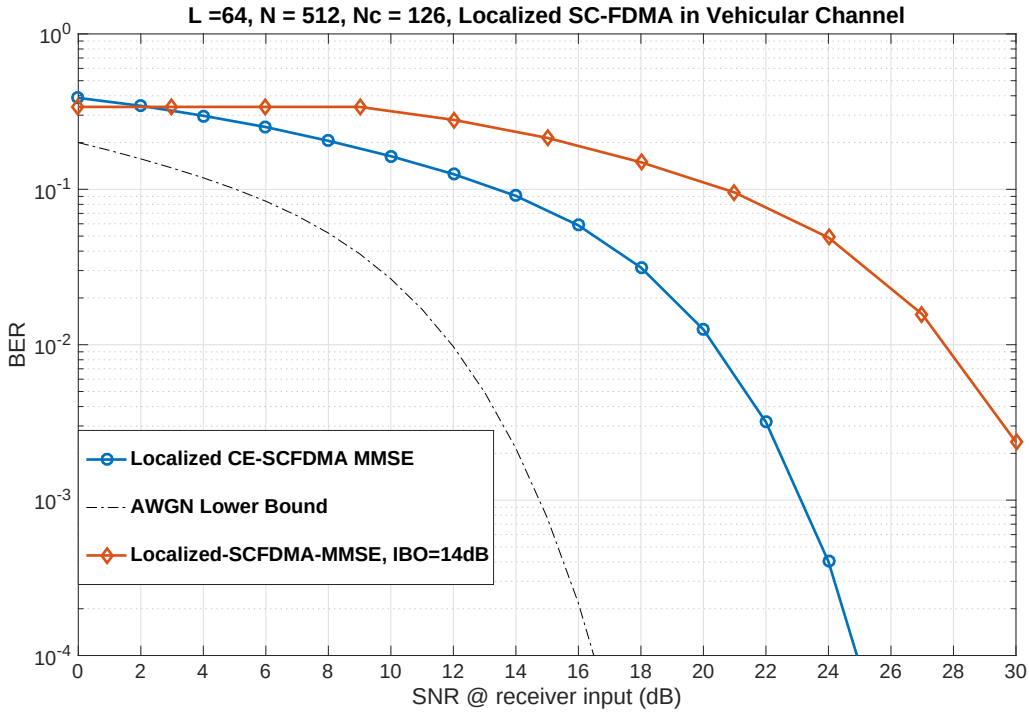

Figure 3.19: Constant Envelope SCFDMA vs. SCFDMA in non-linear vehicular channel, L = 64, N = 512, $N_c = 126$, $2\pi h = 1.5$.

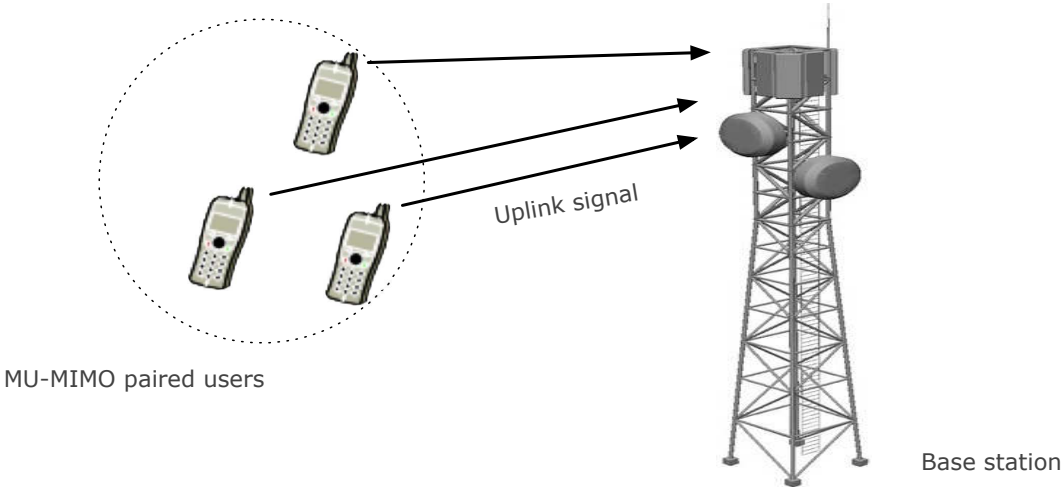

Figure 3.20: Multi-user MIMO user transmitting in LTE-A uplink scenario

3.3.2 Novel Minimum Conditioned Bit-Error Probability Receiver for SCFDMA

In this section, the cost-function for the proposed minimum conditioned bit-error probability (MCBEP) receiver in MU-MIMO SC-FDMA systems will be derived. Unlike classical

linear detectors that aim at maximizing signal-to-interference-noise-ratio (SINR) in multi-user environment, the proposed MCBEP receiver targets the minimization of conditioned bit-error-rate at the output of MUD with computational complexity more-or-less the same as linear MMSE. State-of-the-art show such criterion based on minimum-BER provides close to optimal results.

The frequency domain equalizer weights W are to demodulate the signal at receiver after removal of cyclic prefix and N-point FFT F_N operation, as shown in Fig. 3.21 . The decision variable $\hat{X_k}$ for k-th user is obtained after detection is performed with the help of the derived weights W_k.

The MUD output $\hat{X_k}$is given by,

$$\hat{X_k} = W_k^H HY + W_k^H Z \tag{3.27}$$

where $(\cdot)^H$ is hermitian operator.

$$\hat{X_k} = \hat{S_k} + \hat{Z_k} \tag{3.28}$$

where $\hat{S_k} = W_k^H HY$ and $\hat{Z_k} = W_k^H Z$.

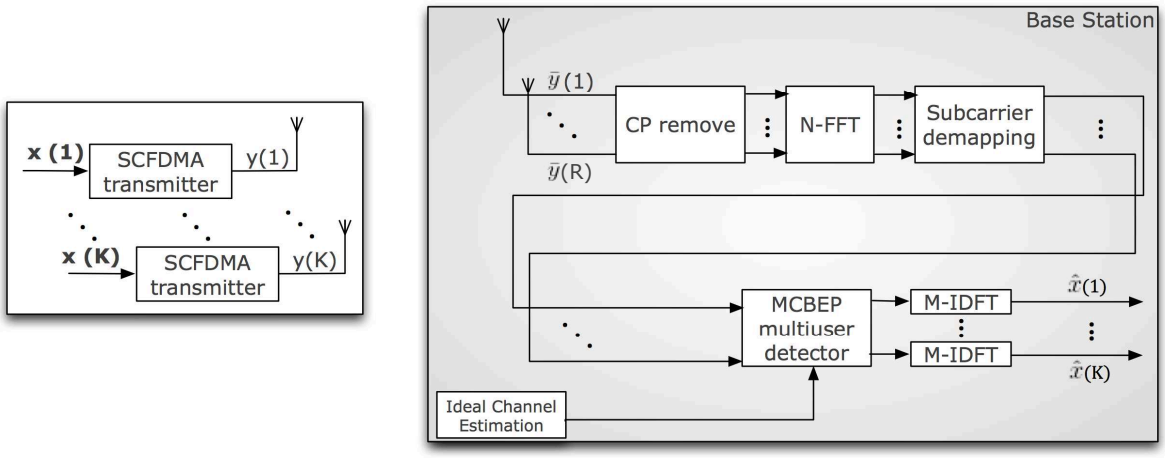

Figure 3.21: Block Diagram of MU-MIMO SCFDMA with receiver equipped with proposed MCBEP MUD.

Performing M-point IDFT F'_M on the noiseless signal $\hat{X_k}$ at the output of MUD for k-th user, the signal $\hat{x_k}$ is passed to decision device.

For only real-valued modulations like cosidered BPSK, the probability of error after decision depends on the real part of decision variable $\hat{x_k}$. The probability density function (PDF) of noisy received signal is the mixture of gaussian distributions associated with each possible symbol transmitted by all the users. The conditional probability of error

MUD takes the μ_k^+ as the mean of $\Re(\hat{S}_k)$ when user k transmits symbol $x_k = 1$, and the mean is μ_k^- when $x_k = -1$. We can write as,

$$\mu_k^+ = \Re\left(\hat{S}_k | x_k = 1\right) \tag{3.29}$$

$$\mu_k^- = \Re\left(\hat{S}_k | x_k = -1\right) \tag{3.30}$$

The effective noise variance of $\hat{Z}$ in (3.28) is given as,

$$\sigma_k^2 = \sigma^2 \left\|W_k\right\|^2 \tag{3.31}$$

The symbols in BPSK are assumed to be equiprobable and with the help of BPSK error probability reported in [46], the conditional bit error probability for BPSK is given as,

$$P_b^c = \frac{1}{2} Q\left(\frac{\mu_k^+}{\sigma_k}\right) + \frac{1}{2} Q\left(-\frac{\mu_k^-}{\sigma_k}\right) \tag{3.32}$$

where $Q(v) = \frac{1}{\sqrt{2}} \int_v^\infty e^{-\frac{t^2}{2}} dt \, , v > 0$. The proposed MCBEP algorithm computes the filter weights W for all the transmit users by minimizing the bit-error probability as given in (3.32). Hence the MCBEP solution is,

$$W_k^c = \arg \min_{W_k} P_b^c \tag{3.33}$$

W_k^c are the weights obtained as a result of minimization of P_b^c. The superscript in W_k^c is acronym for "*conditional*". The MCBER algorithm minimizes the conditional probability given in eq (3.32) with the help of an optimization rule. Different optimization strategies are reported in the literature, namely conjugate gradient descent (CG) [33], genetic algorithm (GA) [13] etc. We will use conugate gradient descent (CG) approach that first computes the conjugate gradient of cost function and iteratively reaches the minima with step size equal to λ. For the i-th iteration with step size λ, we have

$$W_k^c(i+1) = W_k^c(i) - \lambda\left(\bigtriangledown P_{k|\mathbf{x}}\right) \tag{3.34}$$

$\bigtriangledown P_{k|\mathbf{x}}$ is the gradient of (3.32) and can be expressed in full form as,

$$\begin{aligned} \bigtriangledown P_{k|\mathbf{x}} = & -\frac{1}{2\sqrt{2}} exp\left(-\frac{(\mu_k^+)^2}{2\sigma_k^2}\right) \cdot \frac{1}{\sigma_k} \cdot \left(H\mathbf{x}|_{\mathbf{x_k=1}} - \frac{\mu_\mathbf{k}^+ \cdot \mathbf{w}}{\|\mathbf{w}\|^\mathbf{2}}\right) \\ & + \frac{1}{2\sqrt{2}} exp\left(-\frac{(\mu_k^-)^2}{2\sigma_k^2}\right) \cdot \frac{1}{\sigma_k} \cdot \left(H\mathbf{x}|_{\mathbf{x_k=-1}} - \frac{\mu_\mathbf{k}^- \cdot \mathbf{w}}{\|\mathbf{w}\|^\mathbf{2}}\right) \end{aligned} \tag{3.35}$$

The algorithm converges to optimal weights when (3.35) goes to zero or global minima. Step size λ should be adjusted properly because CG algorithm is senstive to step size.

Algorithm might not converge to minima with larger step size, whereas small size will take too long to reach the minima. At the output of MCBEP MUD, the noise-less multi-user signal is,

$$\hat{X}_c = {W_c}^H HY + {W_c}^H Z \tag{3.36}$$

$\hat{X}_c$ is the estimated vector without MUI and is passed to decision quantizer.

3.3.3 Comparison with other related approaches in terms of computational complexity

In our work, we compare the performance of our proposed receiver with other two state-of-the-art approaches, namely MMSE and Adaptive LMS based MMSE. The proposed MCBEP receiver algorithm is derived from MBER algorithm that has computational complexity exponential in the number of users, $O(2^K)$. The complexity is significantly reduced without noticeable loss in performance in case of MCBEP receiver that has computational complexity linear in the number of users comparable to LMS-based MMSE, $O(K)$. Computational complexity of ideal MMSE receiver is $O(K^3)$.

3.3.4 Simulation Results

The proposed MCBEP receiver is tested against state-of-the-art appraoches, namely ideal-MMSE and Least mean square (LMS)-MMSE. The simulations are performed in MATLAB environment and parameters are choosen based on 3rd generation partnership program (3GPP) LTE-A [51] uplink as listed in Tab. 3.3. The receiver antenna number is set equal to the number of users paired transmitting, i.e., $K = N_R$. The first series of simulation results is related to the convergence of the proposed receiver MCBEP. In Fig. 3.22, the measured bit-error probability versus iteration number is shown for the MCBEP MUD, considering 6 transmitting users and transmission per-bit SNR equal to 18dB. The convergence to the final value of the cost function is obtained after 30 iterations in the case of ideal CSI knowledge. For sake of comparison, convergence to the averaged Mean Squared Error (MSE) of the LMS-based MMSE is shown in Fig. 3.23. Under the same condition of noise and interference considered for MCBEP, the convergence of adaptive MMSE is slow and requires higher number of iterations to converge to minima. The convergence of MCBEP is lot faster with a simple-to-implement conjugate gradient algorithm. The second series of simulation results is related to BER performance of proposed MCBEP against the approaches mentioned in Tab. 3.3. The first use-case is single antenna two-user MU-MIMO. The BS forms the pair and allow the paired users to transmit over the same set of radio resource hence it is equivalent to 2x2 MU-MIMO

Table 3.3: Simulation Parameters

Bandwidth	5 MHz
Number of Subcarriers	512
CP length	36
Resource Blocks (RBs)	6
Subcarriers in RB	12
Subcarrier Spacing	15 KHz
Sampling frequency	7.68 MHz
Channel Estimation	Ideal
Channel Impulse response	Extended Vehicular A (EVA)
Transmitter Antennas (Users, K)	2, 4, 6, 8
Receiver Algorithm	MCBEP, MMSE, & LMS-MMSE
Step size (λ)	0.01

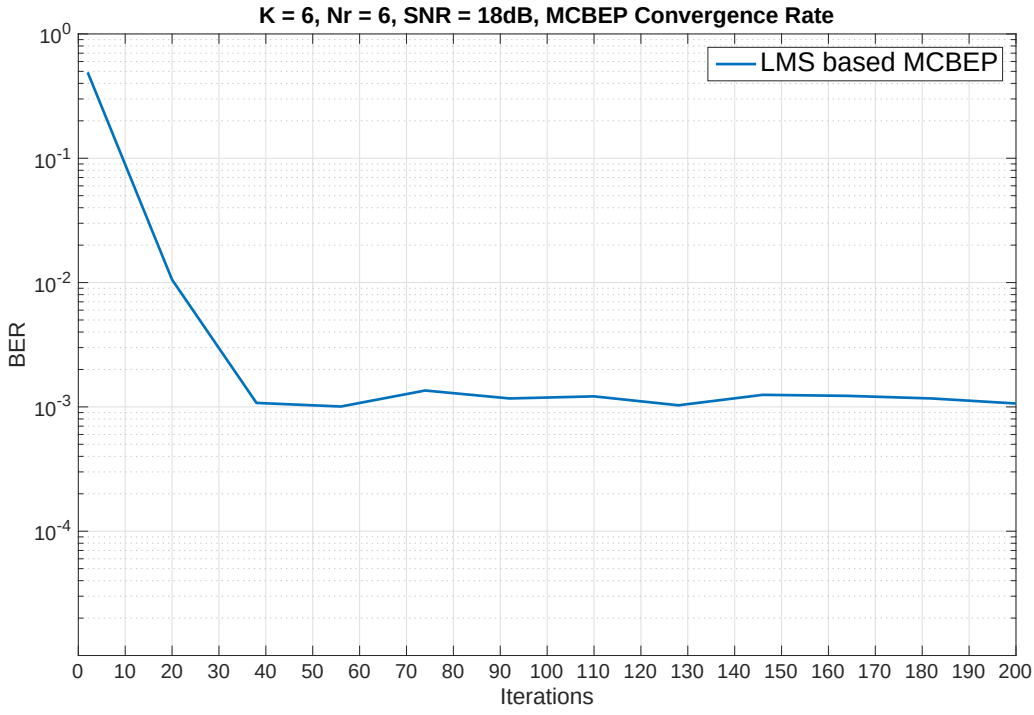

Figure 3.22: Convergence of MCBEP receiver with K=6, $N_R = 6$, SNR = 18dB

system. Due to low interference environment where only one user is causing interference to the other, the receiver is able to distinguish the uplink streams transmitted by users

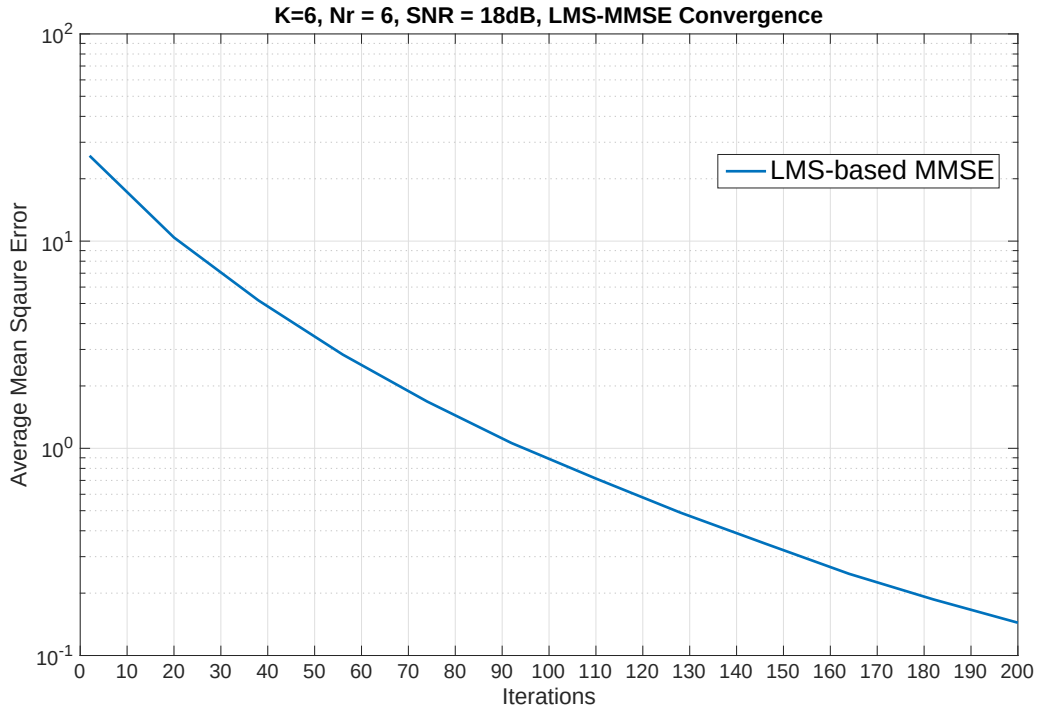

Figure 3.23: Convergence of LMS-based MMSE receiver with K=6, $N_R = 6$, SNR = 18dB

without much performance degradation, as evident in Fig. 3.24. The performance of proposed MCBEP is closer to SISO-AWGN bound and show improvement of around 3dB w.r.t ideal-MMSE MUD detector and $\sim$ 4dB over LMS-MMSE in interference-limited region (high-SNR regime). Exactly the same trend can be observed in Fig. 3.25 when number of paired users increased to 4, thus forming 4x4 MU-MIMO system. It can be seen that in noise-limited region (low SNR regime), the performance of all receivers is the same, whereas, in interference-limited region MCBEP outperforms ideal-MMSE and LMS-based MMSE by $\sim$ 3dB and $\sim$ 5dB, respectively. It is worth mentioning here that adaptive techniques based on maximization of SINR are unfavorable in cancelling the multiuser interference (MUI). The performance gap between MCBEP and ideal MMSE shrinks as the MUI in the system increases. As a consequence the probability density function (PDF) of decision variable is deteriorated due to MUI. Hence the ability with which the receiver detects the symbol reduces. However, MCBEP still manages to acheive 2dB gain over ideal MMSE in Fig. 3.26. The LMS-MMSE continues to perform poorer with increased MUI. Increasing the number of users to eight shows that MCBEP and ideal MMSE has performance quite close to each other (MCBEP shows $\sim$ 1dB of gain over ideal MMSE), Fig. 3.27. It is because, the interference term in the denominator of

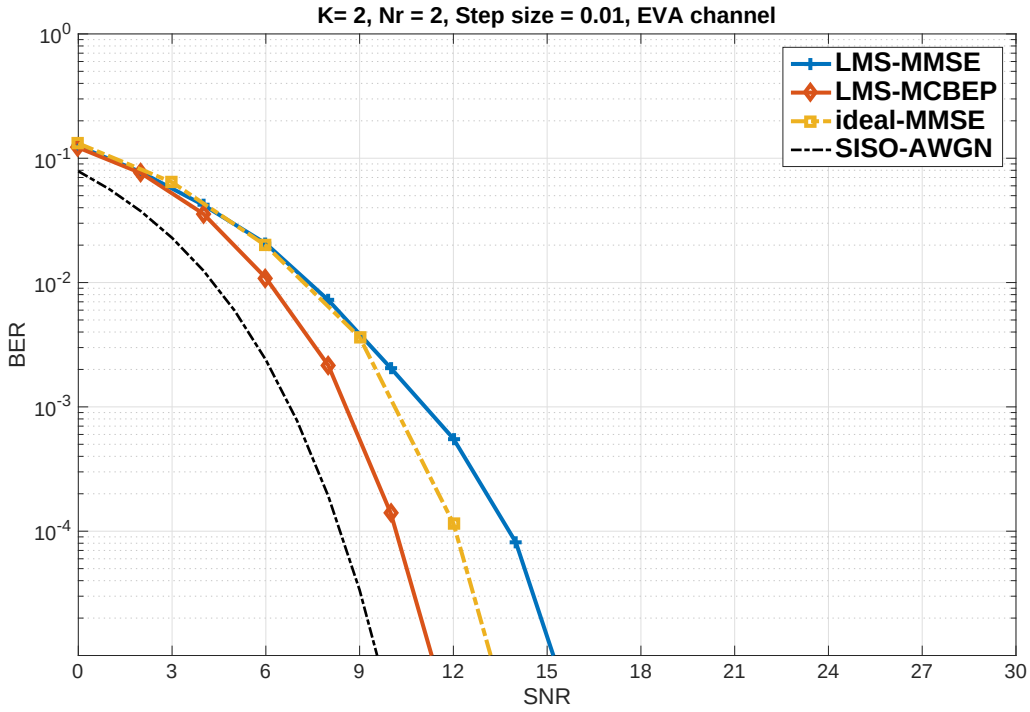

Figure 3.24: BER performance vs. SNR for $K = 2$ of MCBEP, ideal MMSE and adaptive MMSE MUD with ideal CSI knowledge at receiver

SINR becomes gaussian with increasing number of users. The performance of MCBEP is equal to that of ideal-MMSE in gaussian channels. The performance of LMS-MMSE receiver clearly shows suboptimality in high interference environments.

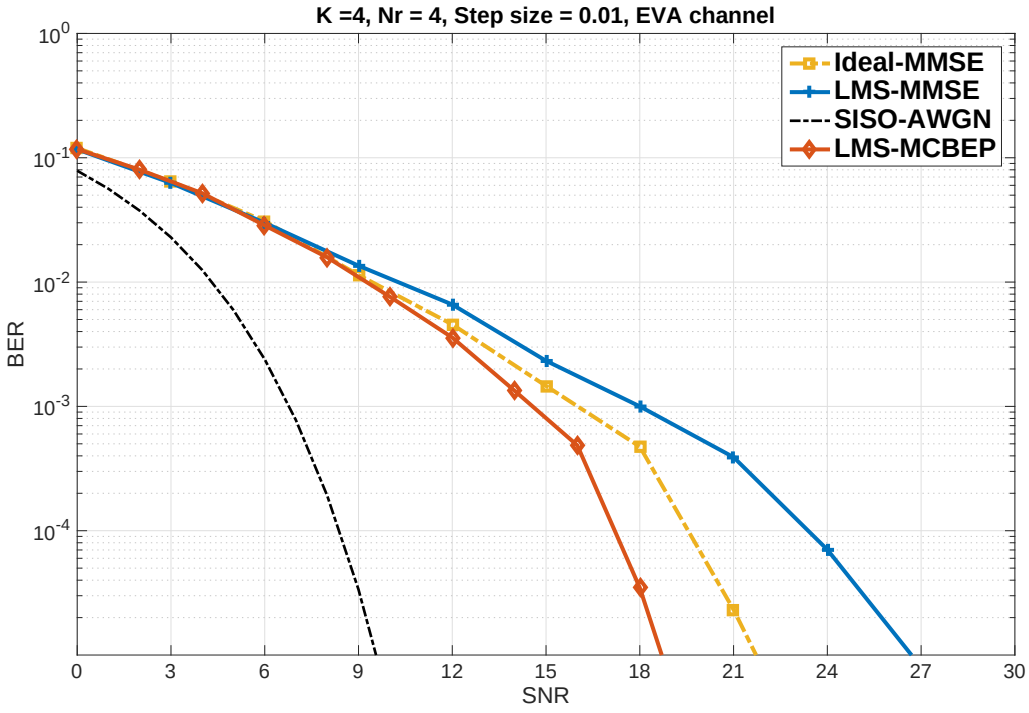

Figure 3.25: BER performance vs. SNR for $K = 4$ of MCBEP, ideal MMSE and adaptive MMSE MUD with ideal CSI knowledge at receiver

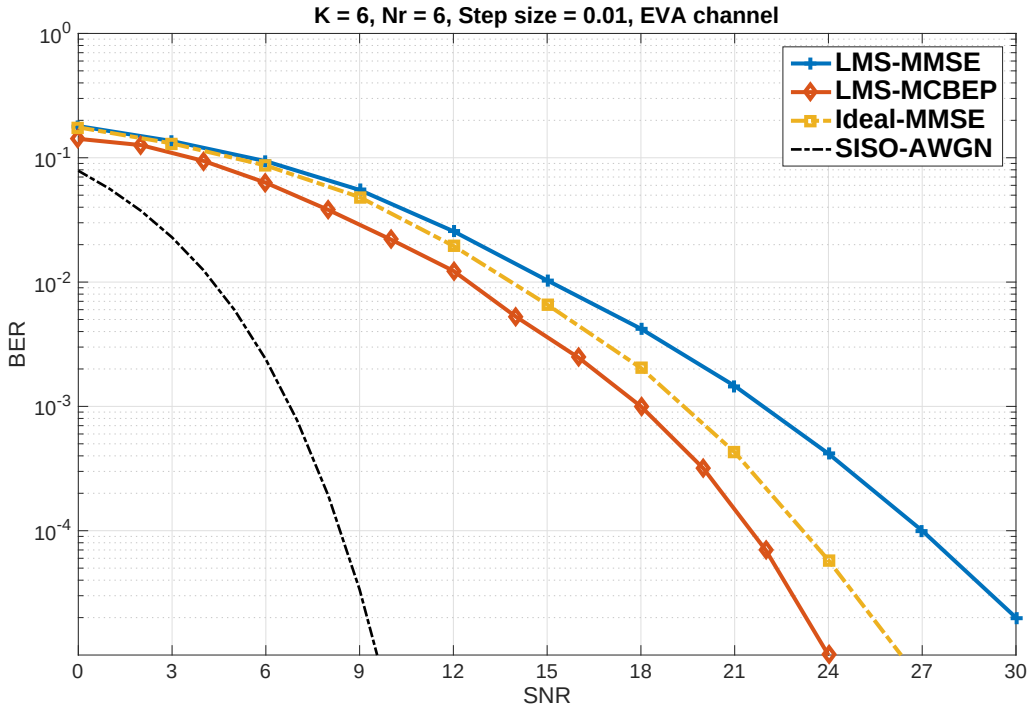

Figure 3.26: BER performance vs. SNR for $K = 6$ of MCBEP, ideal MMSE and adaptive MMSE MUD with ideal CSI knowledge at receiver

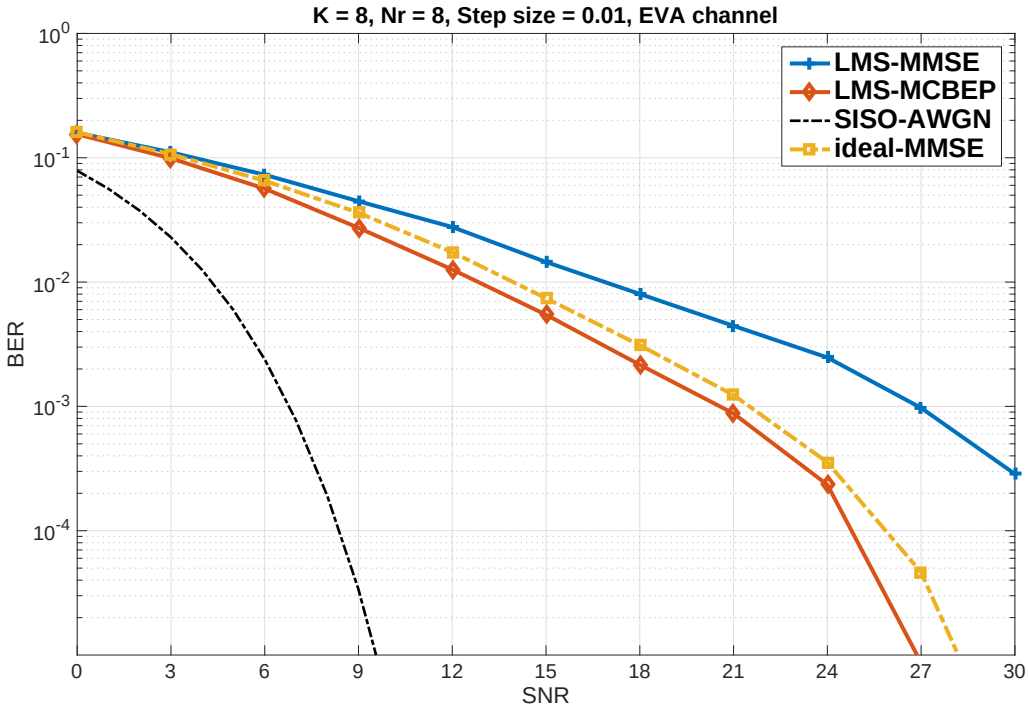

Figure 3.27: BER performance vs. SNR for $K = 8$ of MCBEP, ideal MMSE and adaptive MMSE MUD with ideal CSI knowledge at receiver

Chapter 4

Millimeter wave backhaul for LTE-A small cell

This chapter aims at describing waveform design for wireless backhaul in LTE-A. Wireless links are categorised into line of sight (LOS) and non line of sight (NLOS) links. Currently use microwave frequency bands are too congested to provide high data rates. In order to have wireless gigabit links, higher frequency bands (esp. millimeter wave bands) should be explored due to huge availability of bandwidth. Of millimeter wave (mmWave) frequency bands, 73GHz range or E-band is of particular interest where as high as 10GHz (5GHz each in 73GHz and 83GHz) of free band is available. Making use of it will help in achieving gigabits over wireless links. On the other hand, numerous issues are associated with the wave propagation in E-band, such as atmospheric effects, multipath channel for NLOS links, hardware design for high frequency operations, etc. These challenges are directly related to design of physical layer transmission scheme.

Keeping in mind the issues related to propagation in E-band and efficient use of large bandwidth, ultrawide band (UWB) techniques should be employed. Impulse radio (IR) concepts have been discussed in literature for quite some time and, are known for their low complexity hardware design and efficient use of ultrawide bandwidth. For LOS link, IR techniques are promising because of almost negligible multipath attenuation and atmospheric effects. Impulse radio based on pulse position modulation (PPM) is conceived for LOS backhaul applications where time hopping (TH) is used for multiple access in point-to-multipoint case (P-t-mP). Such a technique is useful in a scenario where base stations are in clear LOS. However, IR performance degrades drastically in NLOS multipath channels. Moreover, despite simple transceiver architecture, IR requires expensive oscillators that are characterized by low phase noise levels.

To counter NLOS multipath channel effects in E-band, a robust transmission technique has to be considered that should be able to provide adequate performance to meet

backhaul requirements. Because of multiple echoes received at the receiver in NLOS case, space-time MIMO techniques can help in attaining significant diversity gains. Therefore, Space time block codes (Alamouti's codes) are able to achieve diversity gains but only for small number of antennas. The performance deteriorates significantly for large antenna arrays. Also the maximum achievable rate with Alamouti's codes is 1. Another form of MIMO technique is spatial multiplexing aiming to boost data rates by transmitting independent information stream from different antennas. However spatial multiplexing requires high signal to noise ratio (SNR) at the receiver for its performance. Hence there is a need to strike a tradeoff between space time codes and spatial multiplexing to have not just the diversity gain but also rate improvement. In this regard, space-time shift keying (STSK) has recently been proposed for applications where both diversity and multiplexing gains are desired. STSK techniques together with multicarrier (OFDM) and single carrier (SC) modulation are studied for NLOS backhaul. Because of severe multipath characteristics in mmWave, diversity gains improving error rate at the receiver is essential and at the same multiplexing gains are also desired to meet backhaul rate requirements. STSK with OFDM and SC is able to meet NLOS backhauls by striking a flexible tradeoff between diversity and multiplexing. Techniques like OFDM and SC in the STSK context are considered for point-to-point (P-t-P) case in this study. However for P-t-mP case, OFDM can employ FDMA or TDMA and TDMA with SC.

In the following section, TH-IR technique with PPM is discussed for LOS backhaul mmWave channels. Later, STSK techniques are with OFDM and SC are considered for NLOS backhaul connections. Simulation results are presented in all case scenarios.

4.1 Time Hopping Impulse Radio (TH-IR) for mmWave LOS Backhaul

As millimeter-wave spectrums have wider frequencies, they allow a larger band to be used for higher capacity transmission. The E-band in particular is called an atmospheric window and has low attenuation caused by water vapor and oxygen which makes it attractive for multi-gigabit radio communications. In addition, the high frequencies provide high rectilinearity and resistance to interference from other systems. UWB impulse radio techniques are discussed in this section because of their simple transceiver architecture and adequate line of sight propagation characteristics.

4.1.1 Impulse Radio Waveforms

Impulse radio technology eliminates the needs for an up-and-down converter composed of a modulator, demodulator, oscillator, multiplier and mixer which used in conventional radio technologies and allows for size reduction facilitating simple configurations and low power consumptions. Implementing those components at very high frequencies (mmWave) is also not trivial and it can demand technologies that cannot be easily integrated. The additional jitter related to the high phase noise of these typical components could also be challenging.

Impulse radio (IR) signaling, a form of ultra-wide-band (UWB) signaling, communicates with baseband pulses of short duration typically in the ranges of nanoseconds. Therefore, it spreads the energy of the radio signal very thinly from near DC to very few gigahertz. In E-band spectrum, huge bandwidth can be made available for IR communications without causing interference. Impulse radio systems employ nonsinusoidal wave shapes that should have certain properties when transmitted from the antenna.

Several nondamped waveforms have been proposed in the literature for IR-UWB systems, such as Gaussian, Rayleigh, Laplacian, cubic waveforms, and modified Hermitian monocycles [112]. In all these waveforms the goal is to obtain a nearly flat frequency domain spectrum of the transmitted signal over the bandwidth of the pulse and to avoid a DC component. Gaussian waveforms, whose mathematical descriptions are similar to Gauss function, are the most prominent ones among all. The zero-mean Gauss function is described by the following equation, where σ is the standard deviation:

$$G(x) = \frac{1}{\sqrt{2\pi\sigma^2}} e^{-x^2/2\sigma^2} \tag{4.1}$$

The basis of these Gaussian waveforms is a Gaussian pulse represented by the following equation:

$$y_{g1}(t) = k_1 e^{-(t/\tau)^2} \tag{4.2}$$

where $-\infty < t < \infty$, τ is the time-scaling factor, and k_1 is a constant. More waveforms can be created by a sort of high-pass filtering of this Gaussian pulse. Filtering acts in a manner similar to taking the derivative of $y_{g1}(t)$. For example, a Gaussian monocycle, the first derivative of a Gaussian pulse, has the form:

$$y_{g2}(t) = k_2 \frac{-2t}{\tau^2} e^{-(t/\tau)^2} \tag{4.3}$$

A Gaussian monocycle has a single zero crossing. Further derivatives yield additional zero crossings, one additional zero crossing for each additional derivative. If the value of is fixed, by taking an additional derivative, the fractional bandwidth decreases, while the centre frequency increases [112] [42]. A Gaussian doublet also called a doublet in IR

communication, as shown in Fig. 4.1 is the second derivative of y_{g2} and is defined by:

$$y_{g3}(t) = k_3 \frac{-2}{\tau^2}(1 - \frac{2t^2}{\tau^2})e^{-(t/\tau)^2} \tag{4.4}$$

Transmitting the pulses directly sent to the antennas results in the pulses being filtered due to the properties of the antennas. This filtering operation can be modeled as a derivative. The same effect occurs at the receiving antenna. The idealized received pulse shape can be written as;

$$p_{rx} = [1 - 4\pi(\frac{t}{\tau})^2]e^{-2\pi(t/\tau)^2} \tag{4.5}$$

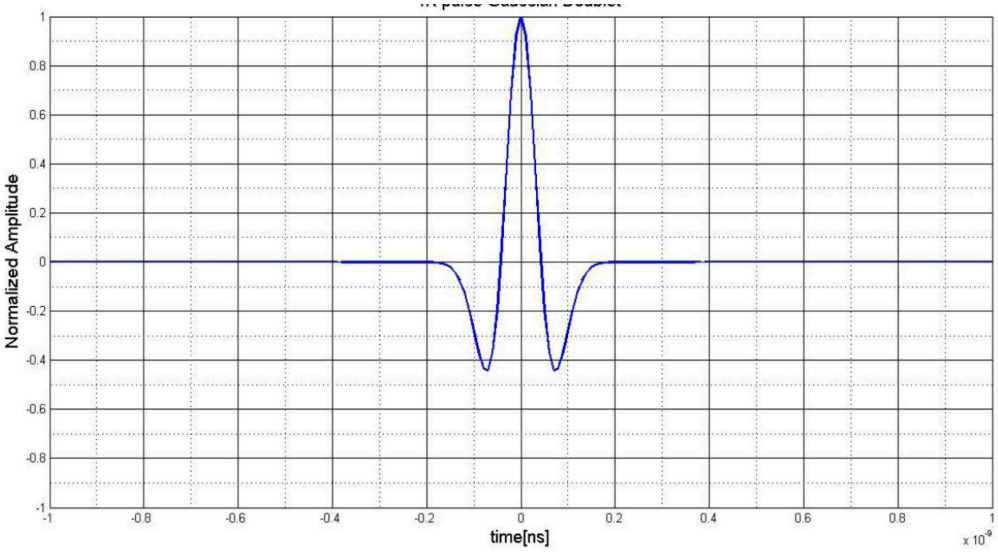

Figure 4.1: IR Gaussian Doublet

When designing the waveforms for desired application, the center frequency and available bandwidth are things which need to be taken into account. The duration of the pulses in time domain determines the bandwidth.

Since one pulse by itself does not communicate a lot of information. Information or data needs to be modulated onto a sequence of pulses called a pulse train. When pulses are sent at regular intervals, another important parameter called pulse repetition rate. In general pulse repetition is a characteristic that may determine the center frequency of a band of transmitted energy.

Sets of pulses which are used for the modulation of digital information onto analog pulse shapes. These sequences of pulses, called pulse trains, which will be able to transmit much larger volumes of information than a single set of pulses. In general, an unmodulated pulse train $s(t)$ with regular pulse output can be written as:

$$s(t) = \sum_{n=-\infty}^{\infty} p(t - nT) \tag{4.6}$$

where T is the pulse-spacing interval and $p(t)$ is the basic pulse.

4.1.2 Impulse Radio Modulation Formats

Impulse radio modulation is based on continuous transmission of very short time pulses where each pulse has an ultra wide spectral occupation in the frequency domain. IR radio modulation techniques are normally categorized into two named time-based technique and pulse-based technique as depicted below.

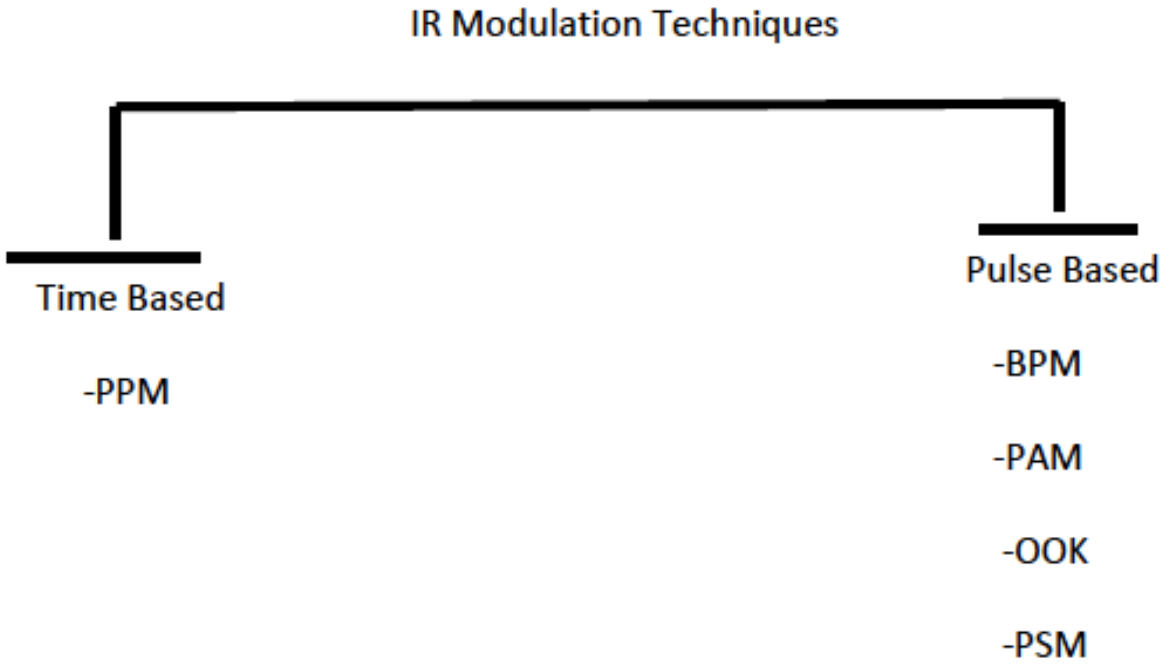

Figure 4.2: Impulse radio Modulation techniques

Bi-Phase Modulation (BPM) is to invert the pulse, that is, to create a pulse with opposite phase. Even though BPM in comparison with pulse positon modulation (PPM) has the 3 dB gain in power efficiency, it is a binary modulation and can not be scaled to multi-level to send multiple bits per symbol to increase data rate. Similarly, on-off keying (OOK) modulation technique, where the absence or presence of a pulse signifies the digital information of '0' or '1', respectively, is simpler to implement but binary only

and has low noise immunity. Pulse amplitude modulation (PAM) is the preferred for short-range IR communications normally. The motive behind this fact is, an amplitude-modulated signal which has smaller amplitude is more susceptible to noise interference than its larger-amplitude counterpart. In addition, more power is required to transmit the higher-amplitude pulse. In sinusoidal systems, AM systems are usually characterized by a relatively low bandwidth requirement and power inefficiency in comparison with angle modulation schemes. Thus, the major advantage (low bandwidth) can be seen to be anti-ethical to IR, as power efficiency is of high importance.

The other interesting modulation technique is Pulse Shape Modulation (e.g. orthogonal pulse modulation (OPM)) which requires special pulse shapes to be generated which are orthogonal to each other. Even though using orthogonal pulses has an advantage for multiple access techniques, it is more complex than the other methods.

By far the most common method of modulation in the literature is pulse position modulation (PPM) where each pulse is delayed or sent in advance of a regular time scale. Thus, a binary communication system can be established with a forward or backward shift in time. By specifying specific time delays for each pulse, an M-ary system can be created. The advantages of PPM mainly arise from its simplicity and the ease with which the delay may be controlled. But, for IR system extremely fine time control is necessary to modulate pulses to sub-nanosecond accuracy.

4.1.3 Time Hopping Impulse radio Transceiver Architecture

In [98, 63, 83] two main approaches have been identified for achieving a pass-band UWB transmitter at mmWave:

1. generation of narrowband pulses following an up conversion stage to E band frequencies [98];

2. generation of pulses with a bandwidth in the order of hundreds of GHz followed by a band-pass filtering stage which puts the signal spectrum around the desired center frequency [63, 83].

The first transceiver architecture contains local oscillators, mixers and millimeter wave bandpass filtering stages in the common UWB transmission chain (and also in the receiving chain). A pulse generator generates pulses of width 350ps for conventional microwave sub-10GHz UWB wireless systems that are translated to millimeter wave frequency band followed by amplification and filtering. The presence of oscillators and mixer increases the implementation complexity and hence the overall costs. On the other hand, the pulse is not affected by shape distortions.

In the second architecture the transceiver has a very simple configuration, consisting of a Wavelet Generator (WG) and a Power Amplifier (PA) in the transmitter. The WG has only a Pulse Generator (PG) and a Band Pass Filter (BPF). Unlike in conventional transceivers, oscillators and mixer are not required in the system. For a transmitter operating at E band, the PG needs to generate picoseconds pulses. The BPF filters a wide spectrum of the pulses to match the spectrum mask and create a narrowband signal. The pulse generator can be implemented through logic gates (XOR or NAND). This architecture needs a strict control on ultra-short pulse generator in order to center the maximum of the pulse spectrum in the desired frequencies. An additional drawback is the need for high transmitter front-end amplification, being the largest part of the power lost during the filtering. Moreover, to prevent the pulse shape from the distortion, the BPF is very critical and must have a flat insertion loss and a small delay group variation in the selected pass-band.

In our system, we used a TH-IR UWB transmission using Gaussian pulses. In Fig. 4.3 and Fig. 4.4, the block diagram of the transceiver is shown.

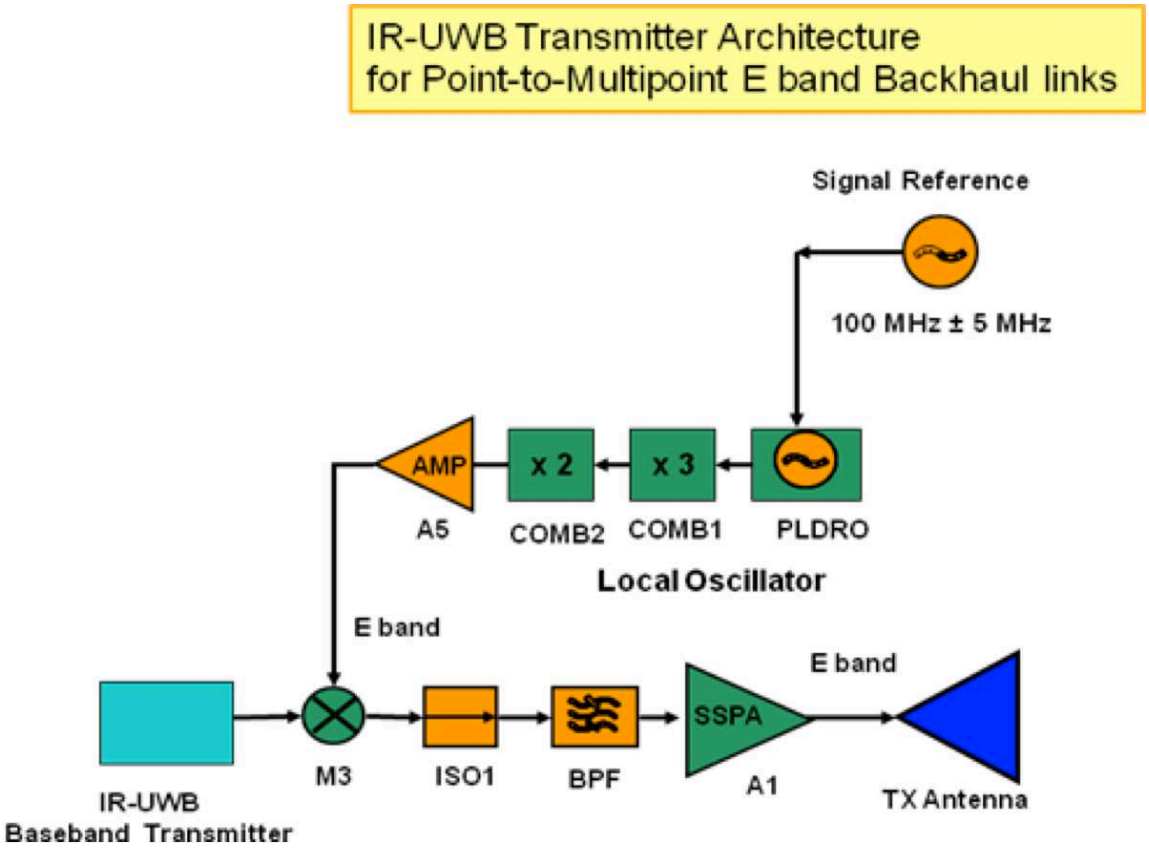

Figure 4.3: IR-UWB Transmitter Architecture E-band Backhauling

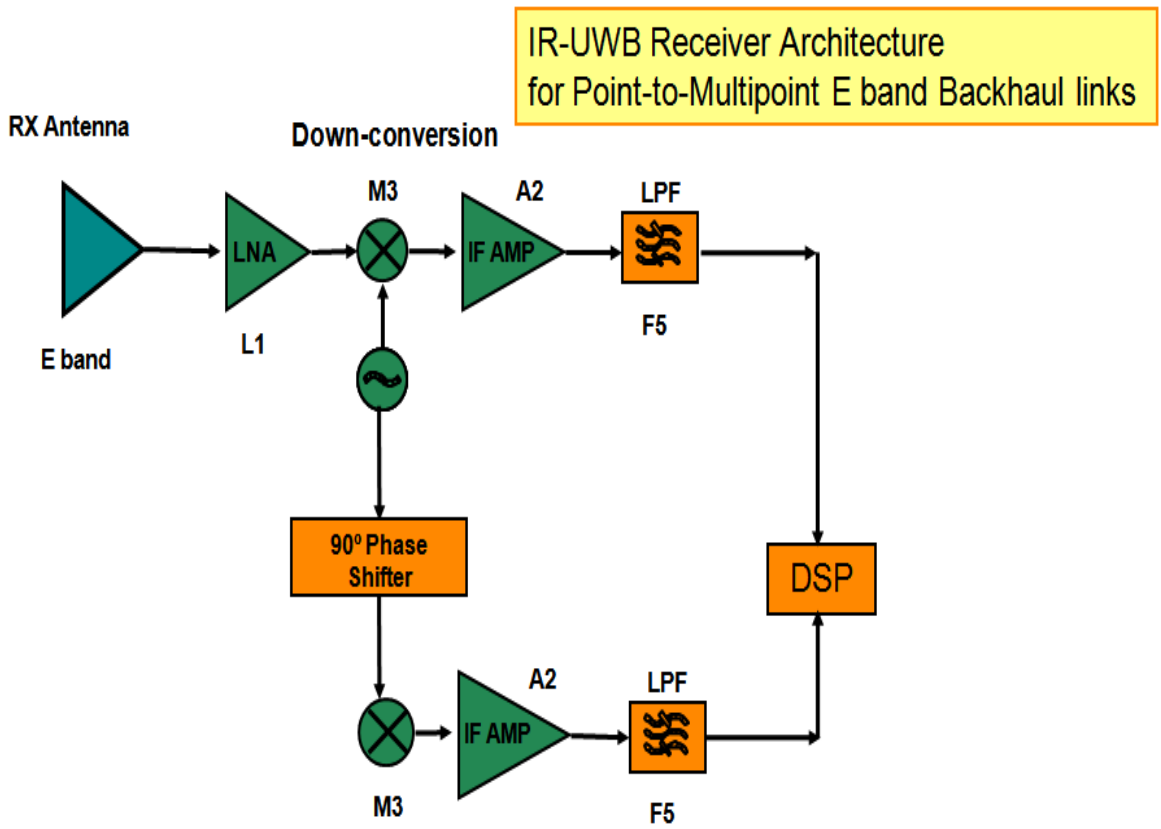

Figure 4.4: IR-UWB Receiver Architecture E-band Backhauling

The UWB baseband transmitter generates very short Gaussian monocycle pulses. In Fig. 4.5 the gaussian monocycle waveform is shown in the time domain, whereas in Fig. 4.6 the related spectrum is plotted.

One can notice at a glance the spectral efficiency of IR technique, allowing to efficiently occupy very large spectrum portions. One transmitted symbol is spread over N_s monocycles to achieve processing gain that may be used to counteract noise and RF distortions. To eliminate catastrophic collisions in multiple accessing, an additional time shift, unique to each user, is added to each pulse in the pulse train through the PPM technique: when the data symbol is 0, no additional time shift is modulated on the monocycle, otherwise (when the symbol is 1) a time shift of δ is added to the pulse waveform.

Therefore, the PPM TH-IR UWB signal for kth user is given by [20]:

$$s^{(k)}(t) = \sum_{j=-\infty}^{\infty} A^{(k)}_{d[j/N_s]} p(t - jT_f - c^{(k)}_j T_c - \delta^{(k)}_{[j/N_s]}) \tag{4.7}$$

where $A^{(k)}$ is the signal amplitude, $p(t)$ represents the second derivative of Gaussian pulse,

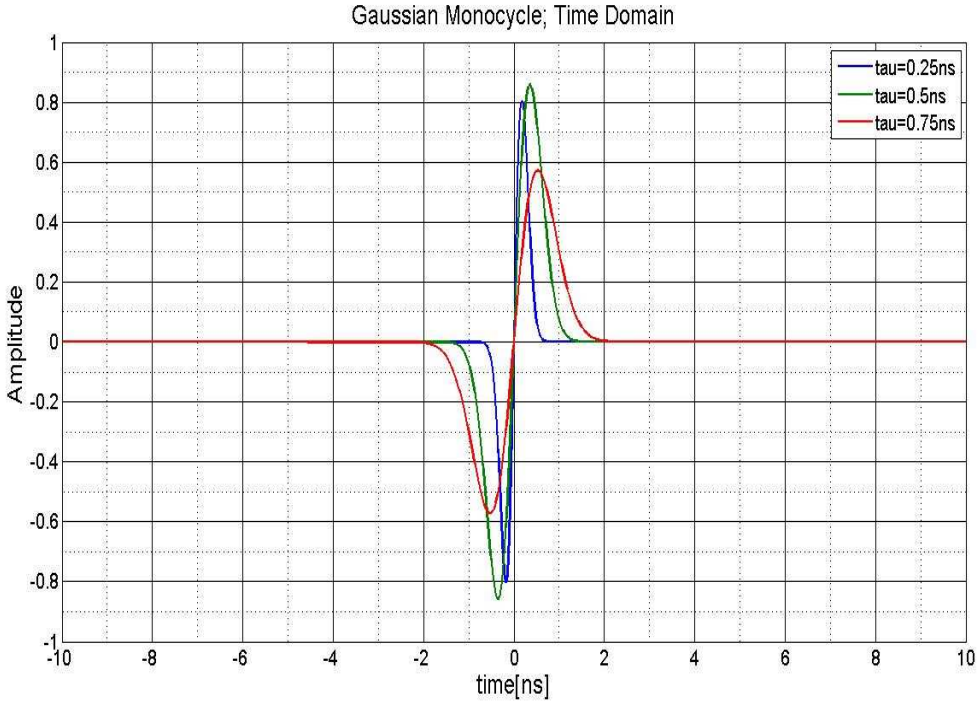

Figure 4.5: Time Domain Gaussian Monocycle

with pulse width T_p , T_f is the frame duration (a frame is divided into time slots with duration T_c). The pulse shift pattern $c_j^{(k)}$, $0 \leq c_j^{(k)} \leq N_{th}$ ($N_{th}T_c = T_f$) is the time hopping sequence for the k-th user and it is pseudorandom with period T_c . $\delta^{(k)}$ is the additional time shift introduced by PPM, as described above. The baseband signal is up-converted to E band, amplified by a SSPA and then transmitted. The UWB receiver uses a direct conversion scheme, thereby eliminating the need of image rejection filter and complicated phase synchronization circuits. In receiver, the received signal is first amplified by a LNA, and then it is down-converted to baseband by two E-band oscillators operating in phase and quadrature. I and Q components are low pass filtered and fed to the DSP (Digital Signal Processing) section, where they are combined, demodulated and decoded.

4.1.4 Simulation Results

The TH-IR backhaul transmission system working in E-band has been simulated in MATLAB environment. The simulations are conducted for pass-band systems, meaning that Radio Frequency (RF) chains are considered in the simulations. Hence, the most significant radio frequency impairment, phase noise effects on oscillator and mixers, is considered

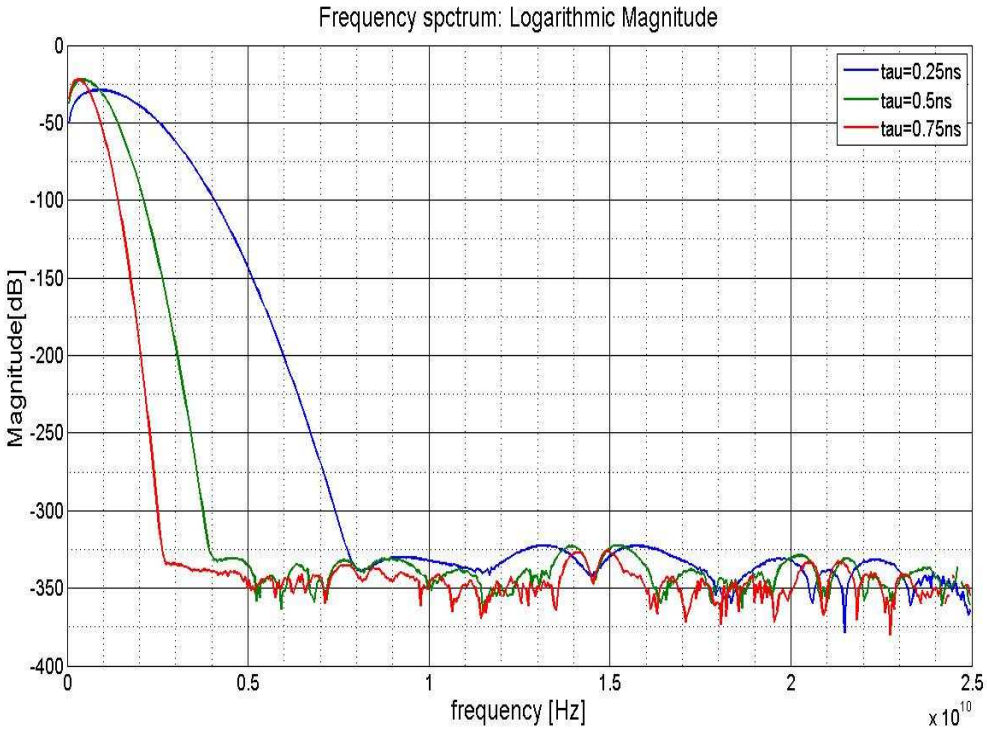

Figure 4.6: Frequency Domain Gaussian Monocycle

together with multi-user interference.

There are several ways of modeling the phase noise process such as an AR (AutoRegressive) filter based model, or by shaping the frequency response of phase noise according to some practical measurements using Leesons noise spectrum model described in [47]. The latter represents the most commonly employed model in practical applications. Such a model is based on two assumptions: i) the phase noise is assumed to be asymptotically stationary, and ii) the oscillator input perturbation u(t) is assumed to be white thermal noise. A more realistic and comprehensive model of phase-noise is given in [68] as:

$$S_{\phi}(f) = 10\log\left[\frac{2FkT}{P_c}\left\{1+\left(\frac{f_c}{2Q\Delta f}\right)^2\right\}\left(1+\frac{\Delta f_{1/f^3}}{|\Delta f|}\right)\right] \tag{4.8}$$

where F is noise factor of the active device, k is the Boltzmann Constant, T is temperature (K), P_c is the Average Carrier Power (W), f_c is centre carrier frequency, Δf represents low-frequency noise spectral components proportional to $1/f$ (like, e.g., flicker noise). Finally, $\Delta f_{1/f^3}$ is a parameter taking into account the presence of non-white noise components affecting the oscillators. The measured phase noise values (used for simulations) are [-100.2 dBc/Hz, -209.9 dBc/Hz] in correspondence of carrier offset frequencies range [1

MHz, 10 MHz].

A point-to-multipoint E-band LOS backhaul link considering 4 small-cells transmitting in the 73GHz band their backhaul information to a macro-cell whose distance in kilometer is a parameter d. The simulated model is a generalized one that can be upgraded to larger number of small cells. Hereinafter, we denote such a backhaul configuration with 4-1 that means four-to-one. The following link budget that is reasonable for terrestrial transmission systems operating in E-band is considered:

- Transmitted power: 1W;
- Aggregate channel data-rate: 4Gbit/sec;
- Channel coding: variable-rate Reed-Solomon (RS) coding;
- Modulation/demodulation losses: 4dB;
- TX/RX antenna gain: 24dBi;
- Gaseous absorption: 3dB/Km;
- Rain attenuation: 17.6 dB/Km; such a value has been derived by the ITU model for mm-wave rain attenuation [8], considering a rainfall intensity of 45 mm/h that is exceeded with a probability of $10^{-}4$ (see the statistical model for cumulative distribution of rain intensity proposed by Luini and Capsoni in [74]);
- Low-Noise Amplifier (LNA) gain: 21 dB;
- Receiver noise figure: 3.5dB.

Given the aforesaid link budget, the expression of the per-bit signal-to-noise available at the input of the demodulator with an availability percentage of 99.999% is given as follows:

$$\left(\frac{E_b}{N_0}\right)_{av} = 99.36 - 20\log_{10}(D_{mt}) - 0.02D_{mt} + \epsilon_{dB}(dB) \tag{4.9}$$

The first series of simulation results are related to the evaluation of the raw Bit-Error-Rate (BER) vs. Eb/N0 coming from the channel, before RS decoding. The ideal lower bound for our transmission system is a BPSK modulation with AWGN (blue curve), Fig. 4.7. We can notice that the performance loss due to Multi-User Interference (MUI), neglecting the effects of phase noise (red curve) ranges from 3dB at low Signal to Noise Ratio (SNR) to 6dB at higher SNR. As expected MUI bounds TH performance with an error-floor. Such an error-floor is more evident when phase noise is introduced and, consequentially, the MUI increases as the relative time jitter increases. In order to improve link performance and to reach the error-free condition, the Reed Solomon (RS) channel coding has been

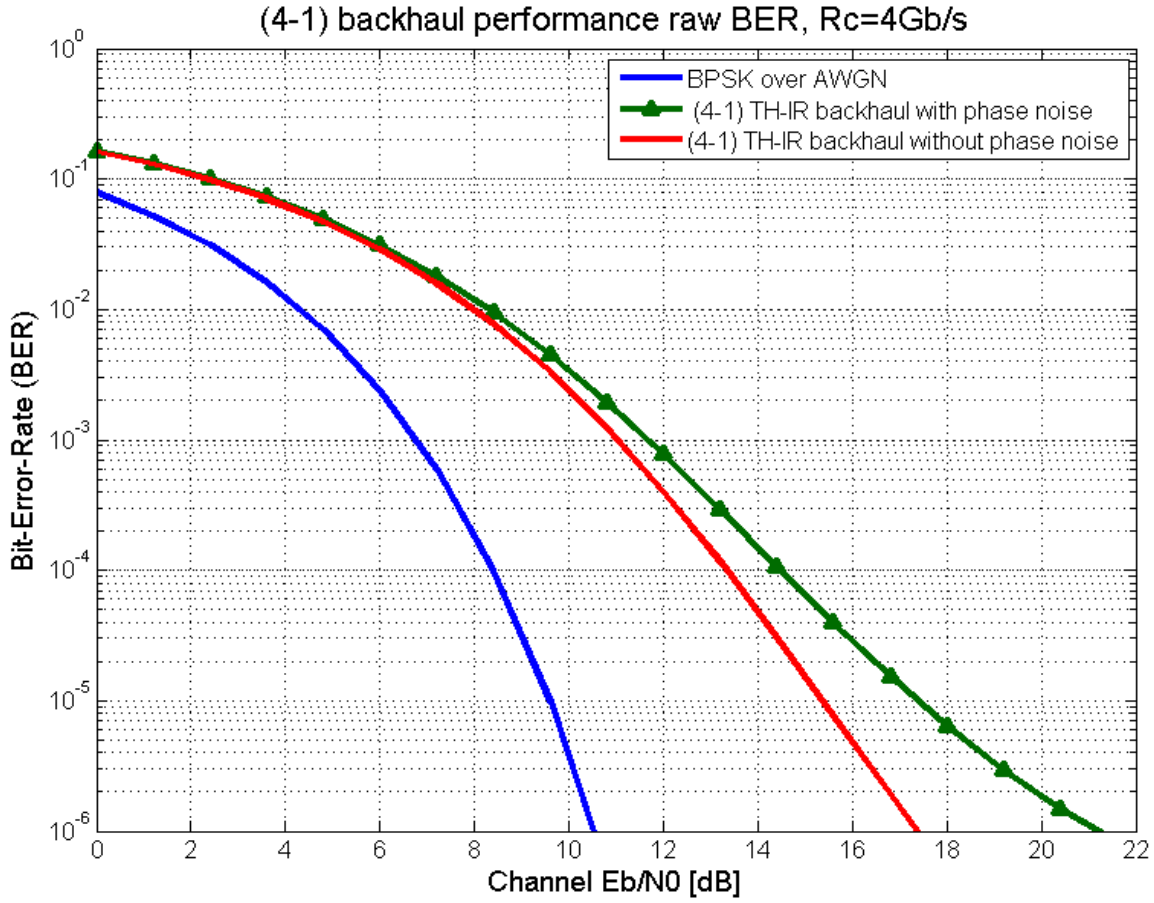

Figure 4.7: Raw (uncoded) BER performance vs. Eb/N0 of E-band 4-1 P-t-mP backhaul based on TH-IR

introduced in our system. RS coding is very simple to be implemented and quite effective also for high code rates, see Fig. 4.8. Variable code rates have been considered, namely:

- RS(31,29): code-rate Rc=0.935, free distance t=1;
- RS(31,27): code-rate Rc=0.871, free distance t=2;
- RS(31,25): code-rate Rc=0.806, free distance t=3;
- RS(31,23): code-rate Rc=0.742, free distance t=4.

Following the guidelines of [28], an error-free BER limit equal to 10^{-6} has been fixed (it is reasonable for an aggregate bit-rate of 4 Gb/s). Such a limit is reached by RS(31,29) code rate at Eb/N0 = 13.5dB, it is reached by RS(31,27) at Eb/N0=12dB, RS(31,25) at Eb/N0=11.25dB and RS(31,23) at Eb/N0=10.5dB as in Fig. 4.8. Link availability curve with 99.999% availability is derived in Fig. 4.9 with the help of (4.9) and coded BER

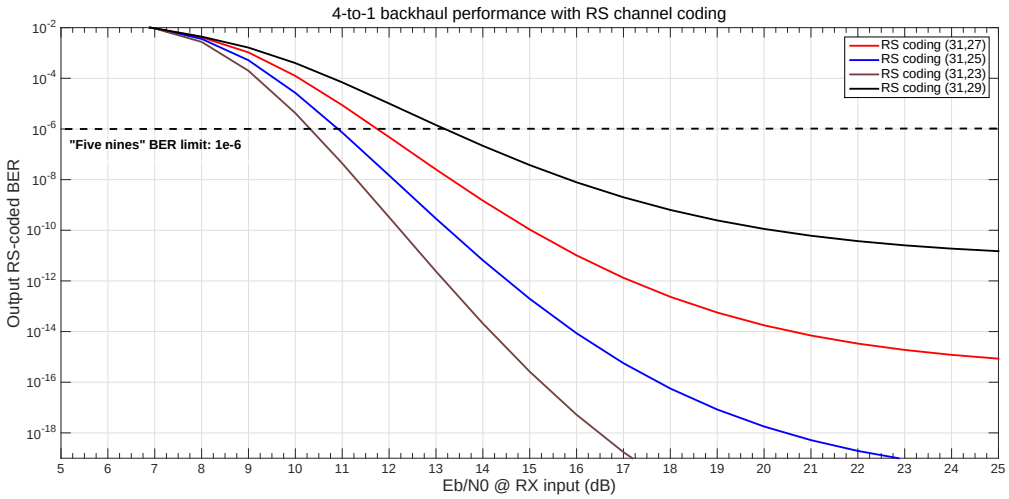

Figure 4.8: BER performance after RS decoding vs. Eb/N0 of E-band 4-1 P-t-mP backhaul based on TH-IR

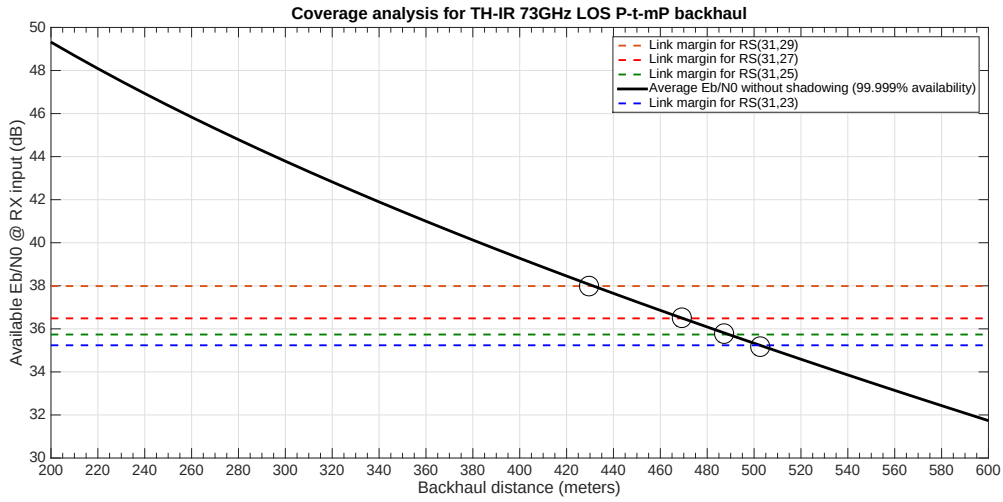

Figure 4.9: Eb/N0 with 99.999% availability vs. backhaul distance and derivation of backhaul coverage for different RS coding rates

data as in Fig. 4.8. The significance of this curve lies in the fact that it gives an idea of how much distance a backhaul link can attain w.r.t data rate. The maximum backhaul distance equal to 500m is reached using RS(31,23) coding with a net aggregate backhaul rate of 2.96 Gb/s. The maximum backhaul capacity of 3.48 Gb/s is reached by RS(31,27) coding at a backhaul distance of 470m. Considering the distances involved in LTE-A small cell backhauling (generally less than 1Km), such results are fully satisfactory in LOS scenario.

4.1.5 Conclusion

The work shows a feasible and effective solution for LOS small-cell wireless backhaul based on UWB TH-IR technique in E-band. Typical channel impairments affecting MM-wave transmission (rain fading, oxygen absorption, phase noise and timing jitter) have been considered in the simulations. Results have shown the capability of TH-IR of reaching a net capacity of 3.48 Gb/s at a distance of 500m in a point-to-multipoint 4-to-1 backhaul configuration. This strategy is feasible for a scenario where central hub (fibre connectivity to core network) makes a star-network with other small BSs over wireless link. TH-IR does not require expensive hardware as signal transmission is done without the need of upconverters. Such a low complexity design is advisable for small BS. In non line of sight (NLOS) the performance of TH-IR techniques degrades dramatically when one channel time delay becomes equal to δ. In case of NLOS, a robust transmission technique should be designed.

4.2 Space-Time MIMO techniques for mmWave NLOS Backhaul

Because the performance of TH-IR UWB is severely limited by non-ideal hardware components and by channel impairments [118], space time shift keying (STSK) techniques are proposed for non-line of sight (NLOS) backhaul. Space-time shift keying relies on dispersion of input energy in space and time dimensions, and harvest gains obtained as a result of multiplexing-gain trade-off. In the following subsection, state-of-the art related to space-time shift keying is discussed.

4.2.1 Related Background on ST-MIMO

The concept of multiple antennas for high data rates is orginated in 2003 when Paulraj in his paper [85] introduces MIMO applications to reach high capacity data rates in wireless fading channels. With multiple antennas in the system, diversity and/or multiplexing gain can be achieved [122]. For example space-time techniques, like space-time block codes (STBC) [12] and, linear dispersion codes (LDC) [50], provide time-diversity gains to the system. STBC provides maximum attainable diversity gain but performance degrades for higher number of transmit antenna elements. In [50], Hassibi *et al.* proposed space-time transmission scheme, called linear dispersion codes (LDC), that is capable of providing flexible trade-off between diversity and multiplexing gain without degrading much the performance. [85] proposes MIMO systems for high data rate applications. Multiple independent streams are multiplexed over multiple antennas. At the receiver, multi-

stream detection is performed to seperate the information streams. However, optimal receiver design (maximum likelihood) is very complex for high order of modulations with medium antenna arrays. Vertical bell laboratories layered space-time (V-BLAST) [**?**] architecture is proposed to achieve significant data rates over rich scattering environments. However, the architecture is still too complex and performance requires high SNR at the receiver.

To overcome the issue of complex receiver design, another variant of MIMO is proposed in [79, 80], called spatial modulation (SM), in which only one out of M transmit antennas is activated for each symbol. Hence ICI is negligible and making maximum liklihood (ML) complexity affordable for optimal performance. It has been reported in [79, 80] SM is capable of outperforming V-BLAST (where the performance is limited by ICI) and Alamouti's STBC (where the maximum feasible diversity order is MN where N is the receiver antennas.). Spatial modulation relies on receive antenna elements in order to combat fading channels. Also to increase transmission rate, the number of transmitting antenna has to be increased exponentially.

Space-time shift keying (STSK) is proposed in [99] that utilizes both space and time dimensions, based on SM and LDC principle of [50]. In contrast to SM, STSK is about activation of Q space-time dispersion matrix within each STSK block duration. Because only single Q matrix is activated for an input symbol, ICI is significantly reduced. Hence STSK is capable of striking a flexible diversity versus multiplexing gain that is function of design of Q dispersion matrix, transmit and receive antennas. The authors in [99] further claimed that no ICI is generated with STSK technique hence single antenna ML detection can be employed for narrowband channels exploiting time-diversity to the fullest. The ML-complexity still poses no threat to wideband OFDM systems where each of the subcarriers is experiencing flat fading [34]. However the ML-complexity of SM/STSK is inevitably high in wideband single carrier systems (e.g., SC-CP and SC-FDMA) for increased number of taps [90]. Thus Single carrier SM/STSK systems have to resort to low complexity near-optimum receivers as proposed in [60].

To summarize the differences among different gain providing techniques, it is obvious that space time block codes (STBC) (Alamouti's codes) provide diversity by transmitting same information over space and time using pre-defined block codes. Spatial Multiplexing (SMUX) transmits independent streams from different antennas and hence increasing capacity by introducing multiplexing gains. Spatial modulation (SM) activates only one antenna in a given time and providing receiver diversity by reducing ICI and making optimal receiver complexity affordable. Space time shift keying (STSK) disperses the input symbol energy over space and time dimensions by designing dispersion matrix thus providing both diversity and multiplexing gains.

Based on the state-of-the art, a tree is constructed where the properties of each of the mentioned techniques is discussed in a hierarchical fashion as seen in, Fig. 4.10. The two extremes represent the diversity (STBC) and multiplexing (SMUX) gains whereas STSK/SM are better at providing the diversity-multiplexing trade-off. Such techniques will be dealt with single carrier (SCCP) and multicarrier waveforms (OFDM) in this work.

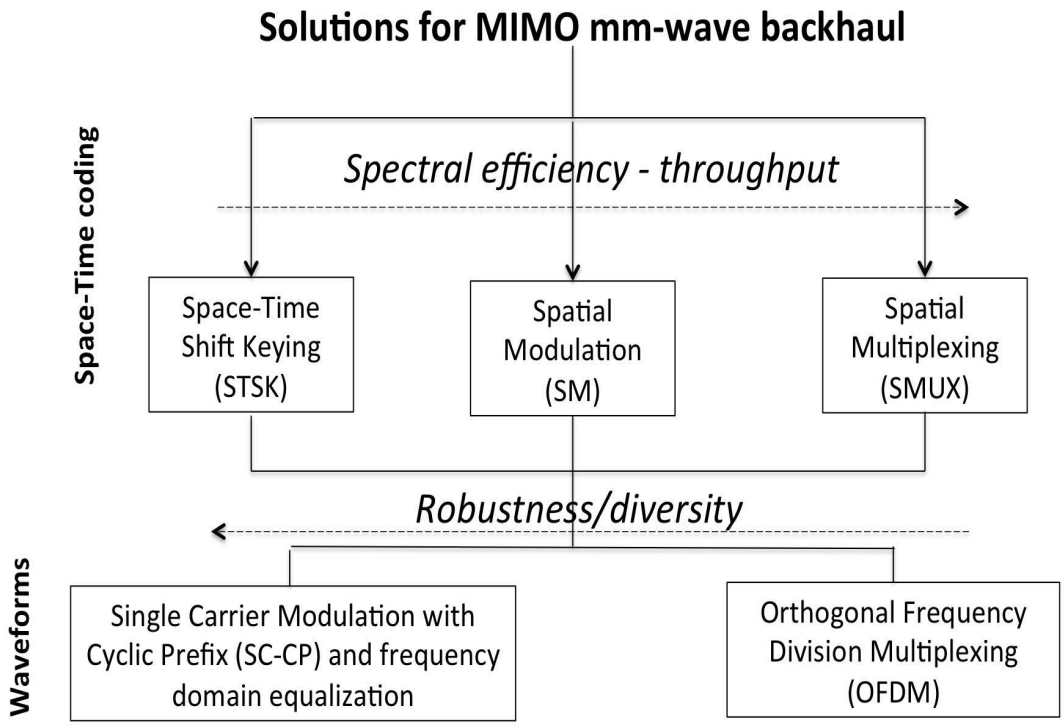

Figure 4.10: Hierarchical description of mmWave backhaul

All previous works that have been mentioned is considered in rich scattering environment at microwave frequency bands where enough echoes of transmitted signal manage to reach receiver and hence diversity gains are exploited. In order to have gigabit-link in the backhaul, millimeter wave bands are considered where the provision of GHz range band is possible. In contrast to channels observed at microwave band, at high frequency band (e.g., 73GHz) lesser number of resolvable multipath components (MPC) are detectable as

compare to that of at lower frequency bands. This is due to the smaller wavelength at high frequency bands that diffuse whenever face obstacle in the way [91] and channels do not exhibit Rayleigh "like" characteristics. Authors in [9] find that even in high NLOS mmWave environments, multiple antennas can be incorporated to leverage diversity and spatial multiplexing gains at different locations where multipath clusters are received.

The choice of E-band for backhaul is motivated in following section.

4.2.2 E-band as backhaul solution

Backhaul system performance is often characterized by availability of links and error rate. Cellular traffic generated inside a cell is transported to core network through backhaul. Availability of backhaul links is essential to guarantee throughput inside a cell. Hence user performance depends not only on access but also on backhaul. Unlike access, continuous link availability plays important role in evaluating backhaul performance. For this reason, high link availability of $\geq 99\%$ is desired in cellular network. For example 4G/LTE-A small cell network demands "*very high*" link availability of 99.999% or *five 9s* at BER less than 10^{-6}. Such analysis are very important when E-band wireless backhaul is being considered because of E-band links are vulnerable to propagation losses if transmission strategies is not well optimized to stand extreme environments.

E-band is of particular interest in mmWave bands because of the provisioning of 5GHz contiguous band in both 70Ghz and 80Ghz. More recently many private companies have commercialized some products for small cells backhauling. Notably CERAGON corporation (Paolo Alto, CA) has commercialized products for small cell backhaul in E-band. The FiberAir-70^{TM} for LOS PtP achieves aggregate data rate of 1Gbps at 81 GHz and the FiberAir-2500^{TM} for NLOS P-t-mP achieves 200Mbps at 6GHz. All these product rely on single carrier transmission technique. Such huge bandwidth paired with MIMO antenna array (4 to 256 elements) can be deployed for high capacity links. Agilent identifies E-band benefits that are summarized as follow :

1. Uncongested frequency band;
2. High antenna directivity with pencil beam;
3. Separate two frequency bands without interference concern;
4. Light licensing scheme;

Agilent [3] has categorized cellular standards based on scalable wireless backhaul solution in E-band. 4G/LTE-A falls in 1st generation of E-band backhaul, whereas future cellular standards are in 2nd and 3rd generation. Hence E-band wireless systems not only

overcome compatibility issues between ceullular generations but also provides scalable solution for wireless backhaul. The key points for first generation E-band wireless are :

- Single carrier modulation with BPSK/QPSK;
- Channel width can be fixed or variable (250MHz – 1GHz);
- Capacity should be less or equal to 1Gbps.

A robust transmission strategy, not only capable of minimizing RF impairments at mmWave but also efficiently exploits time-frequency diversity in mmWave multipath channels, deserves an intention. However, there are some challenges associated with E-band and backhaul that are needed to be addressed in the context of LTE-A small cell framework.

Challenges of E-band

1. Cost effective hardware (i.e. Power amplifier to operate in linear region);
2. Phase noise tolerance;
3. RF component cost for millimeter wave frequency bands;

Challenges of Backhaul (4G/LTE small cells)

1. Good enough link availability e.g., 99.999%;
2. Bit error rate lower than 10^{-6} in presence of phase noise and power amplifier non-linearity;
3. Capacity $\geq$ 500Mbps;

4.2.3 System Model

We are considering non line of sight (NLOS) millimeter wave channel in the backhaul with M transmitting (Tx) and N receiving (Rx) antennas. The tranmitter and receiver are both small base stations (BSs) mounting street poles. In case of NLOS scenario where multiple reflected rays are received at Rx, millimeter wave frequency selective channel is considered between each Tx-Rx antenna pair. In space-time system, the signal Y received at Rx in $i-th$ STSK block duration is

$$Y(i) = H(i)X(i) + Z(i) \tag{4.10}$$

where $Y(i) \in \mathbb{C}^{N\times T}$, $X(i) \in \mathbb{C}^{M\times T}$ is the transmit STSK signal in i-th block duration, $H \in \mathbb{C}^{N\times M}$ is the millimeter wave channel matrix generated as described in previous section, and $Z \in \mathbb{C}^{N\times T}$ is the zero-mean unit variance noise components at the receiver. The transmitted signal $X(i)$ is generated using Q dispersion matrix where input symbol

energy is spread over space M and time T, as shown in Fig 4.11. It can be expressed in mathematical form as

$$X = \boldsymbol{A}\boldsymbol{\kappa}_{q,l} \tag{4.11}$$

$$\boldsymbol{A} = [vec(A_1), \ldots, vec(A_Q)] \in \mathbb{C}^{MT \times Q} \tag{4.12}$$

where $\boldsymbol{\kappa}_{q,l}$ is the vector containing input K-QAM/PSK symbol k_l of index l in the q-th position, as

$$\boldsymbol{\kappa}_{q,l} = [0, \ldots, 0, k_l, 0, \ldots, 0] \tag{4.13}$$

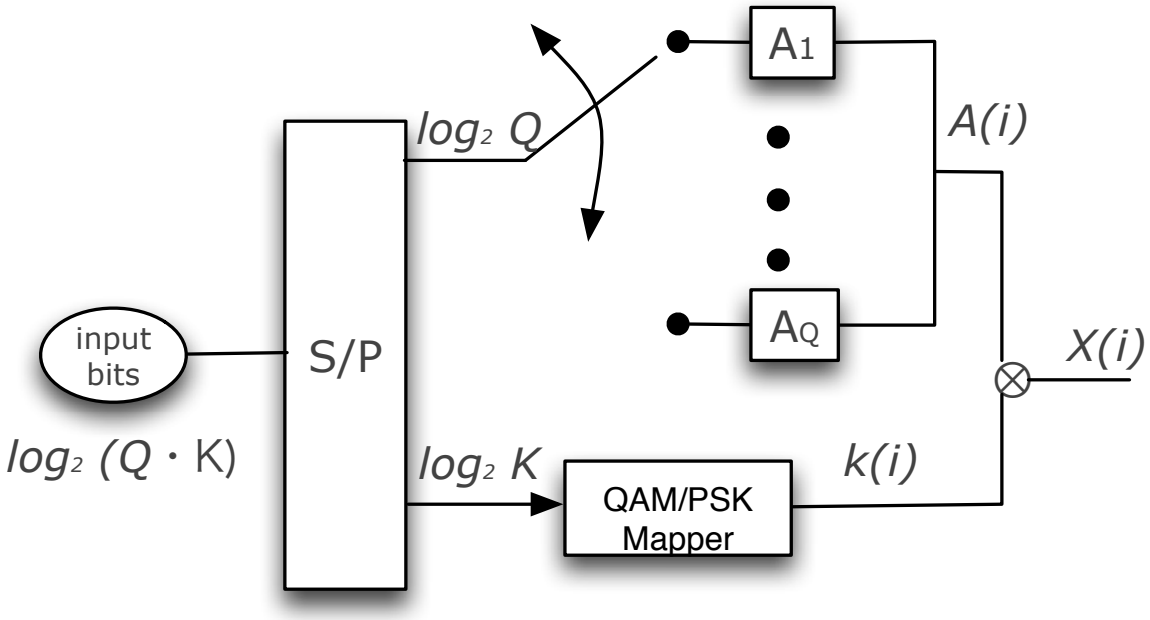

Figure 4.11: Space-time shift keying matrix generator[99]

Single carrier cyclic prefix space-time shift keying

SC-CP is block transmission of N_F symbols appended with cyclic prefix in order to avoid interSymbol interference (ISI). Having complexity similar to that of OFDM, SC-CP enjoys inherent frequency diversity in frequency selective channels. As claimed in [99], in STSK systems ICI is negligible making ML complexity affordable at the receiver; however, it is still a challenging issue in SC-CP systems in case of dispersive channels. The dispersion matrix sets are generated offline using bio-inspired optimization technique, genetic algorithm (GA) [15].

The i-th STSK codeword $X(i)$ is generated as a result of linear multiplication of input K-QAM/PSK symbol k with space-time matrix $A_q \in \mathbb{C}^{M\times T}$. The space-time matrix spreads the symbol energy in M and T dimensions and eventually system benefits from space-time diversity. A single SC-CP STSK codeword consists of T adjacent SC-CP blocks having N_F space-time coded symbols. The dispersion matrix A_q has to satisfy following power constraint,

$$tr\left[A_q^H A_q\right] = T, \quad \forall q \tag{4.14}$$

The input rate is $log_2(Q \cdot K)$ as depicted in Fig 4.11. A block of N_F codewards are generated and transmitted with cyclic prefix (CP) length N_{CP} greater than channel impulse response (CIR) L. Ideal channel state information (CSI) is assumed with the assumption that channel remains static over one STSK block duration T. A simpler and near optimum STSK receiver architecture of [60] that was orginally proposed for OFDMA/SCFDMA can be employed in SC-CP systems, Fig 4.12. The received signal Y gets equalized with frequency domain linear equalizer (FDE) (e.g., MMSE or ZF) performing point-wise multiplication between weight matrix W and Y in frequency domain as in (4.17). The weight matrix W for, ZF and MMSE, is given as,

$$W_{ZF}^H = \left[H^H H\right]^{-1} H^H \tag{4.15}$$

$$W_{MMSE}^H = \left[H^H H + N_0 \mathbb{I}_M\right]^{-1} H^H \tag{4.16}$$

where N_0 is the noise power. For sake of simplicity, we omit ZF and MMSE subscripts from the equations hereafter. The equalized i-th block V is given as

$$\begin{aligned} \bar{V(i)} &= WY \\ &= \bar{X}(i) + \bar{Z}(i) \end{aligned} \tag{4.17}$$

where $\bar{V}(i) = \mathbb{C}^{M\times T}$ and $\bar{Z}(i)$ is gaussian noise and $\bar{X}(i)$ is the i-th channel-free codeword. The block index i will be dropped to make mathematics simpler. To ease the computations, vectorial stacking is applied on $\bar{V}$

$$\widetilde{V} = vec\left(\bar{V}\right) \in \mathbb{C}^{MT\times 1} \tag{4.18}$$

The space-time demapping operation in Fig. 4.12 is

$$V = \frac{1}{T}\boldsymbol{A}^H \widetilde{V} = [v_1, \ldots, v_Q] \in \mathbb{C}^{Q\times 1} \tag{4.19}$$

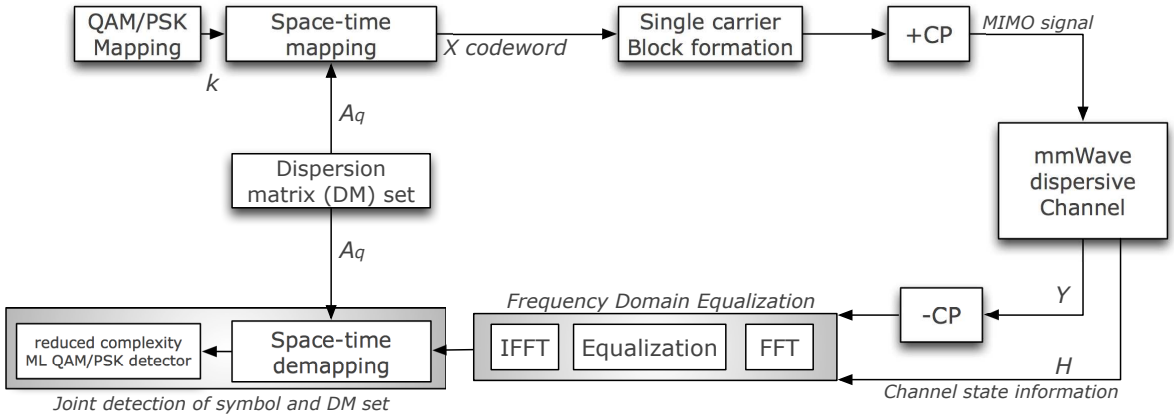

Figure 4.12: Single carrier cyclic prefixed (SC-CP) STSK millimeter wave system

Indexes $\hat{q}$ and $\hat{l}$ can be detected using maximum likelihood (ML) as

$$(\hat{q}, \hat{l}) = arg \underset{q,l}{min} \|V - \boldsymbol{\kappa}_{q,l}\|^2 \tag{4.20}$$

As we can see in (4.20) the channel effect is removed from the signal V using frequency domain equalization (FDE) operation and hence ML detection complexity becomes affordable. SC-CP STSK has potential of attaining joint frequency-time diversity order upto $T(L+1)$.

Othorgonal frequency division multiplex space-time shift keying

Orthogonal frequency division multiplex (OFDM) is robust against frequency selective channels where N_F parallel subcarriers convert frequency selective channel into frequency flat channels. This characteristic allows OFDM to have simpler receiver and hence it has been considered for downlink LTE-A systems. Because the symbols are modulated on othorgonal subcarriers, freqeuncy domain realization of maximum liklihood is possible with affordable computational complexity when number of transmitting antennas and modulation order are not so high. In [60], the sub-optimal receiver is proposed for STSK OFDMA/SC-FDMA systems as discussed in previous section. The optimal ML receiver for OFDM-STSK system is discussed in [99]. The OFDM-STSK system in millimeter wave channels is shown in Fig. 4.13.

The single-stream ML finds the estimates $(\hat{q}, \hat{l})$ from:

$$(\hat{q}, \hat{l}) = arg \underset{q,l}{min} \|Y - \boldsymbol{HAK}_{q,l}\|^2 \tag{4.21}$$

The optimal ML detector performs exhaustive search over an entire space of $(Q \cdot K)$. It should be noted that the search space depends on modulation order K and Q. So the

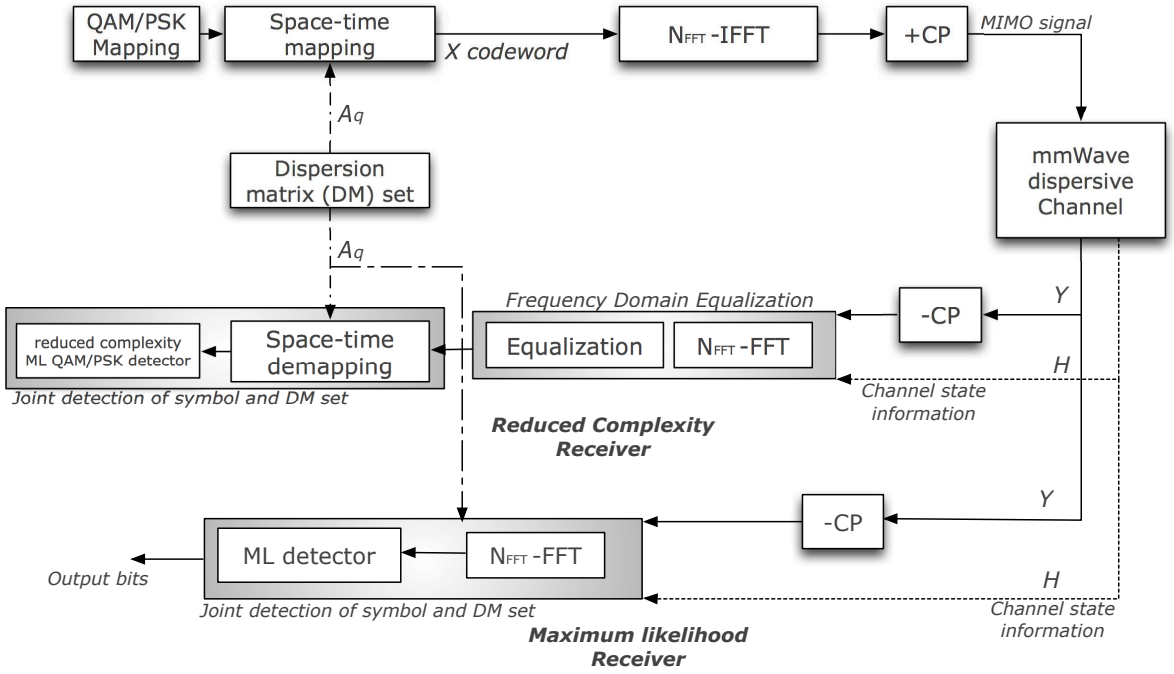

Figure 4.13: OFDM STSK millimeter wave system

computational complexity is realizable with smaller Q and K.

4.2.4 MM-wave link impairments

MM-wave system poses hardware challenges like phase noise and non-linear power amplifier. We highlight such challenges in the framework of space-time coded SC-CP and OFDM.

Impact of phase noise

Non-ideal oscillators give rise to phase noise (PN) in hardware transceivers that results into a particular power spectral density (PSD). This motivates system designers to equip the E-band transceivers with expensive PN high frequency oscillators [77]. Large bandwidths and smaller sampling time will experience unsignificant phase noise. However, such wideband systems require frontend components to operate at higher bandwidths. As a result, this increases the phase pertubation introduced by entire communication system. Hence the question "How much phase noise a receiver can tolerate without compromising the system performance?" deserves an answer. The answer to this question is to test STSK systems, both SC-CP and OFDM, in the presence of phase noise in the hardware.

Lets try to see the effects of PN mathematically in SC-CP and OFDM systems. As

seen in Figs 4.12 and 4.13, low complexity receivers employ FDE to remove contamination done by multipath channel. In the presence of PN in the system, equalized SC-CP signal in (4.17) after FDE can be expanded as,

$$\bar{V}_{SC}^{k} = \bar{X}_k e^{j\theta_k} + \bar{Z}_k \tag{4.22}$$

where, $\bar{X}_k^{M\times T}$ is the equalized k-th STSK codeword block, θ_k is the phase noise component and $\bar{Z}_k$ is frequency domain noise samples. In order to analyze the impact of phase noise on the received signal $\bar{x_k}$, we expand (4.22) as,

$$\bar{V}_{SC}^{k} = \sum_{n=0}^{N_F-1} \bar{x}_k e^{-j\frac{2\pi}{N_F}nk} e^{j\theta_n} + \bar{Z}_k,\ k = 0, 1, 2, ..., N_F - 1 \tag{4.23}$$

Most of the system has very low phase noise (i.e., $\theta_n << 1$), hence we can approximate the phase noise exponential as $e^{j\theta_n} \approx 1 + j\theta_n$. Hence (4.23) can be simplified as,

$$\bar{V}_{SC}^{k} = \sum_{n=0}^{N_F-1} (1 + j\theta_n)\, \bar{x}_n e^{-j\frac{2\pi}{N_F}nk} + \bar{Z}_k \tag{4.24}$$

$$\bar{V}_{SC}^{k} = \sum_{n=0}^{N_F-1} \bar{x}_n e^{-j\frac{2\pi}{N_F}nk} + j\sum_{n=0}^{N_F-1} \bar{x}_n\theta_n e^{-j\frac{2\pi}{N_F}nk} + \bar{Z}_k \tag{4.25}$$

$$\bar{V}_{SC}^{k} = \bar{X}_k + j\bar{X}_k^{pn} + \bar{Z}_k \tag{4.26}$$

It is clear in (4.26), the first term $\bar{X}_k$ is the equalized frequency domain k-th STSK codeword SC-CP symbol and second term $\bar{X}_k^{pn}$ is the common phase noise (CPE) that is same for all symbols in a SC-block.

The impact of phase noise on OFDM is different from that of in SC systems because overlapping subcarriers due to IFFT-precoding in OFDM. The output of FDE can be seen as,

$$\bar{V}_{OFDM}^{k} = \mathbf{\Gamma_k} + \bar{Z} \tag{4.27}$$

where

$$\mathbf{\Gamma_k} = \frac{1}{N_F}\sum_{u=0}^{N_F-1} e^{j\theta_u} \sum_{n=0}^{N_F-1} \bar{X}_n e^{j2\pi(n-k)u/N_F} + \bar{Z}_k \tag{4.28}$$

Substituting $e^{j\theta_n} \approx 1 + j\theta_n$ for very small values of θ_n in (4.28),

$$\mathbf{\Gamma_k} = \frac{1}{N_F}\sum_{u=0}^{N_F-1} (1 + j\theta_u) \sum_{n=0}^{N_F-1} \bar{X}_n e^{j2\pi(n-k)u/N_F} + \bar{Z}_k \tag{4.29}$$

$$\mathbf{\Gamma_k} = \bar{X}_k + j \sum_{n=0}^{N_F-1} \bar{X}_n \Theta_{n-k} + \bar{Z}_k \tag{4.30}$$

where $\Theta_k = \frac{1}{N_F} \sum_{u=0}^{N_F-1} \theta_u e^{\frac{j2\pi}{N_F} nu}$ is the frequency response of phase noise samples θ_u at k-th STSK codeword. The second term in (4.30) can be seen as,

$$j \sum_{n=0}^{N_F-1} \bar{X}_n \Theta_{n-k} = \underbrace{j\bar{X}_k \Theta_0}_{CPE} + \underbrace{j \sum_{n=0, n\neq k}^{N_F-1} \bar{X}_n \Theta_{n-k}}_{ICI} \tag{4.31}$$

We can see in (4.31), k-th OFDM STSK codeword $\bar{X}_k$ is effected by multiplicative term (common phase error) and additive term (ICI). ICI can not be corrected and disturbs the orthorgonality between subcarriers. The multiplicative term reduces the useful signal amplitude due to power leakage from neighbouring subcarriers. Hence OFDM is more prone to system phase noise and the performance degrades with the increase in phase noise floor. One noticeable remark about phase noise in OFDM and SC-CP is that phase noise in OFDM is dependent on number of subcarriers N_F whereas it is independent of block size in SC-CP system. Also SC-CP is not affected by ICI hence SC-CP has proven to be more robust against phase noise effects in non-ideal hardware.

Power Amplifier Non-linearity

Power amplifier (PA) is characterized by input amplitude to output amplitude (AM/AM) and input amplitude to output phase (AM/PM). Lets say, the time-domain input signal to PA is,

$$s_{in}(t) = A_{in}(t)\, exp(j\phi_{in}(t)) \tag{4.32}$$

The output of PA is given as,

$$s_{out}(t) = \varrho\left[A_{in}(t)\right] exp\left[j\left\{\phi_{in}(t) + \varphi\left[A_{in}(t)\right]\right\}\right] \tag{4.33}$$

where ϱ and φ are AM/AM and AM/PM property of power amplifier. In this work, Saleh's model [95] is used whose AM/AM and AM/PM property is given as,

$$\varrho\left[A_{in}(t)\right] = \frac{g_0(t)}{1 + \left[A_{in}(t)/A_{sat,in}\right]} \tag{4.34}$$

$$\varphi\left[A_{in}(t)\right] = \frac{\alpha_\varphi A_{in}^2(t)}{1 + \beta_\varphi A_{in}^2(t)} \tag{4.35}$$

In (4.34) and (4.35) g_0 is the gain , $A_{sat,in}$ is the input saturation amplitude and $\alpha_\varphi, \beta_\varphi$ are AM/PM parameters. $\alpha_\varphi = \pi/50$ and $\beta_\varphi = 1/4$ is used in this work.

The non-linearity of transmit PA at the output of FDE in case of OFDM can be seen using (4.17) as,

$$\bar{V}_{OFDM}^{k} = \lambda_{\mathbf{k}} + \bar{Z}_{k} \tag{4.36}$$

where,

$$\lambda_{\mathbf{k}} = \left(\sum_{u=0}^{N_F-1} \varrho(\mathbf{x_u}) \mathbf{e}^{\mathbf{j}\varphi[\mathbf{x_u}]} \right) \mathbf{x_k} + \sum_{n=0, n\neq k}^{N_F-1} \mathbf{x_n} \sum_{u=0}^{N_F-1} \varrho\left[\mathbf{x_u}\right] e^{j\varphi[\mathbf{x_u}]} e^{j2\pi(n-k)u/N_F} \tag{4.37}$$

As we can see in (4.37), at the transmitter the OFDM codeword $\mathbf{x_n}$ is affected by multiplicative and additive terms that are dependent on ampifier characteristics $\varrho[\cdot]$ and number of subcarrier N_F. In case of SC-CP, the signal is only dependent on amplifier characteristics as seen in (4.38) and is independent of block length N_F,

$$\bar{V}_{SC}^{k} = \mathbf{x_k} \varrho\left[\mathbf{x_k}\right] e^{j\varphi[\mathbf{x_k}]} + \bar{Z}_{k} \tag{4.38}$$

SC-CP STSK has higher resilience against non-linear power amplifier than OFDM STSK. In OFDM, the performance degradation occurs due to loss of othorgonality of subcarriers due to non-linear distortions. On the other hand, SC-CP STSK has higher PAPR than conventional SC-CP system but exhbibits lower PAPR characteristics as compare to OFDM STSK systems. Hence designing lower PAPR systems for backhaul is easier with SC-CP STSK system.

Atmospheric attenuation

Atmospheric attenuations have been acting as propagation hurdle for mmWave transmissions in satellite link. However, they seem to have less impact on mmWave cellular networks as there is a so called 'transmission window' where attenuation level @73 GHz is minimum [92]. It has been reported small cells with 200meters inter-site distance, atmospheric attenuation is approximately 0.06 dB/km and 0.08 dB/km at 28GHz and 38GHz, respectively [43]; whereas it is 0.3 dB/km at frequencies between 70GHz and 90GHz.

Over such small distances, air attenuation due to oxygen absorption is also very low. In [93], rain attenuation is considered to have minimum impact on mmWave with at most 3-6 dB of attenuation in worst rainfall. It would be much less in heavy rain fall. MmWave systems @73 GHz have approximately the same propagation characteristics as that of at 28GHz and 38GHz. With MIMO antenna configuration, atmospheric attenuation is almost negligible over shorter distances (e.g., 200m) as reported in [94].

Table 4.1: Phase noise profiles

	1MHz	10 MHz
PN1	-100dB	-120dB

4.2.5 Computational complexity of receivers

In this section, computational complexity of the two detectors used in previous sections is discussed. Space time shift keying (STSK) and spatial modulation (SM) makes the optimal detection less computational complex due to inherent principle of transmitting single Q matrix in former and activating one out M transmit antennas in latter. Hence optimal maximum liklihood (ML) search space for STSK reduces from Q to one and that of for SM from M to one. As reported in [99], the computational complexity of optimal detector for OFDM-STSK is $\frac{4MNTQ+6NTQL}{\log_2(Q\cdot L)}$ and for SM is $2NM + ML + L$ reported in [56]. The maximum likelihood complexity for spatial multiplexing is too high and increases exponentially with the M. For single carrier with cyclic prefix (SCCP), the optimal reciever complexity is quite high for both STSK and SM. For STSK it is $(QL)^P$ and for SM it is $(ML)^P$ [90]. For this reason, single carrier techniques have to resort to lower complexity sub-optimal techniques. The suboptimal receiver is based on MMSE. The computational complexity of sub-optimal detector for STSK is reported in [60]. For same block size, SCCP and OFDM exhibits same computational complexity that is $4M^2N + 8MN + 4MTQ + 2QL' + Q + 2L$. Suboptimal SM and SMUX, for both OFDM and SCCP, have the same computational complexity as ideal-MMSE.

4.2.6 Simulation Results

To verify the claims made in previous sections, series of simulations are performed in MATLAB environment for a realistic mmWAVE backhaul scenario. Such a scenario is characterized by RF impairments mentioned in previous section. The considered phase noise profile is listed in Tab 4.1. The corresponding phase noise mask for 73GHz frequency band is shown in Fig. 4.14.

A non-linear power amplifier using Saleh's model [95] is considered with input-output backoff characteristics shown in Fig. 4.15. The considered output backoff values are pointed out in the figure for convenience.

The parameters used for simulation are listed in Tab. 4.2

First series of simulations are without channel coding for SC-CP and OFDM. In comparison with STSK, spatial modulation (SM) and spatial multiplexing (SMUX) are simulated in the similar environments where ideal channel knowledge (CSI) is available at the receiver. For all the considered systems, the spectral efficiency η is kept to 3bps/Hz to

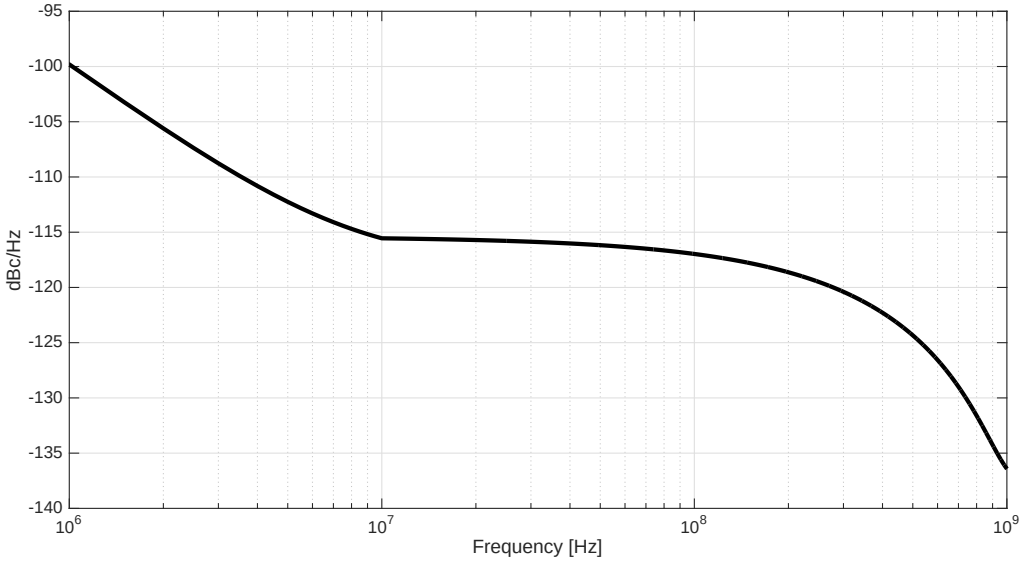

Figure 4.14: Phase Noise Mask for 73GHz Frequency Band

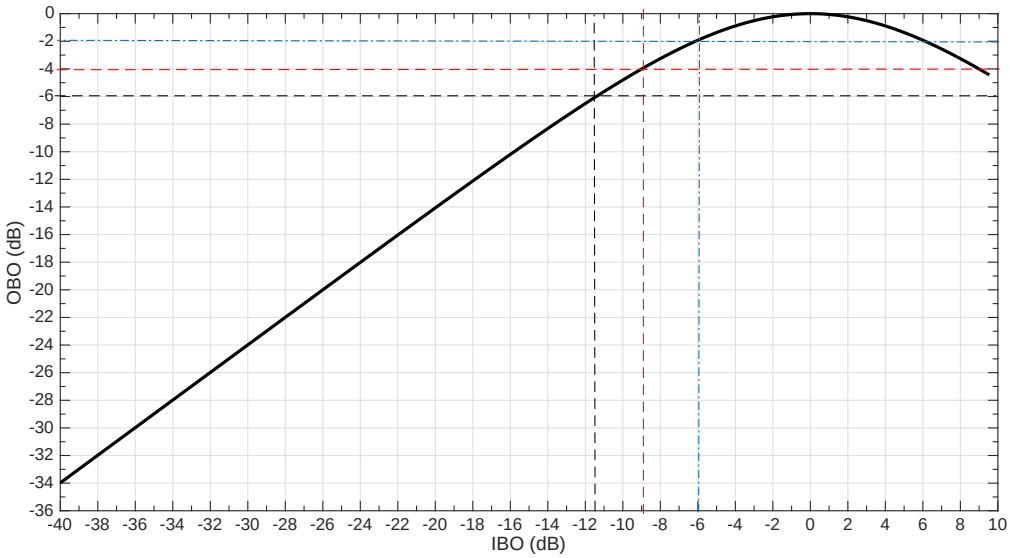

Figure 4.15: Input-Output Backoff characteristics of Non-linear Power Amplifier

have a fair comparison. The spectral efficiency equations are listed in Tab.4.3 It can be seen in Figs 4.16, 4.17, 4.18 for same spectral efficiency STSK systems (both SCCP and OFDM) exploit the diversity efficiently and outperform SM and SMUX counter parts in the absence of hardware impairments.

OFDM makes full use of time diversity in case of optimal receiver where STSK at-

Table 4.2: Parameters

Parameters	Values
Bandwidth	500MHz
Frequency Band	73Ghz
Modulation	BPSK
N_F (OFDM and SC-CP)	512
Cyclic Prefix	150
MIMO antenna configuration	2x2, 4x4
Channel	SSCM [93]
Receiver	SC-CP(MMSE), OFDM(MMSE, ML)
Channel Coding	Trellis code

Table 4.3: Spectral Efficiency (η): SM, SMUX, STSK

	η
SM	$\log_2(M) + \log_2(K)$
SMUX	$M \log_2(K)$
STSK	$\log_2(Q) + \log_2(K)$

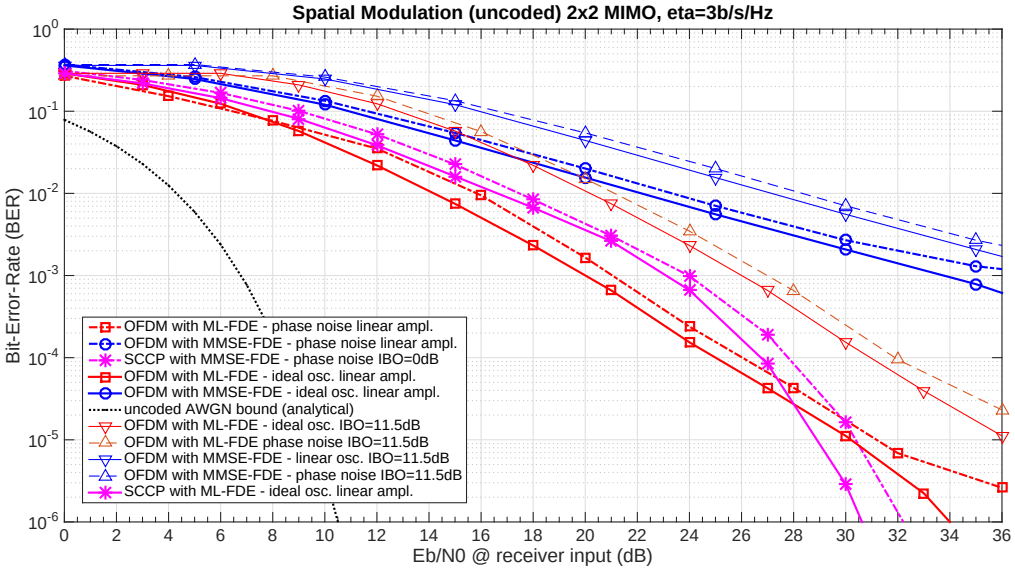

Figure 4.16: Uncoded Spatial Modulation, M = 2, N = 2, $\eta = 3$ bps/Hz, QPSK modulation, in millimeter wave frequency selective channel, SC-CP (sub-optimal detection) and OFDM (optimal and sub-optimal detection)

tains significant gain of ∼13dB over SM. MmWave channels are highly attenuated and occurance of deep fades is highly anticipated. In this regard, OFDM with sub-optimal receiver (i.e., MMSE) has adverse performance in such channels as MMSE receiver is not

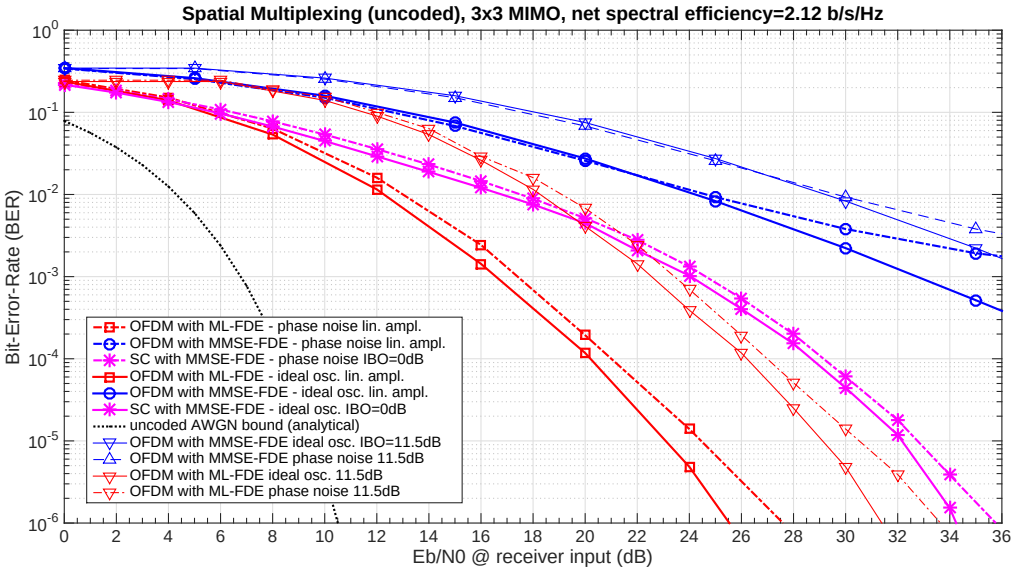

Figure 4.17: Uncoded Spatial Multiplexing, M = 3, N = 3, $\eta = 3$ bps/Hz, BPSK modulation, in millimeter wave frequency selective channel, SC-CP (sub-optimal detection) and OFDM (optimal and sub-optimal detection)

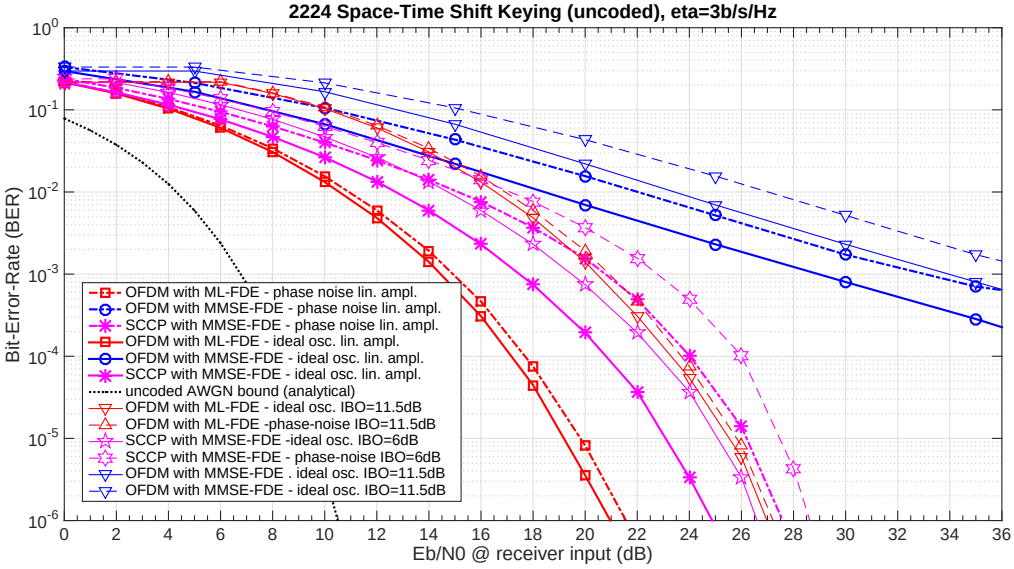

Figure 4.18: Uncoded Space time shift keying, M = 2, N = 2, T = 2, Q =4, $\eta = 3$ bps/Hz, BPSK modulation, in millimeter wave frequency selective channel, SC-CP (sub-optimal detection) and OFDM (optimal and sub-optimal detection)

able to recover symbols that fall in deepfades, see in Figs 4.16, 4.17, 4.18. The situation is rather different in single carrier systems where symbols are spread in frequency domain

before equalization. Such spreading in frequency domain leads to frequency diversity in the system and makes the system robust against channel deep fades. Hence the SCCP with sub-optimal detector has shown performance close to OFDM-ML especially in STSK case where SC-CP takes advantage of frequency and time diversity.

In case of hardware impairments SCCP in all forms has shown remarkable resilience. The single carrier systems due to negligible peak-to-average power (PAPR) requires 0dB of output backoff (OBO). As shown in section 4.2.4, SCCP, due to its single carrier nature, is only affected by common phase error caused by phase noise. OFDM systems, both optimal and suboptimal, are highly vulnerable to hardware impairments due to delicate signal processing functions. OFDM are notorious for having high PAPR and hence high backoff is required to combat non-linear distortions due to power amplifier. Phase noise, on the other hand, disturbs the orthorgonality among subcarriers converting white noise into colored. Hence, performance of OFDM is compromised and is noticeable in Figs 4.16, 4.17, 4.18 where ∼7dB degradation is observable in case of non-ideal RF STSK OFDM-ML w.r.t its ideal couterpart.

Another interesting aspect is to see the performance with higher antenna dimensions while keeping the spectral efficiency $\eta = 3$bps/Hz. Uncoded SMUX system stays the same for $\eta = 3$bps/Hz as in Fig. 4.17. Increasing the antenna dimensions at receiver helps in achieving the array gain as evident in Figs. 4.19 and 4.20. It should be noted that in case of SM OFDM-ML exploits this gain fittingly where a gain of ∼10dB is noticed in case of ideal RF hardware. Phase noise is less effective in case of large antenna array at the receiver. The reason behind such robustness is the effect of phase noise is averaged out at the detection process thanks to receiver antenna diversity. This makes the probability density function (PDF) of decision variables (affected by phase noise) less distorted due to phase noise. SCCP STSK system exhibits PAPR for higher order of antennas. This is due to the dispersion matrix that disperses the input symbol energy in space-time dimensions. Hence a input backoff (IBO) of 4dB is required in case of SCCP that is still low as compare to OFDM-ML for which IBO = 6dB is needed. OFDM-ML STSK system enjoys 4dB gain over SCCP-MMSE STSK. Such a performance gain is due to the use of optimal ML receiver in OFDM STSK that is not possible in SCCP in such frequency selective channel conditions. OFDM-ML STSK has performance very close to uncoded BPSK AWGN bound that shows the resilience against multipath channel and non-ideal hardware impairments.

The channel coding analysis is done in second series of simulations. Trellis coded modulations are considered in the all the considered systems to combat channel imperfections. Adding redundancy to information data makes it robust against deep fades but it also reduces the spectral efficiency i.e., $\eta = 2.12$ bps/Hz. In uncorrelated channels, like mmWave

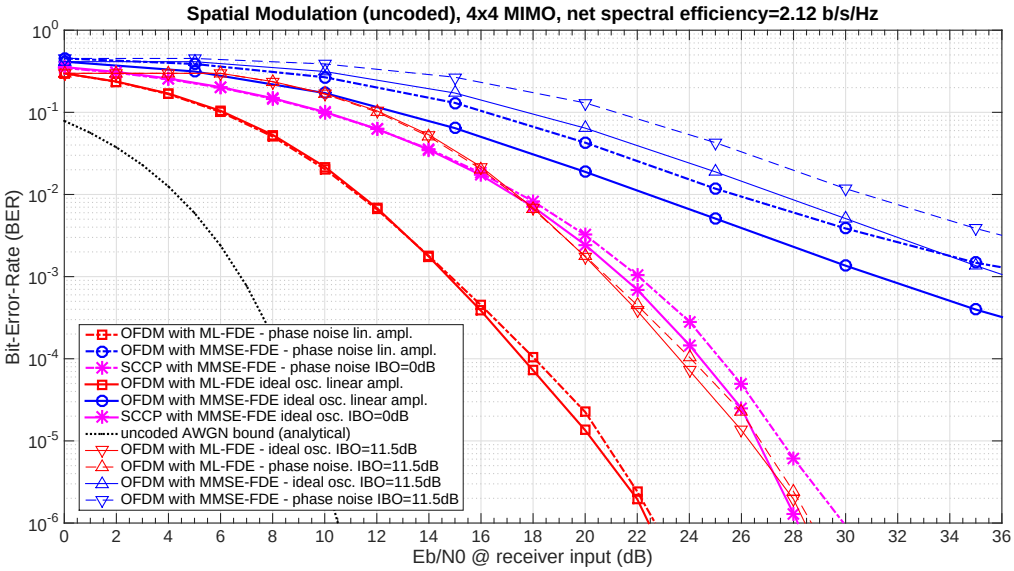

Figure 4.19: Uncoded Spatial Modulation, M = 4, N = 4, $\eta = 3$ bps/Hz, BPSK modulation, in millimeter wave frequency selective channel, SC-CP (sub-optimal detection) and OFDM (optimal and sub-optimal detection)

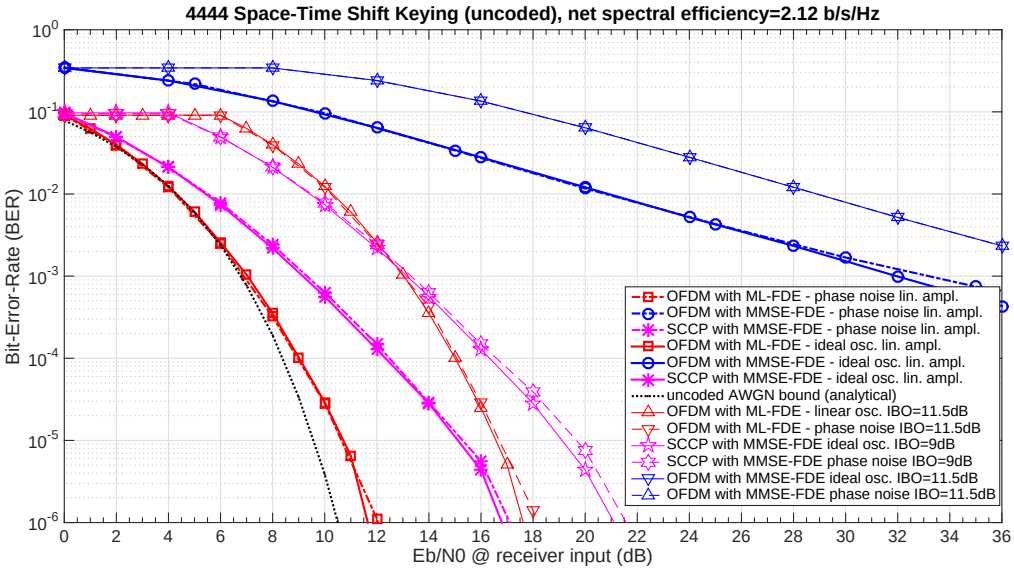

Figure 4.20: Uncoded Space time shift keying, M = 4, N = 4, T = 4, Q = 4, $\eta = 3$ bps/Hz, BPSK modulation, in millimeter wave frequency selective channel, SC-CP (sub-optimal detection) and OFDM (optimal and sub-optimal detection)

frequency selective channels, trellis-coded spatial modulation techniques do not provide coding gain as evident in Figs. 4.21, 4.23. As pointed out in Tab. 4.3, the information

conveyed through antenna index and modulation, i.e., M and K in SM. Hence there exists a splitter as pointed out in [78] that splits the information data into two, i.e. $log_2(M)$ and $log_2(K)$. Only the modulated bits $log_2(K)$ are coded using trellis coding and conveyed to receiver. The fundamental principle is SM and STSK is the same. Hence coding gain is not significant.

In case of SMUX, all input bits are trellis coded before transmission and hence the gain obtained as a result of trellis code is around 6dB over uncoded SMUX in case of OFDM-ML. A similar trend is observed in coded SCCP-SMUX performing better than uncoded counterpart as in Fig 4.22.

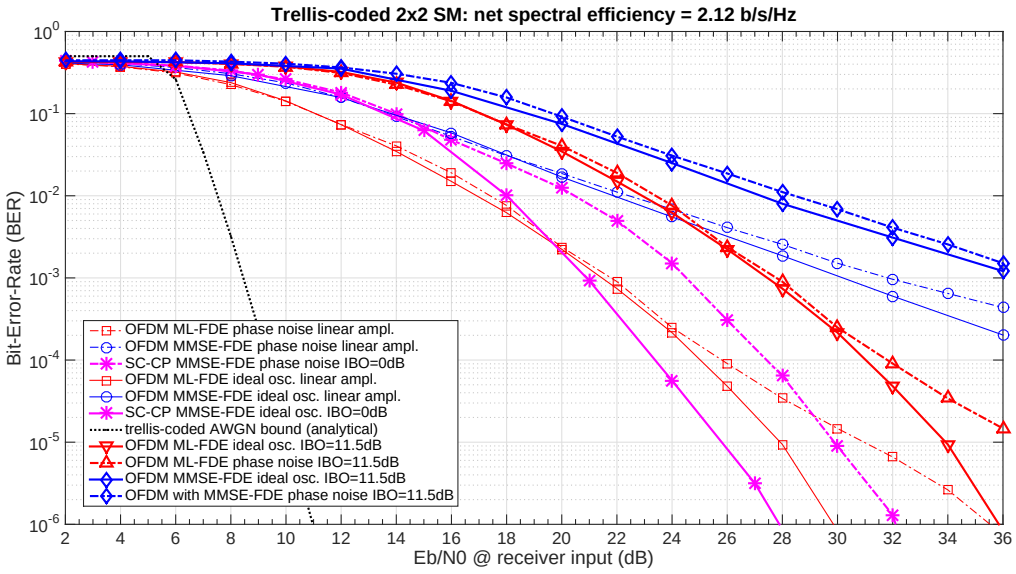

Figure 4.21: Trellis-coded Spatial Modulation, M = 2, N = 2, η = 2.12 bps/Hz, in millimeter wave frequency selective channel, SC-CP (sub-optimal detection) and OFDM (optimal and sub-optimal detection)

Another interesting thing is noted in SM where coded-OFDM exhibits error floor in the presence of non-ideal hardware impairments at high SNR regime. This is due the phase noise impacting the correlation introduced by trellis coding. The same trend can be seen in trellis coded SCCP SM where performance loss of 4dB @10^{-6} is evident between ideal and PN case, see Fig 4.21. Trellis coded STSK schemes have shown more robustness against channel impairments and PN. In Fig 4.23 performance of trellis coded OFDM-ML STSK in the presence of PN is tight w.r.t ideal OFDM-ML STSK. Exactly the same trend can be seen in trellis coded SCCP STSK where PN does degrade the performance by only 1dB. Trellis coded OFDM-MMSE STSK in the presence of PN shows irreducible error floor.

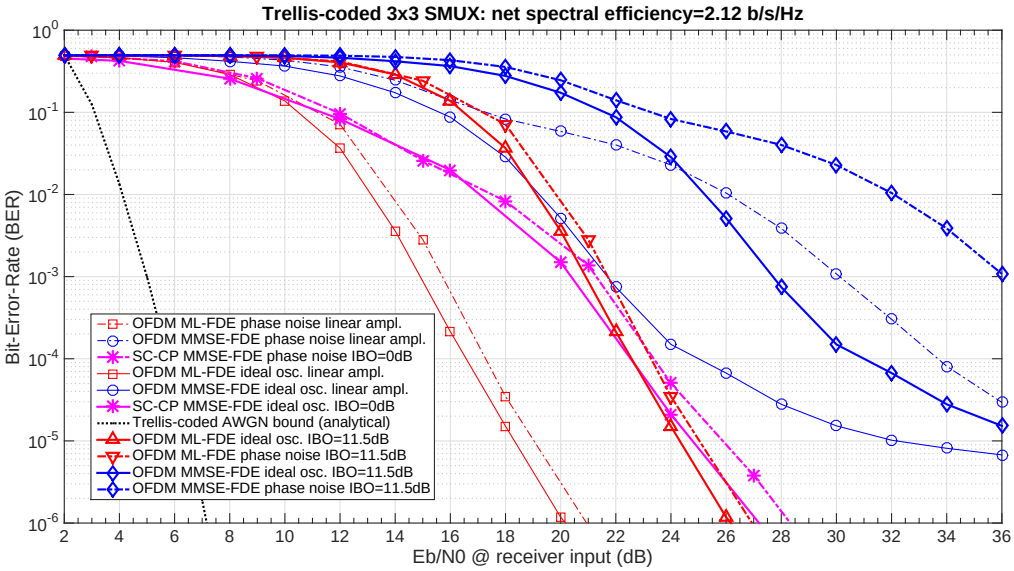

Figure 4.22: Trellis-coded Spatial Multiplexing, M = 3, N = 3, η = 2.12 bps/Hz, in millimeter wave frequency selective channel, SC-CP (sub-optimal detection) and OFDM (optimal and sub-optimal detection)

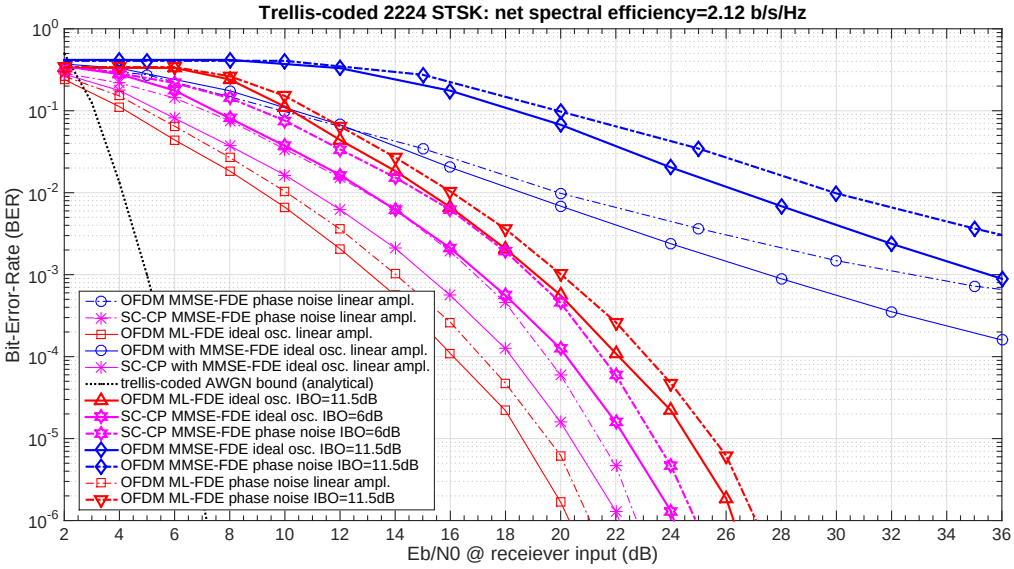

Figure 4.23: Trellis-coded Space time shift keying, M = 2, N = 2, T = 2, Q =4, η = 2.12 bps/Hz, in millimeter wave frequency selective channel, SC-CP (sub-optimal detection) and OFDM (optimal and sub-optimal detection)

Trellis codes provide not much coding gain in the case of large antenna arrays, in case of SM and STSK shown in Figs. 4.24 and 4.25. In case of trellis coded OFDM-ML STSK

with four antennas, around 1dB of gain can be noticed over uncoded OFDM-ML STSK. However an interesting thing to be noted in case 4-antenna systems, phase noise does not harm the correlation introduced by trellis code as it is the case in 2-antenna system. It can be seen that OFDM-ML STSK and SCCP-MMSE STSK performance are tight w.r.t the performance in the presence of phase noise, as seen in Fig. 4.24. OFDM-MMSE STSK is not able to perform fitter and has performance not adequate for backhaul applications. On the other hand, SM with 4-antenna shows some resilience against phase noise but

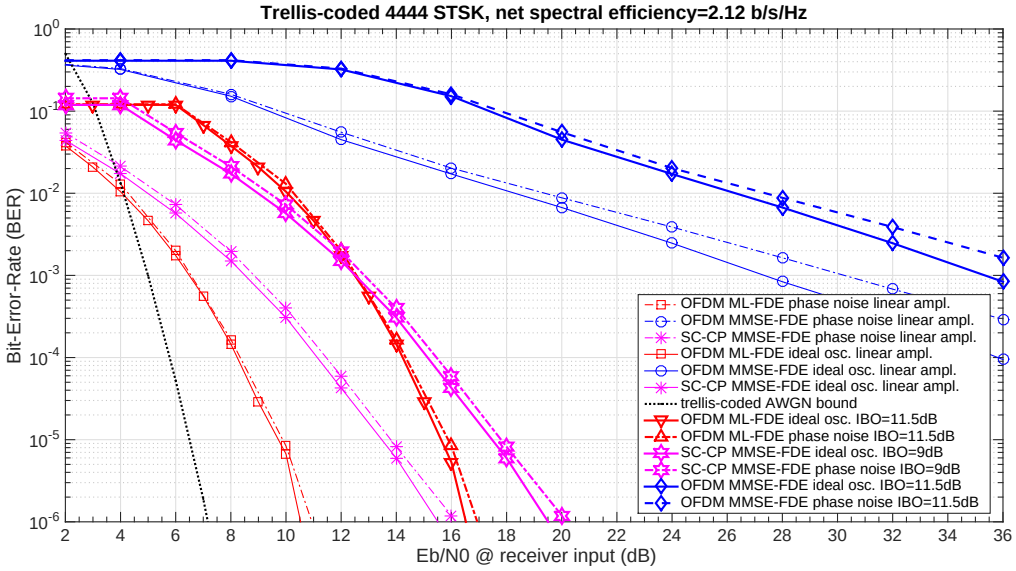

Figure 4.24: Trellis-coded Space time shift keying, M = 4, N = 4, T = 4, Q =4, η = 2.12 bps/Hz, in millimeter wave frequency selective channel, SC-CP (sub-optimal detection) and OFDM (optimal and sub-optimal detection)

overall performance is uncomparable with STSK systems. Due to low complex system design, SM has the edge over STSK but the inability of exploiting the full diversity gain makes them not viable for backhaul applications.

Based on the link performance, ranges are derived for each of transmission schemes in uncoded and coded case with the help of link budget,

$$E_b/N_0 = 109.712 - 24.5\log_{10}(D_{mt}) - 0.02D_{mt} + \varepsilon_{dB} \tag{4.39}$$

The expression in (4.39) is derived by using pathloss for 73GHz as reported in [9] and rain attenuation with 99.999% link availability reported in [74]. The receiver parameters are listed in Tab.4.4.

Based on the values considered in Tab.4.4 and (4.39), ranges are derived as listed in Tab. 4.5 Tab. 4.6. In coded case, tt can be seen that 4-antenna STSK has longest hop

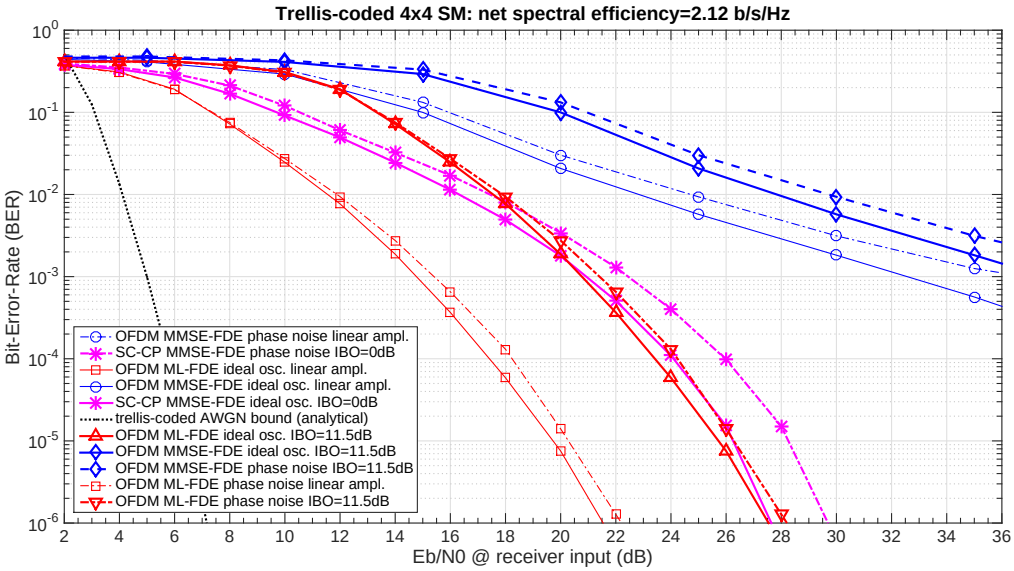

Figure 4.25: Trellis coded Spatial Modulation, M = 4, N = 4, η = 3 bps/Hz, QPSK modulation, in millimeter wave frequency selective channel, SC-CP (sub-optimal detection) and OFDM (optimal and sub-optimal detection)

distance reaching 270meters with OFDM-ML in the absence of hardware impairments, whereas 4-antenna SCCP-MMSE STSK systems can reach upto 187meters with ideal hardware. OFDM-MMSE is clearly not the suitable choice backhauling due to its poor link level performance in mmWave channels. In the presence of hardware impairments, the hop distance for OFDM-ML STSK reduces to 172meters whereas it becomes 142meters in case of SCCP-MMSE STSK. Hence, OFDM systems suffer alot in the presence of phase noise and non-linear power amplifier. The degradation is not significant in case of SCCP-MMSE, indicating that SCCP-MMSE is more robust to hardware impairments as compare to OFDM-ML.

Table 4.4: Receiver Parameters for computation of link budget

Parameters	**Numerical value**
Rx gain G_a	30.7 dB [107]
LNA gain P_a	30 dB [62]
Synchronisation loss, L_{dem}	1.5 dB
Feeder loss, L_{fed}	0.15 dB
Polarization loss, L_{pol}	0.15 dB
Antenna noise temp, T_{ant}, °K	290
Feeder noise temp, T_{fed}, ° K	290
Receiver Noise Figure, F_{rec}	5.5

OFDM SMUX reaches distances upto 115meters with ML and ideal hardware impairments that is greater than 2-antenna OFDM STSK and OFDM SM systems, and 4-antenna SM system. Such a gain is due to trellis coding as SMUX exploits channel coding gain efficiently as compare to SM and STSK where only partial information is coded. On the other hand, SCCP SMUX has greater range as compared to SCCP SM.

Uncoded case is not very different from coded one in the sense the coverage reduces noticeably in case of SMUX whereas it not significant in STSK and SM. However, 4-antenna STSK OFDM-ML still manages to reach 250meters of distance with ideal RF front end. With the same antenna configuration and ideal RF front end, SCCP-MMSE waveform travels upto 177meters. Reducing antenna configuration to 2-antenna, the coverage reduces to the half of the maximum attained with 4-antenna. In all cases, STSK is observed to be the stand out technique covering larger distances.

Table 4.5: NLOS backhaul distances reachable by different trellis-coded ST-MIMO techniques considering *five nines* Link availability and RF hardware impairments

		MIMO CONFIGURATION AND SPACE-TIME TECHNIQUE					
		2x2			4x4		
WAVEFORM AND FDE	**RF HARDWARE CHARACTERIZATION**	SM	STSK	SMUX (3x3)	SM	STSK	SMUX (3x3)
OFDM with ML-FDE	ideal	65 mt.	138 mt.	142 mt.	131 mt.	270 mt.	142 mt.
	non ideal	<10 mt.	82 mt.	82 mt.	77 mt.	172 mt.	82 mt.
OFDM with MMSE-FDE	ideal	<10 mt.	<10mt.	<10 mt.	<10 mt.	<10 mt.	<10 mt.
	non ideal	<10 mt.	<10 mt.	<10 mt.	<10 mt.	<10 mt.	<10 mt.
SC-CP with MMSE-FDE	ideal	77 mt.	115 mt.	79 mt.	80 mt.	187 mt.	79 mt.
	non ideal	55 mt.	98 mt.	73 mt.	68 mt.	142 mt.	73 mt.

Table 4.6: NLOS backhaul distances reachable by different ST-MIMO techniques considering *five nines* Link availability and RF hardware impairments

		MIMO CONFIGURATION AND SPACE-TIME TECHNIQUE					
		2x2			4x4		
WAVEFORM AND FDE	**RF HARDWARE CHARACTERIZATION**	SM	STSK	SMUX (3x3)	SM	STSK	SMUX (3x3)
OFDM with ML-FDE	ideal	47 mt.	130 mt.	94 mt.	118 mt.	250 mt.	94 mt.
	non-ideal	<10 mt.	81 mt.	48 mt.	71 mt.	165 mt.	48 mt.
OFDM with MMSE-FDE	ideal	<10 mt.	<10 mt.	<10 mt.	<10 mt.	<10 mt.	<10 mt.
	non-ideal	<10 mt.	<10 mt.	<10 mt.	<10 mt.	<10 mt.	<10 mt.
SC-CP with MMSE-FDE	ideal	61 mt.	97 mt.	48 mt.	75 mt.	177 mt.	48 mt.
	non-ideal	53 mt.	72 mt.	40 mt.	65 mt.	128 mt.	40 mt.

Chapter 5

SDR-based reconfigurable solutions for LTE-A

In this chapter, the goal is to demonstrate the viability of software-defined radio-based implementation of reconfigurable cooperative LTE-A communication strategies, in particular: cooperative downlink relaying. By designing and emulate SDR cooperative relaying in the downlink, it is shown that LTE-A fully enables the network reconfigurability. Such characteristics of a system allows the adaptation of transmission considering the change in the status of network.

5.1 GNUradio Framework

The GNU Radio Framework is an open source framework that allows the use of Python and C++ for the development of signal processing algorithms. An online community exists dealing with the framework at (*www.gnuradio.org*). The gnuradio library can be downloaded from the same website. An online repository is available from where libraries can be downloaded and utilized for experimentation.

The framework contains a large number of built in blocks, defined in C++, that imitate in software, the functions of the incorporated radio components, for example, mixers and filters, to mention but a few. Additionally, it is possible for developers to design their own blocks in C++ which increases the possibilities of what the GNU Radio framework can be used for. This is particularly an important aspect since the flexibility is needed in order to be able to design the SDR-based system.

The use of the GNU Radio Framework may proceed in either of two ways: One could adopt the use of the graphical user interface which is incorporated into the software- It is called the GNU Radio Companion (GRC). With this approach, graphs within the GUI are connected together with a goal of ensuring a definite signal path from source to sink

whilst taking care to match the signal types that flow from block to block. GRC is an open-source Visual programming language useing GNURadio libraries, and providing its users an easy way to create GNURadio flowgraphs. Fig. 5.1 shows the the GRC interface.

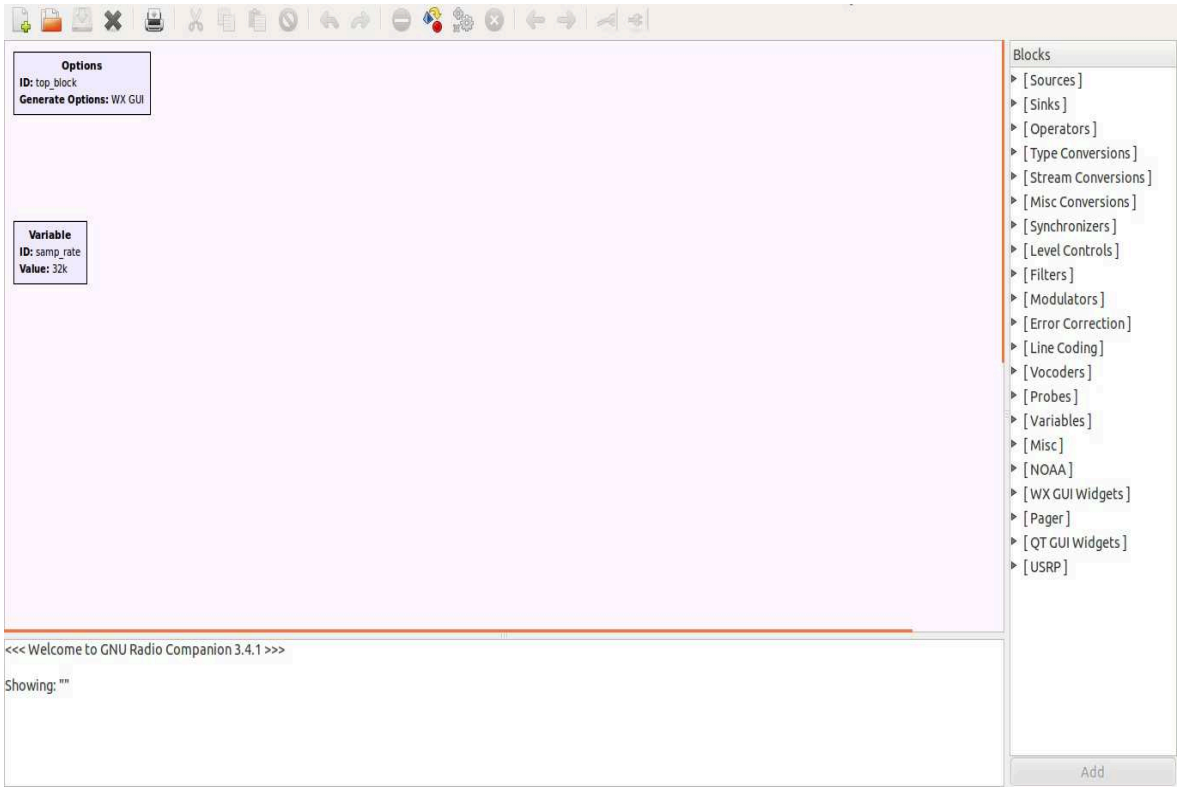

Figure 5.1: Emulation scenario: configuration and topology

With simply drag-and-drop and configuring the modules, GRC provides the ease and rapid developement of applications. A python code is generated as a result, which runs the application. However, GRC lacks the flexibility in the sense that it only allows to change the parameters within a block but does not help in creating new blocks. Rather, XML file is used to create new modules that can be added to GRC environment.

Alternatively, the non graphical interface can be used: In this, one would develop the system by using a python script which connects the signal path(called the graph) by calling the underlying GRC blocks. Of course writing code in python is time consuming but it gives the control in system design to its users where users can add functionalities of their choice to newly created GRC blocks.

Making blocks in GNU radio is about programming in C++ in order to keep GNUradio as fast as it is. With the help of already available libraries, new blocks can be created. The Simplified Wrapper and Interface Generator (SWIG) interface is used in the GNU

Radio Framework to interface between the python scripts and the C++ blocks.

5.2 Universal Software Radio Peripheral (USRP)

GNU Radio is strictly only a software library and can be used in a simulation like environment. An interesting feature it incorporates, is the fact that it can be connected to some low cost hardware, e.g., front end RF equipment, thus enabling over the air communication. An advantage accruing from this is, these radios can be used in experimental research instead of relying on only simulations to assess the performance of the developed system. USRP boards were connected to a commodity PC running the GNU Radio Software to enable over the air communications amongst them. Fig. 5.2 shows an USRP of bus series from Ettus research. It provides an entry level RF processing capabilities where two RF daughterboards are in place making it ideal for applications where high isolation is required between transmit and receive chains [5].

Figure 5.2: USRP1 of Ettus Research

Ettus Research, now a National Instruments company, has developed a number of USRP boards which use motherboards with either the USB 2.0 or Gigabit Ethernet interfaces to connect to the commodity PC. The boards can support, ideally, sampling rates from 8MSps for the USB 2.0 interfaces to 100MSps on the Gigabit Ethernet Interfaces. Another USRP board from ettus for demanding applications is shown in Fig. 5.3. This

USRP belongs to networked series and provides high bandwidth and high-dynamic range processing capabilities. It also enables MIMO configuration with frequency ranging from DC to 6GHz. A gigabit ethernet connectivity is provided to stream data to and from

Figure 5.3: USRP-N210 of Ettus Research

host processors. All these boards are interfaced to the GNU Radio Framework, or to other frameworks on which they operate(like MATLAB and Simulink or LabView), by the Universal Hardware Driver (UHD driver).

5.3 System Setup and SDR implementation

The system was designed and emulated using the GNU Radio Framework installed on a commodity PC connected to USRP boards acting as the RF Front end. This meant that the software for the baseband algorithms was implemented on the PC using Python for the higher level and less computationally intensive operations and C++ for the more computationally intensive operations. The main bottleneck to such a system lies in the

transfer rate that is possible between the USRP board as the front end and the PC. This bottleneck has been handled by providing in later designs of the USRP, models based on gigabit ethernet instead of the USB 2.0 Interface. In the previous, essential components for building up the GNUradio-based SDR testbed are discussed. Possbility of emulating a cooperative relaying scenario using these tools and a performance analysis of the system was carried out thereafter.

The emulated system was implemented to consider the effect a relaying scenario has on the performance of the Physical Downlink Shared Channel (PDSCH) in an LTE-A "like" downlink using the available hardware(a commodity PC(s) connected to a USRP board(s)). The available hardware components for the system emulation are two USRP N210 boards and two USRP1 boards and commodity PCs for each of them to run on. The difference between USRP N210 and USRP1 is shown in Tab. 5.1.

Table 5.1: Features of the ADCs and DACs in both the USRP1 and USRP N210 boards

Features	USRP1	USRP N210
ADC Sampling Rate (MSps)	64	100
ADC Resolution	12	14
DAC Sampling Rate (MSps)	128	400
DAC Resolution	14	16
Number of ADCs and DACs	4	

The system was designed as an OFDMA-based half duplex(all boards use XCVR2450 daughterboards that are half duplex) dual hop system. Basically, what this means is that the design of this system incorporated having one of the USRP boards as the main node(imitating the function of the eNodeB in an LTE-A network), and then other USRP boards as the end users(Fig. 5.4). Two of the USRP boards were used as relays (USRP N210s) to enhance and improve coverage to those boards that are identified by the main node to have a very poor channel gain. The relay nodes were emulated in such a way that it is possible to have them act as both receivers or relays depending on the functionality chosen for them by the main node. Since the focus of this emulation was the downlink, we used a MySQL database implemented on the main node's PC to keep a store of feedback information about the channel gain on each subcarrier, transmitted by each of the end users via the internet. From this information, the choice of whether to opt for the direct link or the cooperative link (via the relay node) was made by the main node observing the channel gain.Whenever the channel gain of the direct link is less than that of the cooperative link for the end user, the cooperative link(shown as the dotted path in Fig. 5.4) was chosen for the transmission. Additionally, users were assigned subcarriers in resource blocks in which they had, compared to other users in the system, a higher

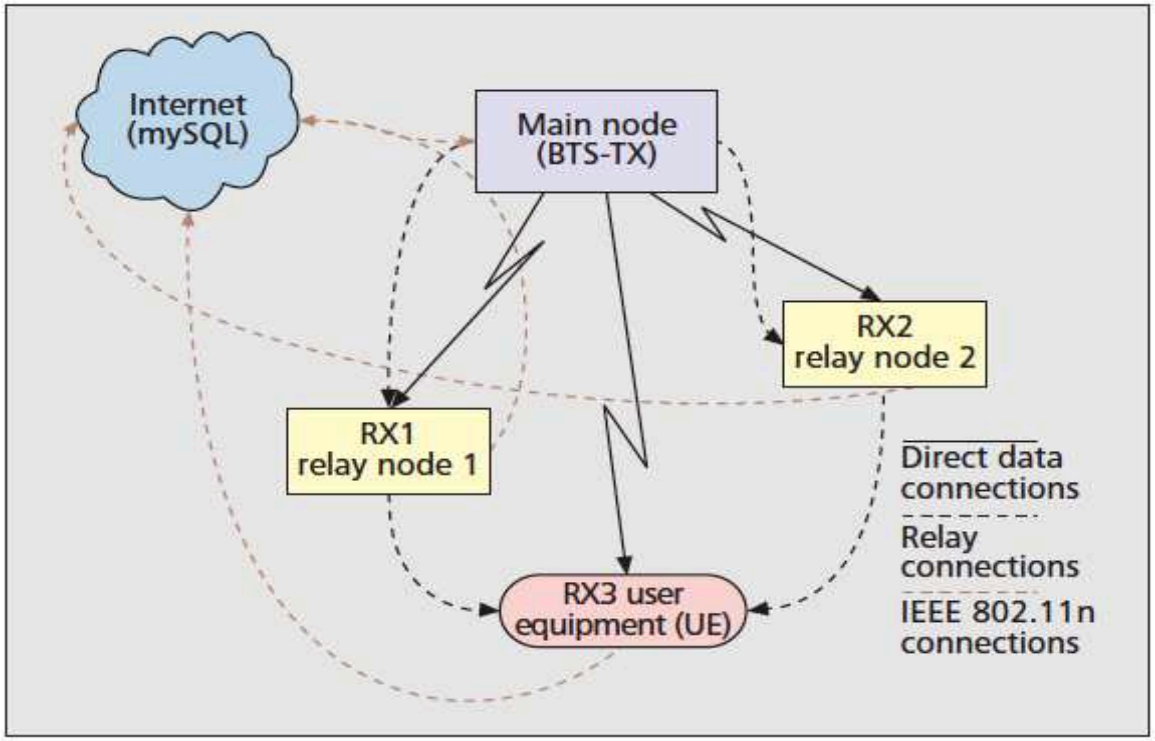

Figure 5.4: Emulation scenario: configuration and topology

channel gain and hence better performance.

The two hop implementation in the downlink implies that for the data destined for the relay attached UEs, resource allocation had to be done twice. However, for simplicity, we opted to emulate the cooperative relaying scenario in which there is only one end node attached to the node acting as a relay at a time. For the first hop, the main node transmits to the other nodes attached to itself (those that do not need a relay) and to the Relay Station(RS). The node chosen to act as a relay in a given transmission relays data to the node incapable of being served sufficiently by the main node in that transmission. All the data to the relay attached UEs is transmitted over the link established between the main node and the RS. For the second hop, the RS allocates resources to the UEs attached to it using the Maximum Sum Rate resource allocation algorithm.

The system design parameters are summarized in Tab.5.2.

5.3.1 OFDMA Transmitter Design

The SDR based implementation of the LTE -A downlink was focused on emulating the physical (PHY) layer of the LTE-A protocol. An emphasis has been placed on the fact that

Table 5.2: Emulated system parameters

Parameters	Values
N_{fft}	128
Max. number of user nodes	3
Size of payload (Bytes)	400
Size of Header and CRC (Bytes)	9
Size of user' transmitting data (Mb)	1
Single bandwidth (KHz)	500
Modulation Scheme	QPSK

the designed and emulated system is based on an LTE-A "like" scenario. This is because of the limitations imposed by the USRP hardware and software design. The GNURadio platform provides an OFDM based modulation and demodulation scheme. This section describes how this modulation scheme was enhanced to create a system using cooperative relaying in an LTE-A like scenario with a focus on the downlink. For this system, we chose to use the non-graphical user interface in developing the software so as to increase the flexibility of the design. Within GNU Radio, a software implementation of the single user orthogonal frequency-division multiplexing (OFDM) transmitter and receiver is already available. This implementation is extended to multi-user OFDMA, which is used in the LTE-A downlink. Following are the assumption made during the implementation:

- Channel is assumed stationary over each subcarrier and varies slowly.
- The number of subcarriers is same for all the nodes.
- Transmission buffer is full for all transmitters.
- RBs are available for transmission.
- The users have homogeneous service requirements.

The transmitter design of this system contains modules defined in python that create graphs for the signal flow from source to the RF front end by interconnecting blocks created using C++. The flow graph (I) of Fig. 5.5 illustrates the interconnection between blocks in the transmitter. In the Fig. 5.5 AWGN noise source module is used only for software simulations. The input data are generated for all users and assembled in packets, the payload size of which is specified in Table 5.2. One by one, the packets are passed to the module `Transmit_Path`.py. The module `Transmit_Path`.py is elaborated in flowchart (II) of Fig. 5.5 within which a sub-module of name Modulator.py is present. This sub-module is responsible for radio resource allocation, subcarrier mapping, inverse fast fourier transform (IFFT), and cyclick prefix addition, as seen in flowchart (III) of Fig. 5.5.

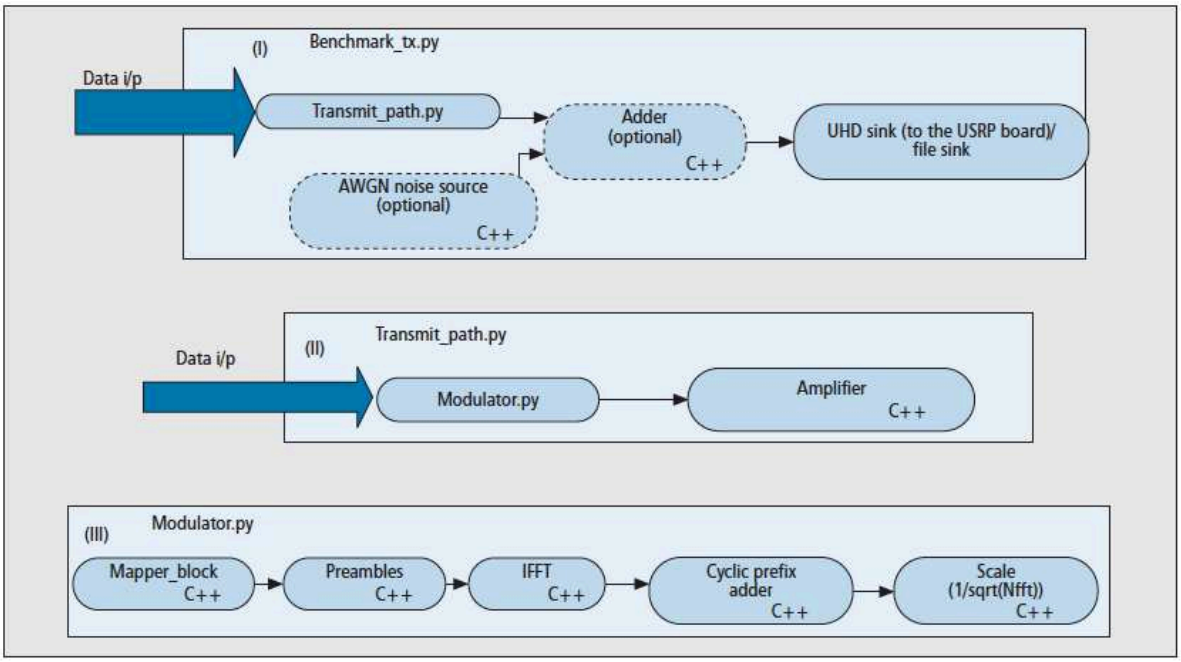

Figure 5.5: Software implementation of OFDMA downlink transmitter

Radio resource allocation and subcarrier mapping are performed by the `Mapper_block`.py (written in C++). Within this script, three tasks are created:

- The incoming data is seperated into users' pipe prior to transmission (Say, 4 users are seperated into 4 pipes).
- Each user is assigned to a RB on the basis of the maximum sum rate (MSR) criterion. The choice of MSR as the radio resource allocation strategy is motivated by its low complexity and ease of implementation. In this scheme, CSI is acquired from the MySQL database that has feedback from the receiver. The feedback information is the channel gain measured over each subcarrier. The information on the assigned RBs is then passed down to the mapper module. In such a way, it is possible to assign to each user those subcarriers in an RB over which that user has the best channel gain (greedy optimization for the MSR resource allocation scheme is adopted). To ensure fairness, equal number of resources is allocated to each user before providing more RBs to the best performers.
- The user messages are retrieved, one at a time, from pipes and mapped onto the delineated subcarriers as per resource allocation scheme in use.

The multi-user signal, generated by the OFDMA baseband transmitter, is finally amplified in RF front-end of USRP boards and transmitted on the wireless channel.

5.3.2 OFDMA Receiver Design

The single-user OFDM receiver implementation available in GNU Radio performs the basic OFDM demodulation tasks. However, the implementation is extended to encompass the functionalities required by both multiuser OFDMA detection and cooperative relaying. The flowchart of Fig. 5.6 shows the flow of signal through the software-implemented blocks for OFDMA downlink receiver. The additional block in standard OFDM GNU

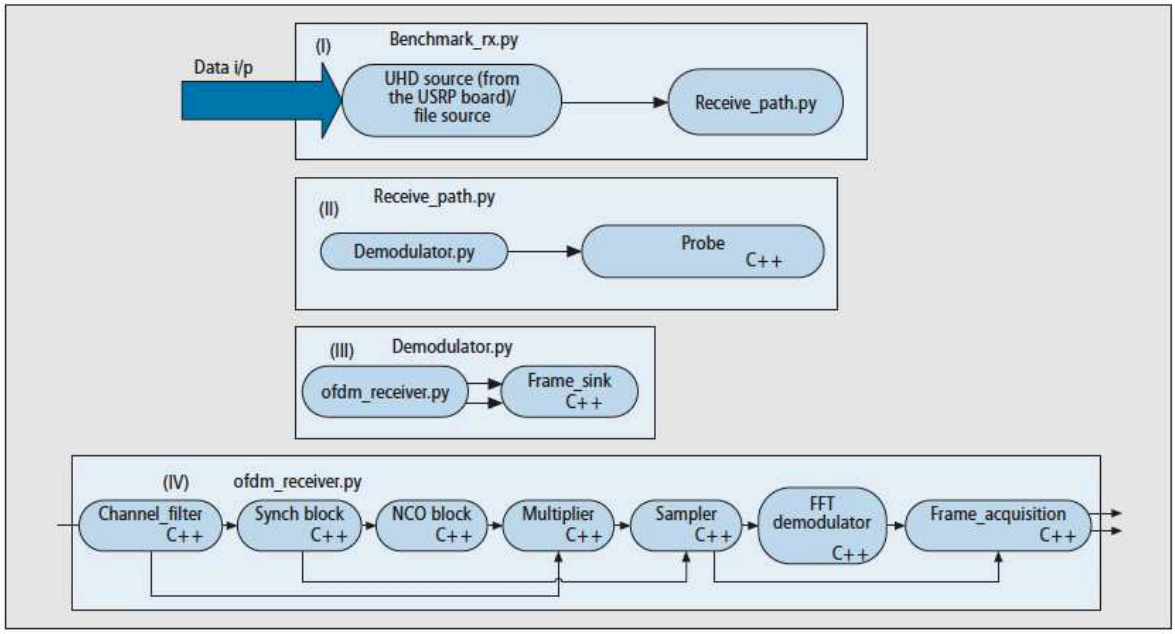

Figure 5.6: Software implementation of OFDMA downlink receiver

radio receiver is `Frame_acquisition` block, written in $C++$ (flowchart IV, Fig. 5.6). The channel estimation is performed in this block and sent to the next block, that is, the `Frame_sink` $C++$ block (flowchart (III), Fig. 5.6). The input signal is then demodulated according to the intended receiver ID.

The `Frame_sink` block performs this operation in a series of states as would a state machine (Fig. 5.7). In the control handling state, the receiver extracts the data symbols sent over allocated RBs labelled with receiver ID. So the receiver ID is enabled to decode the expected data sent from transmitter. As the RBs are determined, the control handling state sets the receiver to acquire the transmitted information from the subcarriers in the assigned RBs and then reassigns the machine to the previous state. The operation then continues on through the other states until the next start of frame flag is received, regardless of the specific state of `Frame_sink`. Indeed, whenever it receives a "Synch rxd" flag, the state machine resets to the Sync search state again, starts the detection

process afresh, and the previous packet is dropped. In this block, an additional capability

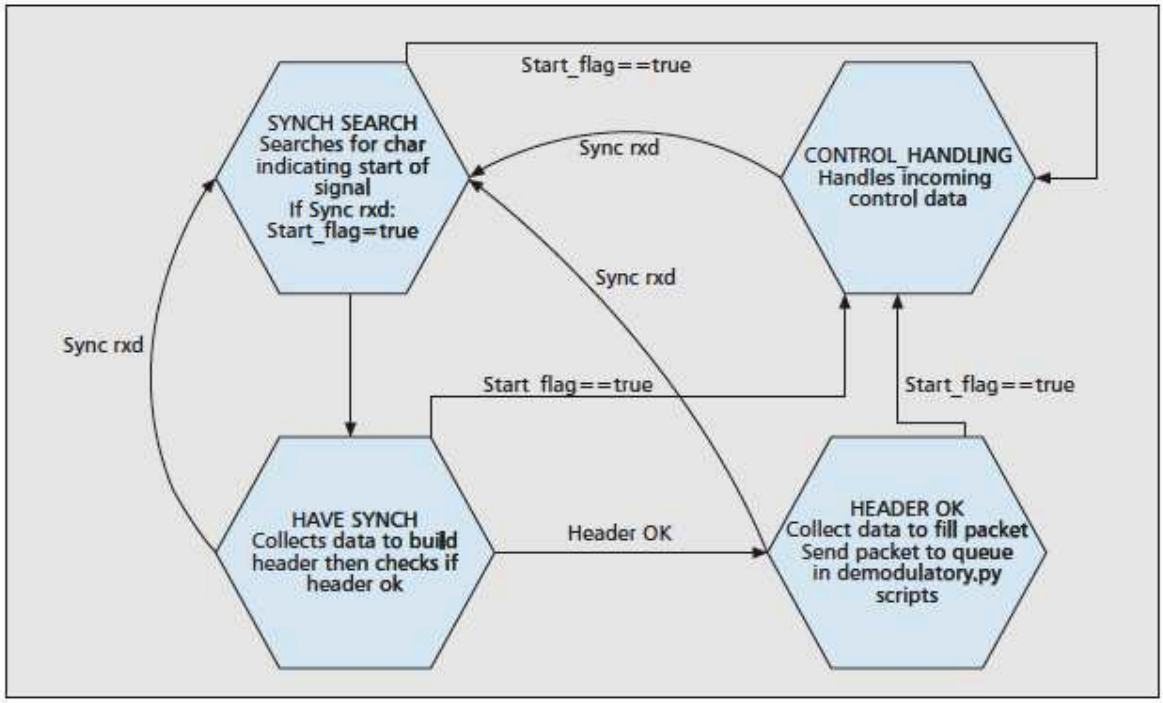

Figure 5.7: Frame synchronization state machine

of inserting the estimated channel gains into an object (accessed from Python script) is considered. A thread, running in parallel to the main flow graph program, updates the database about receiver CSI whenever a new channel estimate is available. Since a premable is used to do channel estimation, so as soon as the preamble is received in every packet, this thread inserts an update about the channel feedback to the MySQL database. Thus, the CSI updates do not slow down the USRP device during data demodulation, as they are executed and stored concurrently.

5.3.3 Cooperative Relay Design

The adopted relay strategy is of type 1, decode-and-forward (DF) first proposed in the LTE Release 8 specification. The protocol enables the relay node to decode the information by suppressing the noise and re-encodes the information for next-hop transmission. Decode-and-forward relaying exhibits higher performance gain with respect to other relaying alternatives at the cost of an increased algorithmic complexity. The half-duplex relay nodes are unidirectional as in typical downlink scenario. Because of the RF daughterboards used by USRP transceiver are half-duplex, the relay can only transmit when it is not in receiving mode. The cooperative relaying algorithm is described in the flowchart

of Fig.5.8. Each relay node is designed to start its functionality as a receiver. For the

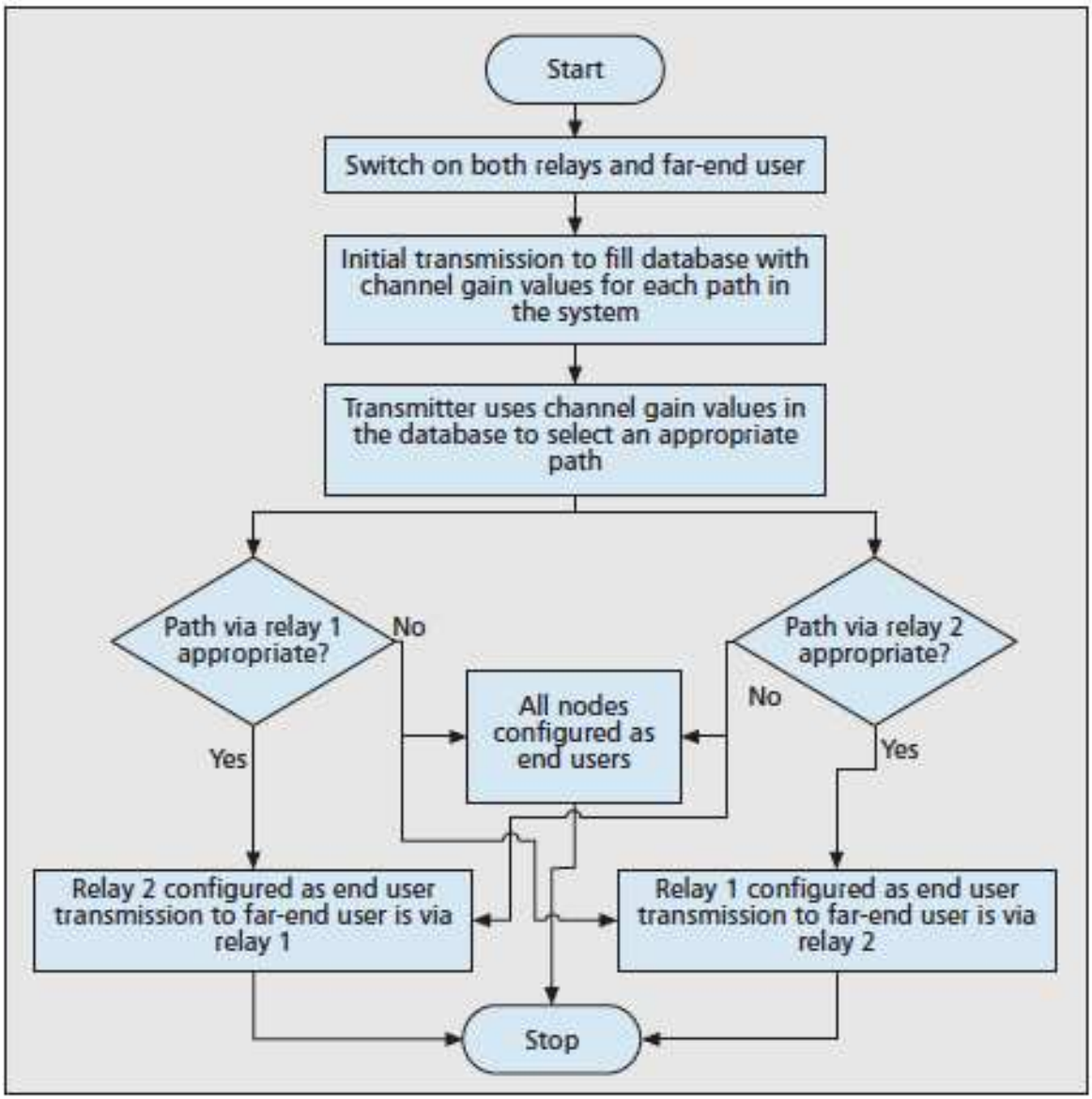

Figure 5.8: Cooperative relaying algorithm

sake of simplicity in emulation, the relay nodes in the system retransmit to a single UE. In order to facilitate cooperative relaying, the design included a further feature where the relay could retransmit or not depending on a parameter contained in the control information sent by the transmitter along with data. This parameter describes the channel conditions between the relay node and the UE. Depending on the value of this parameter, the decision on relay selection is performed, as shown in Fig. 5.8. If both relay paths are

evaluated as appropriate, double relaying is issued, and two relay nodes are activated. At the receiver side, selective diversity combining technique is applied to two relay paths by selecting the one with highest signal-to-noise ratio.

5.3.4 Experimental Results

The experiments shown in this section have been carried out in an indoor environment, more precisely, in two corridors located on the premises of the Department of Information Engineering and Computer Science (DISI) at the University of Trento. The first corridor (wide) is broader and longer than the second corridor (narrow). More precisely, the dimensions are 3 m 55 m for the wide corridor and 1.70 m 30 m for the narrow corridor, respectively. Both environments are open spaces with no objects except for occasional people passing through the corridors.

Figure 5.9: Open-field emulation scenario: Narrow Corridor

In Figs.5.9 and 5.10, two considered emulation scenarios are shown. The positions of main nodes have been fixed in the corridors, whereas positions of UE terminal and relay nodes are varied w.r.t to main node. The relay-UE distance was also varied in the same manner. The relay-UE distance of 2 m was finally chosen because it was observed from ad-hoc experimental trials that this was the optimal distance to improve the coverage from the main node to the UE.

Figure 5.10: Open-field emulation scenario: Wide Corridor

The performance metric chosen to assess the effectiveness of the proposed relaying methodology is the packet error rate (PER) vs. link distance, measured at the UE terminal. Due to random practical channel conditions, sample average of observed PER values were computed after several emulation trails. The confidence intervals for the statistical averages are 5 percent of the sample average for the wide and 10 percent for the narrow corridor, respectively, with a confidence level of 95 percent. Performance bounds were considered from [71], where analytical expressions about bit error rate (BER) achieved by a downlink transmission with single and double cooperative relaying and binary modulations have been derived. PER curves have been obtained by using the approximation $PER = 1 - (1 - BER)^L$, L being the payload size. The AWGN signal-to-noise ratio vs. distance has been computed using the path loss model of [111], while the variance of the multipath attenuation has been estimated using the CSI data stored in the MySQL database. PER results for wide corridor scenario is shown in Fig. 5.11 where performance of testbed with single relaying (UE from relay1) and that of with double relaying (UE from both relays) is depicted. Fig. 5.12 shows the performance of testbed only with double relaying in narrow corridor case. It has been observed during experiments that

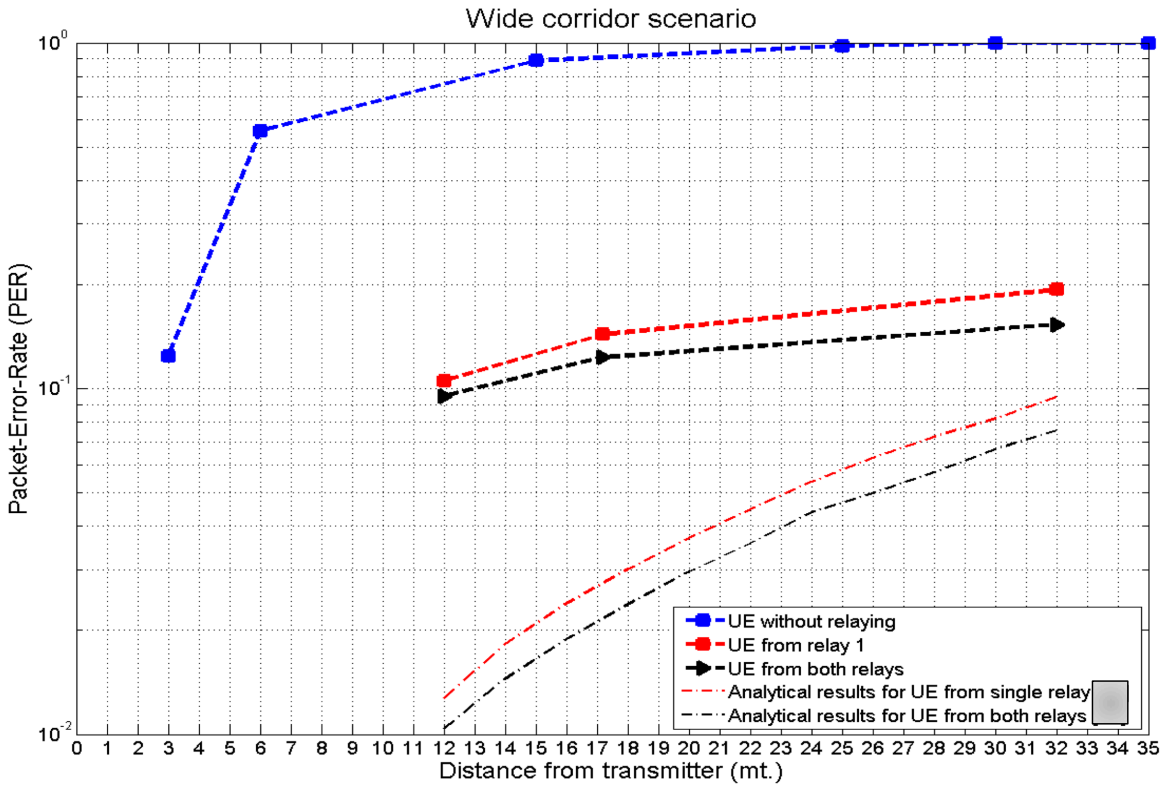

Figure 5.11: Emulation results in terms of PER vs. link distance: Wide Corridor

channel conditions are more severe in the narrow corridor scenario, as clearly evidenced by the higher PER values achieved. The plots obtained in Figs. 5.11-5.12 show the significance of relay nodes in the system as the PER performance increases significantly with respect to direct connection, i.e., main-node to UE (without relaying) for almost all the link distances and conditions considered in the emulations. Due to decode-and-forward protocol used, the usage of relays enables the system to operate nearly at the same performance level as in the case of short-range direct link between transmitter and receiver. This affirms the potential of relaying in future cellular networks. The trend of PER curves is rather similar, but analytical results represent lower bounds on real results. Indeed, analytical evaluation does not take into account inevitable non-idealities of the open-field transmission, e.g., in-band interference, real multipath propagation, wear-tear from low-cost communication hardware, finite precision arithmetic, and so on.

From achieved results, one can understand the ease of experimenting with cutting edge technology using open source hardware and software platforms. The developed cooperative relay test-bed indicates the successful analysis of a technology in academia by performing real experiments. With real experiment trails, interesting insights can be

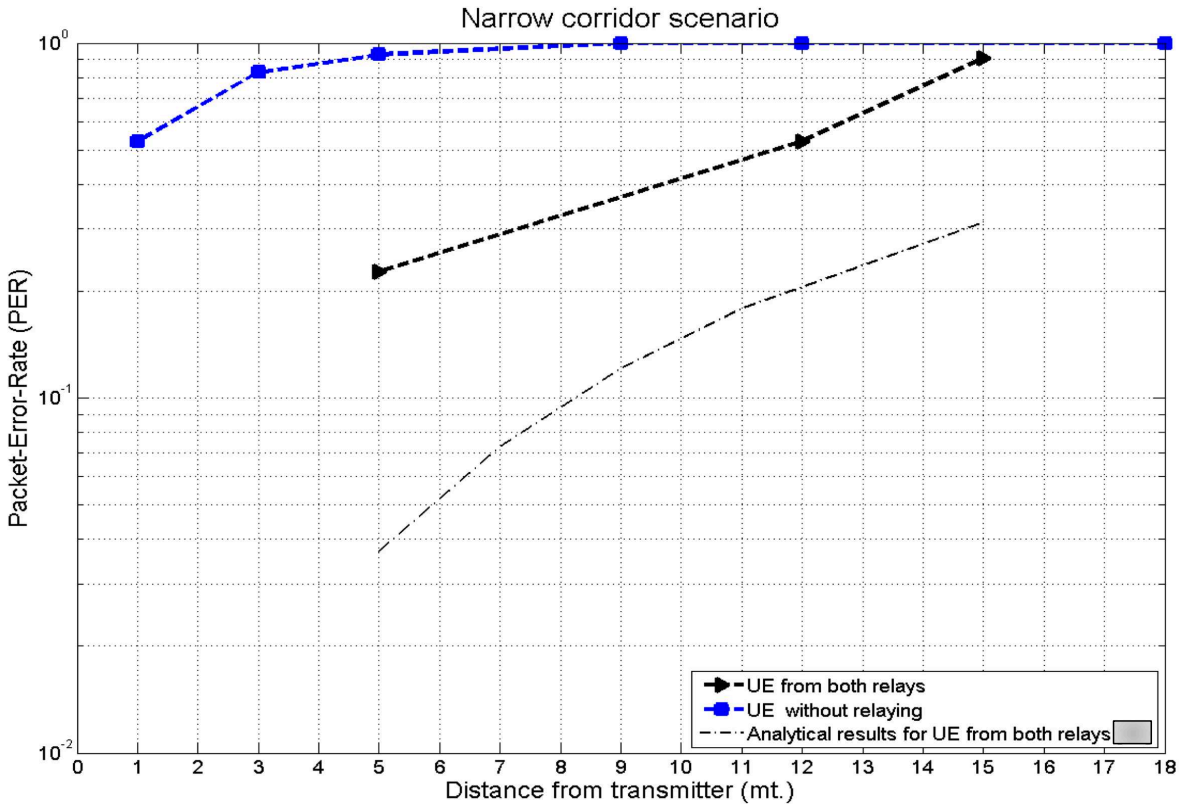

Figure 5.12: Emulation results in terms of PER vs. link distance: Narrow Corridor

derived related to real communication channel that are, otherwise, difficult to capture in software simulations or analytical works. The only bottleneck related to hardware implementation is that experiments can only be performed at a scaled-down level since the low-cost hardware supporting GNU Radio is limited in performance. Nevertheless, even in the presence of limitations, the results are significant and useful for the interested community.

Chapter 6

Conclusion and Future Directions

In this chapter, the methodology and results presented in this thesis are discussed and possible future directions are proposed. The main goal is to study and development of innovative techniques for physical layer of LTE-A uplink in the context of smart city applcations and future upcoming cellular standards (5th generation, 5G). In particular, uplink MIMO transmission is accessed through cooperation between base stations. Moreover, uplink MIMO detection scheme is discussed by proposing a low complexity minimum conditonal bit error probability (MCBEP) in a multiuser scenario. Later on, a power efficient transmission scheme is proposed in the context of upcoming standards that is based on constant envelope SCFDMA (CE-SCFDMA) showing remarkable improvement over current SCFDMA scheme. Wireless backhauling is conceived for connecting small cells where both LOS and NLOS cases are considered. UWB techniques like impulse radio (IR) is considered for LOS scenarios and space time MIMO techniques are relied upon for NLOS. Lastly, LTE-A downlink cooperative relaying is implemented using software-defined radio (SDR) testbed to prove the reconfigurability of future cellular networks.

In chapter 3 section 3.1 uplink cooperative multipoint (CoMP) LTE-A is accessed for improved link performance and energy efficient transmission. A typical LTE-A small-cell scenario has been considered, under the hypothesis of ideal backhaul characterized by error-free and zero latency, which is quite realistic if mmWave wireless backhauling techniques are adopted. Cooperation is conceived at base station level, where neighboring base stations made to cooperate in order to enhance link quality by making full use of energy received on the antennas. In this regard energy efficiency of user equipments (UEs) is analysed. An energy efficiency model is considered for fixed power transmission. It has been shown that a significant perfomance improvement for cell-edge UE obtained by CoMP without any increase of the hardware complexity at the UE. Such a strategy does not require cell-edge users to transmit at high power in order to have high signal to noise ratio at BS and hence energy efficiency is achieved. Performance gains are witnessed over

non-cooperative approach both in ideal and non-ideal channel estimations. Maximum gain is observed with two base stations in case of non-ideal channel estimation. Hence such a strategy is prone to system imperfections. It can be concluded that CoMP strategies are beneficial, in terms of QoS, from UE point of view and it provides green solution to smart cities because users are not required to transmit at exceeded power when located at far distances from eNBs.

Future works may concern with the study of CoMP strategies where the cooperating BSs are selected on the basis of link performance and energy efficiency optimization criteria. Game theory may provide interesting solutions to this problem. MU-MIMO would be an interesting aspect in CoMP strategies where paired users can use same set of radio resources for transmission. In this regard, the link performance and energy efficiency is also limited by multi-user interference (MUI). Another field for research investigation may be related the study of efficient cooperative channel estimation and multi-user detection techniques that can effectively work also in the case of massive MU-MIMO configurations, characterized by the intensive reuse of the radio resources among increasing populations of UEs. Finally, the case of UEs equipped with multiple antennas (two, at most) should be studied in the framework of enhanced MIMO diversity systems.

In section 3.2 a novel constant-envelope multicarrier transmission technique, namely: Constant-Envelope Single-Carrier FDMA (CE-SCFDMA) has been proposed for future uplink cellular systems. The idea is to apply non-linear phase modulation to real-valued SCFDMA signal and that results into constant envelope. Such CE operation is conducive for SCFDMA signals exhibiting lower envelope fluctuations. Hence SCFDMA signals have inherit immunity against nonlinear CE transformation.
Results have shown that CE-SCFDMA is more robust against multipath channels w.r.t SCFDMA. Significant gains are observed at high level of modulations where the performance of SCFDMA is compromised due to high IBO. CE-SCFDMA requires larger modulation index for high modulation order (16QAM, 64QAM) that reduces the spectral efficiency. Sacrificing spectral efficiency results in high performance gains in terms of power efficiency. This makes CE-SCFDMA is a promising candidate for uplink applications in future cellular network. Of course, both spectral and power efficiency are desired due to heavy exchange of data (in the range of Gbps) between the terminal and network operator. Spectral and power in cellular network complement each other. Hence a right tradeoff has to be conceived.
Future works could be based on analysing the effect of non-ideal oscillator causing phase noise in the presence of multiple antennas (MIMO). The spectral efficiency in the system can be improved greatly through the use of multi-user MIMO (MU-MIMO). CE-SCFDMA together with MU-MIMO will be an interesting research in future.

Section 3.3 gives a detail about an iterative minimum conditional bit error probability (MCBEP) multi-user detector that is proposed for uplink SCFDMA. Least mean square (LMS) strategy is applied to minimize the output bit-error probability. State-of-the-art approaches, aiming at maximization of output SINR, namely ideal-MMSE and LMS-MMSE are also discussed for comparison. Fast convergence and near-optimum results advocate the use of proposed MCBEP solution for MU-MIMO. MCBEP outperforms the LMS-MMSE in terms of convergence, indicating the low complexity of the algorithm. It is evident through simulations that minimum bit error rate criterion achieves near optimum results when number of transmitting user K are smaller. The performance of MCBEP appraoches that of ideal-MMSE with the increase in K. The practical implementation of ideal-MMSE is not trivial and usually done through iterative strategy. The iterative LMS-MMSE technique has performance far from optimality as evident in simulation results. Hence a low complex MU-MIMO detector in the shape of MCBEP provides satisfactory results at minimum computational cost. Such a strategy works well in smart city applications where low cost eNBs/BS that are smaller in size and do not intake alot of power for its operations.
In future work, the proposed approach can be applied together with beamforming techniques to further reduce the corrupted effect of MAI and multipath channel. Such a technique works well with in massive MIMO systems where pilot contamination is a big issue. MCBEP does not require pilot but short training symbols for detection. Another interesting research would be the use of recursive least square (RLS) optimizer in MCBEP context together with higher order of modulations. Optimization rules, like bio-inspired, can also be conceived at an affordable computational complexity.

In chapter 4 physical layer transmission schemes for wireless backhaul is considered. Section 4.1 shows a feasible and effective solution for LOS small-cell wireless backhaul based on UWB TH-IR technique in E-band. Typical channel impairments affecting mmWave transmission (rain fading, oxygen absorption, phase noise and timing jitter) have been considered in the simulations. Results have shown the capability of TH-IR of reaching a net capacity of 3.48 Gb/s at a distance greater than 1 Km in a point-to-multipoint 4-to-1 backhaul configuration. This strategy is feasible for a scenario where central hub (fibre connectivity to core network) makes a star-network configuration with other small BSs over wireless link. TH-IR does not require expensive hardware as signal transmission is done without the need of upconverters. Such a low complexity design is advisable for small BS.
In non line of sight (NLOS) the performance of TH-IR techniques degrades dramatically when one channel time delay becomes equal to δ. In case of NLOS, a robust transmission technique should be designed. In future, effectivenss of TH-IR with MIMO is to be

analysed in the presence of NLOS multipath.

Section 4.2 considered a NLOS wireless backhaul scenario where different waveforms are tested over millimeter wave (mmWave) frequency bands. Due to multipath characteristics of the channel, diversity techniques are studied keeping in mind the the issues and challenges in E-band and backhaul. Space-time shift keying (STSK) MIMO with multicarrier (OFDM) and single carrier with cyclic prefixed (SCCP) waveforms are tested and link performance is evaluated. Spatial modulation and spatial multiplexing MIMO techniques with considered waveforms are shown as comparative studies. STSK techniques are able to exploit diversity conveniently in multipath channels especially in case of optimal ML detection for OFDM and suboptimal MMSE detection in case of SCCP. Because of negligible ICI, optimal ML detection, in STSK and SM, has lower complexity. In uncoded case, STSK outperforms SM and SMUX in terms of link performance. Trellis coded STSK and SM do not provide significant gains over uncorrelated channels because only partial information is encoded at the transmitter and hence coding gain is not significant. OFDM-ML STSK technique is preferred choice for long range backhaul with optimal performance at affordable computational complexity. Since OFDM-ML STSK is vulnerable to phase noise and power amplifier effects, expensive transceiver design is required for satisfactory performance. On the other hand, SCCP-MMSE STSK does not require expensive oscillators to work with due to inherent resilience against phase noise but performance is slightly degraded as compare to OFDM-ML due to sub-optimality of MMSE receiver.
Trellis code does not provide sufficient gains for SM and STSK in uncorrelated channels. However increasing the modulation order and decreasing Q in STSK will help in attaining coding gains and coverage extension is possible. Current work is based on point-to-point links which can be extended to point-to-multipoint (P-t-mP) using OFDMA and TDMA in case of SCCP. This is an interesting future direction where the impact of interference can play decisive role in link performance analysis.

Feasibility of software-defined radio (SDR) using an open source GNU Radio platform to emulate cooperative relaying in LTE-A downlink is demonstrated in chapter 5. The system was developed and tested to observe, how a reconfigurable SDR helps the system in attaining benefits of cooperative relaying in LTE-A downlink. Additionally, this testbed provides a platform to test hardware/software applications that involve other typologies of resource allocation in different relaying techniques. The experimental results are achieved in open field testifying the effectiveness of cooperative relaying in LTE-A scenario. Constraints are associated with hardware in terms of processing power, still the experimental analysis represent a preliminary study about the viability of SDR implementation of cooperative communications in LTE-A applications.

SDR can enable several infrastructure gains in case of unusual events (e.g., emergency events, festivals etc). The service provider can reconfigure the network by adding functionalities to cope with the needs originated during the event. This can be accomplished through SDR that makes the reconfigurability easy. In this regard, future LTE-A network, for smart city applications, takes help from SDR that enables the terminal and network reconfigurability by simply downloading the software.
In future work An SDR-based uplink cooperative relaying strategy is being devised for LTE-A 'like' scenarios. The understudy testbed is based on USRP1 and USRP-N210 where the aim is to analyse advantages, in terms of range and link level performance, of relaying in uplink scenarios.

Bibliography

[1] 3GPP TR 36.912 - Feasibility study for further advancements for EUTRA (LTE-Advanced).

[2] ABI research. http://venturebeat.com/tag/abi-research/. [Online].

[3] Agilent Technologies. http://www.agilent.com. [Online].

[4] E-band Communications. http://www.e-band.com/index.php?id=86. [Online].

[5] Ettus Research. www.ettus.com. [Online].

[6] EU OUTSMART project. http://fi-ppp-outsmart.eu/. [Online].

[7] SDR: The Future of Radio. Available ONLINE. [Online: Accessed on 25/01/2013].

[8] Specific attenuation model for rain for use in prediction methods. Rec. ITU-R P.838-3,. [Online].

[9] M.R. Akdeniz, Yuanpeng Liu, M.K. Samimi, Shu Sun, S. Rangan, T.S. Rappaport, and E. Erkip. Millimeter Wave Channel Modeling and Cellular Capacity Evaluation. *IEEE Journal on Selected Areas in Communications,*, 32(6):1164–1179, June 2014.

[10] Ian F. Akyildiz, David M. Gutierrez-Estevez, and Elias Chavarria Reyes. The Evolution to 4G Cellular Systems: LTE-Advanced. *Phys. Commun.*, 3(4):217–244, December 2010.

[11] Md Shamsul Alam, Jon W. Mark, and Xuemin Sherman Shen. Relay Selection and Resource Allocation for Multi-User Cooperative OFDMA Networks. *IEEE Transactions on Wireless Communications,*, 12(5):2193–2205, May 2013.

[12] S. Alamouti. A simple transmit diversity technique for wireless communications. *IEEE Journal on Selected Areas in Communications,*, 16(8):1451–1458, Oct 1998.

[13] M.Y. Alias, Sheng Chen, and L. Hanzo. Multiple-antenna-aided OFDM employing genetic-algorithm-assisted minimum bit error rate multiuser detection. *IEEE Transactions on Vehicular Technology*, 54(5):1713–1721, Sept 2005.

[14] M.Y. Alias, A.K. Samingan, S. Chen, and L. Hanzo. Multiple antenna aided OFDM employing minimum bit error rate multiuser detection. *Electronics Letters*, 39(24):1769–1770, Nov 2003.

[15] F. Babich, A. Crismani, M. Driusso, and L. Hanzo. Design Criteria and Genetic Algorithm Aided Optimization of Three-Stage-Concatenated Space-Time Shift Keying Systems. *IEEE Signal Processing Letters,*, 19(8):543–546, Aug 2012.

[16] Fulvio Babich, Guido Montorsi, and Francesca Vatta. On rate-compatible punctured turbo codes design. *EURASIP Journal on Applied Signal Processing*, 2005:784–794, 2005.

[17] C.F. Ball, R. Mullner, J. Lienhart, and H. Winkler. Performance analysis of Closed and Open loop MIMO in LTE. In *European Wireless Conference, 2009. EW 2009.*, pages 260–265, May 2009.

[18] P. Baracca, S. Tomasin, and N. Benvenuto. Backhaul Rate Allocation in Uplink SC-FDMA Systems with Multicell Processing. *IEEE Transactions on Wireless Communications*, 13(3):1264–1273, March 2014.

[19] Zubin Bharucha, Harald Haas, Andreas Saul, and Gunther Auer. Throughput enhancement through femto-cell deployment. *European Transactions on Telecommunications*, 21(5):469–477, 2010.

[20] Gangadhar S Biradar, SN Merchant, and Uday B Desai. Frequency and time hopping PPM UWB multiple access communication scheme. *journal of communications*, 4(1):14–19, 2009.

[21] Y.W. Blankenship. Achieving high capacity with small cells in LTE-A. In *50th Annual Allerton Conference on Communication, Control, and Computing (Allerton), 2012*, pages 1680–1687, 2012.

[22] A. Caragliu, C. Del Bo, and P. Nijkamp. Smart cities in Europe. In *VU University Amsterdam, Faculty of Economics, Business Administration and Econometrics*, page 0048, 2009.

[23] R.L.G. Cavalcante, S. Stanczak, M. Schubert, A. Eisenblaetter, and U. Tuerke. Toward Energy-Efficient 5G Wireless Communications Technologies: Tools for decoupling the scaling of networks from the growth of operating power. *IEEE Signal Processing Magazine,*, 31(6):24–34, Nov 2014.

[24] CELTIC/CP5-026 WINNER+,. D1.4 initial report on advanced multiple antenna systems. In *Tech. Report*, January 2009.

[25] I. Cianci, G. Piro, L.A. Grieco, G. Boggia, and P. Camarda. Content Centric Services in Smart Cities. In *6th International Conference on Next Generation Mobile Applications, Services and Technologies (NGMAST), 2012*, pages 187–192, Sept 2012.

[26] Antonio Cimmino, Tommaso Pecorella, Romano Fantacci, Fabrizio Granelli, Talha Faizur Rahman, Claudio Sacchi, Camillo Carlini, and Piyush Harsh. The role of small cell technology in future Smart City applications. *Transactions on Emerging Telecommunications Technologies*, pages n/a–n/a, 2013.

[27] M. Coldrey, J.-E. Berg, L. Manholm, C. Larsson, and J. Hansryd. Non-line-of-sight small cell backhauling using microwave technology. *IEEE Communications Magazine,*, 51(9):78–84, September 2013.

[28] Claudio Colombo and Massimo Cirigliano. Next-generation Access Network: A Wireless Network Using E-band Radio Frequency (71-86GHz) to Provide Wideband Connectivity. *Bell Lab. Tech. J.*, 16(1):187–205, June 2011.

[29] Shuguang Cui, A.J. Goldsmith, and A. Bahai. Energy-efficiency of MIMO and cooperative MIMO techniques in sensor networks. *IEEE Journal on Selected Areas in Communications,*, 22(6):1089–1098, Aug 2004.

[30] P.M. Dayal, U.B. Desai, and A. Mahanta. Minimum conditional probability of error detection for MC-CDMA. In *IEEE Eighth International Symposium on Spread Spectrum Techniques and Applications, 2004*, pages 51–55, Aug 2004.

[31] M. De Sanctis, E. Cianca, T. Rossi, C. Sacchi, L. Mucchi, and R. Prasad. Waveform design solutions for EHF broadband satellite communications. *IEEE Communications Magazine,*, 53(3):18–23, March 2015.

[32] C. Dehos, J.L. Gonzalez, A. De Domenico, D. Ktenas, and L. Dussopt. Millimeter-wave access and backhauling: the solution to the exponential data traffic increase in 5G mobile communications systems? *IEEE Communications Magazine,*, 52(9):88–95, September 2014.

[33] Leandro D'orazio, Claudio Sacchi, Massimo Donelli, Jérôme Louveaux, and Luc Vandendorpe. A near-optimum multiuser receiver for STBC MC-CDMA systems based on minimum conditional BER criterion and genetic algorithm-assisted channel estimation. *EURASIP Journal on Wireless Communications and Networking*, 2011(1):351494, 2011.

[34] M. Driusso, F. Babich, M.I. Kadir, and L. Hanzo. OFDM Aided Space-Time Shift Keying for Dispersive Downlink Channels. In *2012 IEEE Vehicular Technology Conference (VTC Fall),*, pages 1–5, Sept 2012.

[35] V. Dyadyuk, J.D. Bunton, J. Pathikulangara, R. Kendall, O. Sevimli, L. Stokes, and D.A. Abbott. A Multigigabit Millimeter-Wave Communication System With Improved Spectral Efficiency. *IEEE Transactions on Microwave Theory and Techniques,*, 55(12):2813–2821, Dec 2007.

[36] M. El-Sayed and P. Gagen. Mobile Data explosion and planning of heterogeneous networks. In *XVth International Telecommunications Network Strategy and Planning Symposium (NETWORKS), 2012*, pages 1–6, 2012.

[37] Levin G. White Paper: The Economics of Gigabit 4G Mobile Backhaul.

[38] J.A. Galache, J.R. Santana, V. Gutierrez, L. Sanchez, P. Sotres, and L. Munoz. Towards experimentation-service duality within a Smart City scenario. In *9th Annual Conference on Wireless On-demand Network Systems and Services (WONS), 2012*, pages 175–181, 2012.

[39] Xiaohu Ge, Hui Cheng, M. Guizani, and Tao Han. 5G wireless backhaul networks: challenges and research advances. *IEEE Network,*, 28(6):6–11, Nov 2014.

[40] M. Geles, A. Averbuch, O. Amrani, and D. Ezri. Performance Bounds for Maximum Likelihood Detection of Single Carrier FDMA. *IEEE Transactions on Communications,*, 60(7):1945–1952, July 2012.

[41] D. Gesbert, S. Hanly, H. Huang, S. Shamai Shitz, O. Simeone, and Wei Yu. Multi-Cell MIMO Cooperative Networks: A New Look at Interference. *IEEE Journal on Selected Areas in Communications,*, 28(9):1380–1408, December 2010.

[42] Mohammad Ghavami, Lachlan Michael, and Ryuji Kohno. *Ultra wideband signals and systems in communication engineering*. John Wiley & Sons, 2007.

[43] A. Ghosh, T.A. Thomas, M.C. Cudak, R. Ratasuk, P. Moorut, F.W. Vook, T.S. Rappaport, G.R. Maccartney, Shu Sun, and Shuai Nie. Millimeter-Wave Enhanced Local Area Systems: A High-Data-Rate Approach for Future Wireless Networks. *IEEE Journal on Selected Areas in Communications,*, 32(6):1152–1163, June 2014.

[44] Arunabha Ghosh, Jun Zhang, Jeffrey G. Andrews, and Rias Muhamed. *Fundamentals of LTE*. Prentice Hall Press, Upper Saddle River, NJ, USA, 1st edition, 2010.

[45] F. Gil-Castineira, E. Costa-Montenegro, F.J. Gonzalez-Castano, C. Lopez-Bravo, T. Ojala, and R. Bose. Experiences inside the Ubiquitous Oulu Smart City. *Computer*, 44(6):48–55, 2011.

[46] Andrea Goldsmith. *Wireless Communications*. Cambridge University Press, New York, NY, USA, 2005.

[47] Nan Guo, Robert C Qiu, Shaomin S Mo, and Kazuaki Takahashi. 60-GHz millimeter-wave radio: Principle, technology, and new results. *EURASIP Journal on Wireless Communications and Networking*, 2007(1):48–48, 2007.

[48] Weisi Guo and T. O'Farrell. Capacity-Energy-Cost Tradeoff in Small Cell Networks. In *IEEE 75th Vehicular Technology Conference (VTC Spring), 2012*, pages 1–5, May 2012.

[49] Z. Hasan, H. Boostanimehr, and V.K. Bhargava. Green Cellular Networks: A Survey, Some Research Issues and Challenges. *IEEE Communications Surveys Tutorials,*, 13(4):524–540, Fourth 2011.

[50] B. Hassibi and B.M. Hochwald. High-rate codes that are linear in space and time. *IEEE Transactions on Information Theory,*, 48(7):1804–1824, Jul 2002.

[51] Dr Harri Holma and Dr Antti Toskala. *LTE for UMTS - OFDMA and SC-FDMA Based Radio Access*. Wiley Publishing, 2009.

[52] J. Hoydis, M. Kobayashi, and M. Debbah. Green Small-Cell Networks. *IEEE Vehicular Technology Magazine,*, 6(1):37–43, March 2011.

[53] J. Hoydis, M. Kobayashi, and M. Debbah. Green Small-Cell Networks. *IEEE Vehicular Technology Magazine,*, 6(1):37–43, 2011.

[54] G. Huang, A. Nix, and S. Armour. Decision feedback equalization in SC-FDMA. In *IEEE 19th International Symposium on Personal, Indoor and Mobile Radio Communications, 2008. PIMRC 2008*, pages 1–5, Sept 2008.

[55] Guo J. CSIRO Submission 09/348 - Department of Broadband Communications and the Digital Economy - Response to the Blackspots Initiative Stakeholder Consultation Paper.

[56] J. Jeganathan, A. Ghrayeb, and L. Szczecinski. Spatial modulation: optimal detection and performance analysis. *IEEE Communications Letters,*, 12(8):545–547, Aug 2008.

[57] Dajie Jiang, Qixing Wang, Jianjun Liu, Guangyi Liu, and Chunfeng Cui. Uplink Coordinated Multi-Point Reception for LTE-Advanced Systems. In *5th International Conference on Wireless Communications, Networking and Mobile Computing, 2009. WiCom '09.*, pages 1–4, Sept 2009.

[58] V. Jungnickel, S. Jaeckel, K. Borner, M. Schlosser, and L. Thiele. Estimating the mobile backhaul traffic in distributed coordinated multi-point systems. In *IEEE Wireless Communications and Networking Conference (WCNC), 2012*, pages 3763–3768, April 2012.

[59] V. Jungnickel, K. Manolakis, S. Jaeckel, M. Lossow, P. Farkas, M. Schlosser, and V. Braun. Backhaul requirements for inter-site cooperation in heterogeneous LTE-Advanced networks. In *IEEE International Conference on Communications Workshops (ICC), 2013*, pages 905–910, June 2013.

[60] M.I. Kadir, S. Sugiura, Jiayi Zhang, Sheng Chen, and L. Hanzo. OFDMA/SC-FDMA Aided Space Time Shift Keying for Dispersive Multiuser Scenarios. *IEEE Transactions on Vehicular Technology,*, 62(1):408–414, Jan 2013.

[61] S. Kadloor and R. Adve. Relay selection and power allocation in cooperative cellular networks. *IEEE Transactions on Wireless Communications,*, 9(5):1676–1685, May 2010.

[62] O. Katz, R. Ben-Yishay, R. Carmon, B. Sheinman, F. Szenher, D. Papae, and D. Elad. High-power high-linearity SiGe based E-BAND transceiver chipset for broadband communication. In *IEEE Radio Frequency Integrated Circuits Symposium (RFIC), 2012*, pages 115–118, June 2012.

[63] Y. Kawano, Y. Nakasha, T. Suzuki, T. Ohki, T. Takahashi, K. Makiyama, Tatsuya Hirose, and K. Joshin. Sub-10 ps Pulse Generator with Biphase Modulation Function in 0.13-micron InP HEMT. In *36th European Microwave Conference, 2006.*, pages 1821–1824, Sept 2006.

[64] Brian Kelley. Software defined radio for broadband OFDM protocols. In *Systems, Man and Cybernetics, 2009. SMC 2009. IEEE International Conference on*, pages 2309–2314, Oct 2009.

[65] F. Khan. Capacity and Range Analysis of Multi-Hop Relay Wireless Networks. In *IEEE 64th Vehicular Technology Conference, 2006. VTC-2006 Fall. 2006*, pages 1–5, Sept 2006.

[66] G. Korinthios, E. Theodoropoulou, N. Marouda, I. Mesogiti, E. Nikolitsa, and G. Lyberopoulos. Early experiences and lessons learned from femtocells. *IEEE Communications Magazine,*, 47(9):124–130, 2009.

[67] Daewon Lee, Hanbyul Seo, B. Clerckx, E. Hardouin, D. Mazzarese, S. Nagata, and K. Sayana. Coordinated multipoint transmission and reception in LTE-advanced: deployment scenarios and operational challenges. *IEEE Communications Magazine,*, 50(2):148–155, February 2012.

[68] T.H. Lee and A. Hajimiri. Oscillator phase noise: a tutorial. *IEEE Journal of Solid-State Circuits,*, 35(3):326–336, March 2000.

[69] Qian Li, R.Q. Hu, Yi Qian, and Geng Wu. Intracell Cooperation and Resource Allocation in a Heterogeneous Network With Relays. *IEEE Transactions on Vehicular Technology,*, 62(4):1770–1784, May 2013.

[70] Zihuai Lin, Pei Xiao, B. Vucetic, and M. Sellathurai. Analysis of receiver algorithms for LTE SC-FDMA based uplink MIMO systems. *IEEE Transactions on Wireless Communications*, 9(1):60–65, January 2010.

[71] Peng Liu and Il-Min Kim. Average BER analysis for binary signallings in decode-and-forward dissimilar cooperative diversity networks. *IEEE Transactions on Wireless Communications,*, 8(8):3961–3968, August 2009.

[72] Sheng Liu, Jianjun Wu, Chung Ha Koh, and V.K.N. Lau. A 25 Gb/s(/km2) urban wireless network beyond IMT-advanced. *IEEE Communications Magazine,*, 49(2):122–129, 2011.

[73] Wenyu Liu, Xiaohua Li, and Mo Chen. Energy efficiency of MIMO transmissions in wireless sensor networks with diversity and multiplexing gains. In *IEEE International Conference on Acoustics, Speech, and Signal Processing, 2005. Proceedings. (ICASSP '05).*, volume 4, pages iv/897–iv/900 Vol. 4, March 2005.

[74] L Luini and C Capsoni. Estimating the spatial cumulative distribution of rain from precipitation amounts. *Radio Science*, 47(1), 2012.

[75] R. Madan, N.B. Mehta, A.F. Molisch, and Jin Zhang. Energy-Efficient Cooperative Relaying over Fading Channels with Simple Relay Selection. *IEEE Transactions on Wireless Communications,*, 7(8):3013–3025, August 2008.

[76] P. Marsch and G. Fettweis. Uplink CoMP under a Constrained Backhaul and Imperfect Channel Knowledge. *IEEE Transactions on Wireless Communications,*, 10(6):1730–1742, June 2011.

[77] H. Mehrpouyan, M.R. Khanzadi, M. Matthaiou, A.M. Sayeed, R. Schober, and Yingbo Hua. Improving bandwidth efficiency in E-band communication systems. *IEEE Communications Magazine,*, 52(3):121–128, March 2014.

[78] R. Mesleh, M. Di Renzo, H. Haas, and Peter M. Grant. Trellis Coded Spatial Modulation. *IEEE Transactions on Wireless Communications,*, 9(7):2349–2361, July 2010.

[79] R. Mesleh, H. Haas, Chang Wook Ahn, and Sangboh Yun. Spatial Modulation - A New Low Complexity Spectral Efficiency Enhancing Technique. In *First International Conference on Communications and Networking in China, 2006. ChinaCom '06.*, pages 1–5, Oct 2006.

[80] R.Y. Mesleh, H. Haas, S. Sinanovic, Chang Wook Ahn, and Sangboh Yun. Spatial Modulation. *IEEE Transactions on Vehicular Technology,*, 57(4):2228–2241, July 2008.

[81] R. Mulinde, T.F. Rahman, and C. Sacchi. Constant-envelope SC-FDMA for nonlinear satellite channels. In *IEEE Global Communications Conference (GLOBECOM), 2013*, pages 2939–2944, Dec 2013.

[82] T. Nakamura, S. Nagata, A. Benjebbour, Y. Kishiyama, Tang Hai, Shen Xiaodong, Yang Ning, and Li Nan. Trends in small cell enhancements in LTE advanced. *IEEE Communications Magazine,*, 51(2):98–105, 2013.

[83] Y. Nakasha, Y. Kawano, T. Suzuki, T. Ohki, T. Takahashi, K. Makiyama, T. Hirose, and N. Hara. A W-band wavelet generator using 0.13-mu m InP HEMTs for multi-gigabit communications based on ultra-wideband impulse radio.

[84] Hoondong Noh, Myoungseok Kim, Jaesang Ham, and Chungyong Lee. A practical MMSE-ML detector for a MIMO SC-FDMA system. *IEEE Communications Letters,*, 13(12):902–904, December 2009.

[85] A.J. Paulraj, D.A. GORE, R.U. Nabar, and H. Bolcskei. An overview of MIMO communications - a key to gigabit wireless. *Proceedings of the IEEE*, 92(2):198–218, Feb 2004.

[86] Zhouyue Pi and F. Khan. An introduction to millimeter-wave mobile broadband systems. *IEEE Communications Magazine,*, 49(6):101–107, June 2011.

[87] John G. Proakis and Dimitris G. Manolakis. *Digital Signal Processing (3rd Ed.): Principles, Algorithms, and Applications*. Prentice-Hall, Inc., Upper Saddle River, NJ, USA, 1996.

[88] M. Rahman, S. Latif, T. Ahad, P.K. Dey, M.F. Rabbi Ur Rashid, B. Rashid, and S. Ahmed. The Study of OFDM ICI Cancellation Schemes in 2.4 GHz Frequency Band Using Software Defined Radio. In *7th International Conference onWireless Communications, Networking and Mobile Computing (WiCOM), 2011*, pages 1–6, Sept 2011.

[89] T.F. Rahman and C. Sacchi. A cooperative radio resource management strategy for mobile multimedia lte uplink. In *Aerospace Conference, 2014 IEEE*, pages 1–8, March 2014.

[90] R. Rajashekar, K.V.S. Hari, and L. Hanzo. Spatial Modulation Aided Zero-Padded Single Carrier Transmission for Dispersive Channels. *IEEE Transactions on Communications,*, 61(6):2318–2329, June 2013.

[91] T.S. Rappaport, G.R. Maccartney, M.K. Samimi, and Shu Sun. Wideband Millimeter-Wave Propagation Measurements and Channel Models for Future Wireless Communication System Design. *IEEE Transactions on Communications*, 63(9):3029–3056, Sept 2015.

[92] T.S. Rappaport, J.N. Murdock, and F. Gutierrez. State of the Art in 60-GHz Integrated Circuits and Systems for Wireless Communications. *Proceedings of the IEEE*, 99(8):1390–1436, Aug 2011.

[93] T.S. Rappaport, Shu Sun, R. Mayzus, Hang Zhao, Y. Azar, K. Wang, G.N. Wong, J.K. Schulz, M. Samimi, and F. Gutierrez. Millimeter Wave Mobile Communications for 5G Cellular: It Will Work! *IEEE Access,*, 1:335–349, 2013.

[94] C. Sacchi, C. Stallo, and T. Rossi. Space and frequency multiplexing for MM-wave multi-gigabit point-to-point transmission links. In *IEEE Aerospace Conference, 2013*, pages 1–10, March 2013.

[95] A.A.M. Saleh. Frequency-Independent and Frequency-Dependent Nonlinear Models of TWT Amplifiers. *IEEE Transactions on Communications,*, 29(11):1715–1720, November 1981.

[96] S.J. Silverman. Games theory and software defined radios. In *IEEE Military Communications Conference, 2006. MILCOM 2006.*, pages 1–7, Oct 2006.

[97] Smart City. Smart city — Wikipedia, the free encyclopedia, 2015. [Online; accessed 27-October-2015].

[98] Cosimo Stallo, Ernestina Cianca, Sandeep Mukherjee, Tommaso Rossi, Mauro De Sanctis, and Marina Ruggieri. UWB for multi-gigabit/s communications beyond 60 GHz. *Telecommunication Systems*, 52(1):161–181, 2013.

[99] S. Sugiura, Sheng Chen, and L. Hanzo. Coherent and Differential Space-Time Shift Keying: A Dispersion Matrix Approach. *IEEE Transactions on Communications,*, 58(11):3219–3230, November 2010.

[100] A.A. Tabassam, F.A. Ali, S. Kalsait, and M.U. Suleman. Building Software-Defined Radios in MATLAB Simulink - A Step Towards Cognitive Radios. In *13th International Conference on Computer Modelling and Simulation (UKSim), 2011 UkSim*, pages 492–497, March 2011.

[101] Y. Tachwali and H. Refai. Implementation of a BPSK Transceiver on Hybrid Software Defined Radio Platforms. In *3rd International Conference on Information and Communication Technologies: From Theory to Applications, 2008. ICTTA 2008.*, pages 1–5, April 2008.

[102] R. Taori and A. Sridharan. Point-to-multipoint in-band mmwave backhaul for 5G networks. *IEEE Communications Magazine,*, 53(1):195–201, January 2015.

[103] Y.B. Thakare, S.S. Musale, and P.G. Shete. Next generation communication towards open wireless standard and software defined radio. In *IET International Conference on Wireless, Mobile and Multimedia Networks, 2008.*, pages 168–171, Jan 2008.

[104] The Global mobile Suppliers Association. GSM/3G market update. Feburary 2010.

[105] S.C. Thompson, A.U. Ahmed, J.G. Proakis, J.R. Zeidler, and M.J. Geile. Constant envelope ofdm. *IEEE Transactions on Communications*, 56(8):1300–1312, August 2008.

[106] A.C. Tribble. The software defined radio: Fact and fiction. In *IEEE Radio and Wireless Symposium, 2008*, pages 5–8, Jan 2008.

[107] Lei Wang, Yu Jian Cheng, Da Ma, and Cheng Xiang Weng. Wideband and Dual-Band High-Gain Substrate Integrated Antenna Array for E-Band Multi-Gigahertz Capacity Wireless Communication Systems. *IEEE Transactions on Antennas and Propagation,*, 62(9):4602–4611, Sept 2014.

[108] Qixing Wang, Dajie Jiang, Guangyi Liu, and Zhigang Yan. Coordinated Multiple Points Transmission for LTE-Advanced Systems. In *5th International Conference on Wireless Communications, Networking and Mobile Computing, 2009. WiCom '09.*, pages 1–4, Sept 2009.

[109] Qixing Wang, Jing Jin, Guangyi Liu, and Shuguang Cui. Coordinated multi-cell beamforming for TD-LTE-advanced systems. In *2011 Conference Record of*

the Forty Fifth Asilomar Conference on Signals, Systems and Computers (ASILOMAR),, pages 1304–1308, Nov 2011.

[110] Yangyang Wang and Yanhui Zhou. Cloud architecture based on Near Field Communication in the smart city. In *7th International Conference on Computer Science Education (ICCSE), 2012*, pages 231–234, 2012.

[111] Ye Wang, Wen-jun Lu, and Hong-bo Zhu. An empirical path-loss model for wireless channels in indoor short-range office environment. *International Journal of Antennas and Propagation*, 2012, 2012.

[112] Moe Z. Win and Robert A. Scholtz. Impulse radio: how it works. *IEEE Communications Letters*, 2:36–38, 1998.

[113] M.P. Wylie-Green, E. Perrins, and T. Svensson. Introduction to CPM-SC-FDMA: A Novel Multiple-Access Power-Efficient Transmission Scheme. *IEEE Transactions on Communications,*, 59(7):1904–1915, July 2011.

[114] E. Yaacoub. Green communications in LTE networks with environmentally friendly small cell base stations. In *IEEE Online Conference on Green Communications (GreenCom), 2012*, pages 110–115, 2012.

[115] Yuyu Yan, Huiyu Yuan, Naizheng Zheng, and S. Peter. Performance of uplink multiuser MIMO in LTE-advanced networks. In *International Symposium on Wireless Communication Systems (ISWCS), 2012*, pages 726–730, Aug 2012.

[116] Hen-Geul Yeh and P. Ingerson. Software-defined radio for OFDM transceivers. In *4th Annual IEEE Systems Conference, 2010*, pages 261–266, April 2010.

[117] H. Yoshida, H. Tsurumi, and Yasuo Suzuki. Broadband RF front-end and software execution procedure in software-defined radio. In *IEEE VTS 50th Vehicular Technology Conference, 1999. VTC 1999 - Fall.*, volume 4, pages 2133–2137 vol.4, 1999.

[118] Guangrong Yue, Lijia Ge, and Shaoqian Li. Performance of UWB time-hopping spread-spectrum impulse radio in multipath environments. In *The 57th IEEE Semiannual Vehicular Technology Conference, 2003. VTC 2003-Spring.*, volume 3, pages 1644–1648 vol.3, April 2003.

[119] Tae-Won Yune, Chan-Ho Choi, Gi-Hong Im, Jong-Bu Lim, Eung-Sun Kim, Yoon-Chae Cheong, and Ki-Ho Kim. SC-FDMA with iterative multiuser detection: improvements on power/spectral efficiency. *IEEE Communications Magazine,*, 48(3):164–171, March 2010.

[120] Jiayi Zhang, Lie-Liang Yang, and L. Hanzo. Energy-Efficient Channel-Dependent Cooperative Relaying for the Multiuser SC-FDMA Uplink. *IEEE Transactions on Vehicular Technology,*, 60(3):992–1004, March 2011.

[121] Qian Zhang, Chenyang Yang, and A.F. Molisch. Downlink Base Station Cooperative Transmission Under Limited-Capacity Backhaul. *IEEE Transactions on Wireless Communications*, 12(8):3746–3759, August 2013.

[122] Lizhong Zheng and D.N.C. Tse. Diversity and multiplexing: a fundamental trade-off in multiple-antenna channels. *IEEE Transactions on Information Theory,*, 49(5):1073–1096, May 2003.

[123] Ruolin Zhou, Qian Han, R. Cooper, V. Chakravarthy, and Zhiqiang Wu. A Software Defined Radio Based Adaptive Interference Avoidance TDCS Cognitive Radio. In *IEEE International Conference on Communications (ICC), 2010*, pages 1–5, May 2010.